MAY - AUG. 2007
Volume XIII Number II
ISSN 0859 144X

THE ASEAN JOURNAL OF RADIOLOGY

Published by The Radiological Society and
The Royal College of Radiologists of Thailand,
Bangkok, Thailand

Started through an educational grant from Bracco since 1995

THE IMAGE OF INNOVATION

MAY - AUG. 2007
Volume XIII Number II

ISSN 0859 144X

THE ASEAN JOURNAL OF RADIOLOGY

Published by The Radiological Society and
The Royal College of Radiologists of Thailand,
Bangkok, Thailand

Started through an educational grant from Bracco Since 1995

Chief Editor

Professor Kawee Tungsubutra
Kaweevej Hospital, 318 Tarksin Road, Dhonburi, Bangkok 10600, Thailand.

Asean Journal of Radiology.
Instructions for Authors.

1. The Asean Journal of Radiology publishes the papers on Radiological Sciences, such as research work, review articles, case reports, innovations in Medical Sciences related to all branches of Radiology, and letters to the editor. The aforementioned materials can be written in English only.

2. The authors have to submit 2 copies of the manuscript and a diskette: **to Prof. Dr. Kawee Tungsubutra.** 318 Kaweevej Hospital, Tarksin Road, Dhonburi, Bangkok 10600, Thailand.

3. The original copy to be submitted must be typed in a double space on one side of the page of 8.1/2" x 11.1/2" paper.

4. The format of the article must include :
   a. Title page and address of the author (s)
   b. Abstract
   c. Introduction (Background)
   d. Material and Method
   e. Results and discussion (Tables and Illustrations)
   f. Acknowledgement (if any)
   g. References (Follow the Vancouver style developed by ICMJE)

5. We will provide 5 copies of reprints for the author (s) who submit (s) an article for publication in the Asean Journal.

6. The illustrations and tables must be clearly prepared with legends in English as they are the art works to be reproduced.

7. The authors are reponsible for the contents of the article as to its facts and findings.

8. Ethics.

Paper reporting studies which might be interpreted as human experimentation (e.g. controlled trials) should conform to the standards of the Declaration of Helsinki (see British Medical Journal 1964: 2: 177) and should indicate that, approval that such studies may proceed, has been granted by the local or hospital Ethics Committee.

When reporting experiments on animals indicate whether the institution's or the National Research Council's guide for, or any national law on, the care and use of laboratory animals was followed.

THE ASEAN JOURNAL OF RADIOLOGY

Volume XIII Number II MAY - Aug. 2007

CONTENTS

THE ASEAN JOURNAL OF RADIOLOGY

Volume XIII Number II MAY - AUG. 2007

CONTENTS

MAMMOGRAPHIC AND ULTRASONOGRAPHIC FINDINGS CHARACTERISTICS OF INVASIVE DUCTAL CARCINOMA OF THE BREAST IN KING CHULALONGKORN MEMMORIAL HOSPITAL (KCMH*)

Kewalee SASIWIMOLPHAN, MD.[1], Darunee BOONJUNWETWAT, MD.[1]

ABSTRACT

Purpose: To review mammographic, ultrasonograhic findings and histological grades of invasive ductal carcinoma (IDC) of breast in King Chulalongkorn Memorial Hospital.

Materials and methods: A total of 263 proven cases of IDC of breast and histological grading whose 252 mammographic studies and 233 ultrasoud studies were retrospective reviewed for mammographic and ultrasonographic features.

Results: Two hundred and twenty two abnormal masses have been found in 217 mammography. Another 35 cases whose mammographic findings showed no mass lesions; 5 were normal, 19 were asymmetrical density and 11 were architectural distortion and adjunction ultrasound images could detect these lesions. The most common mammographic findings of IDC were abnormal mass with irregular shape (86.5%). The most frequent margin of mass from mammography was spiculate margin (39.6%) which most were histological grade 1 and 2 (77.27%) followed by indistinct (ill-defined) margin (33.7%). Malignant-type microcalcifications were observed in 111 cases (44%) and the most common type of microcalcifications were granular type(52.3%). Mammography was better than ultrasonography in depicting microcalcifications (111 Vs 58 lesions). Axillary lymphadenopathy was detected in 46% of cases. Ultrasonography was better than mammography in depicting soft tissue masses. Two hundred and forty four lesions have been found by ultrasonography. The most common ultrasonographic findings for IDC of breast cancer were irregular shape (80%) and thick echogenic rim (80%). Nearly most of lesions were hypoechoic lesions (hypoechoic lesions 83.2% and very low echoic lesions 7.38%). Most frequent posterior attenuation from ultrasonography was posterior enhancement (29.5%) followed by posterior shadowing (28.3%). In-group of posterior enhancement lesions were mostly in histological grade 3 and 2, while in posterior shadow group most lesions were in grade 1 and 2. Doppler study, available in 240 lesions, found that 79.9% have one or more feeding vessels to lesions.

Conclusion: Most common malignant mammographic features are spiculated margin (39.6%) and irregular shape (86.5%). Multiple suggestive malignancy signs such as malignant microcalcifications, axillary lymphadenopathy and skin thickening should be used to increase confidence of the diagnosis. Most common features on ultrasound are irregular mass, angular margin, thick echogenic rim and hypervascularity from Doppler study. Posterior shadowing of the mass tends to be found in grade 1 and 2 tumor, whereas posterior acoustic enhancement tends to be found in grade 3 tumor. Adjunctive ultrasonography was suggested to improved the confidence of diagnosis.

[1] Department of Radiology, Faculty of Medicine, King Chulalongkorn Memorial hospital.

INTRODUCTION

Breast cancer is the most prevalent cancer among women throughout the world and one of the mortality causes among women in the world today[1] without knowing the actual cause, probably due to multiple factors.[2] The risk of breast cancer increases with age and drops off at 80 years of age. However, the incidence of breast cancer is increasing in younger women and many cases of this disease are being reported in women in their twenties and thirties. The incidence of breast cancer among women across all ages are also continue to be rising.

In Thailand, breast cancer is the second most common cancer, leading by cervical cancer, and second cause of death in women today. The number of new breast cancer cases has been increased by approximately 17.2 per 100,000 women.[3] Invasive ductal carcinoma breast cancer is the most common pathological type of breast cancer.[2]

Early and accurate diagnosis of breast cancer is a cornerstone of successful treatment. Mammography is the role acceptable method for breast cancer screening and diagnosis. Pre-operative mammographic features can predict patients likely to have residual microscopic disease or extensive intraductal carcinoma following conservation surgery for breast cancer. The sensitivity of the mammography to the index cancer range from 63% to 98% and has been reported to be as low as 30%-48% in dense breast.[4] The use of ultrasound as an adjunct to mammography in the diagnosis of breast cancer is well established[4-6] with increase in diagnostic accuracy of the breast cancer detection.[7] An abnormal mass on mammography is reported in 50% of carcinomas of less than 10-mm diameter and 88% of those greater than 10 mm diameter8. A spiculated mass on mammography has been reported in up to 84% of breast malignancies.[9] However in Gershon-Cohen J et al study10 in 1969 showed that up to 60% of malignant lesions showed no classical sign of breast cancer.

Historically, at ultrasound examination posterior acoustic shadowing was said to be associated with the majority of malignant breast mass: 70%-80% over all and almost 100% of speculated lesions.[5] However, it is now widely recognized that not all-invasive breast mass demonstrate posterior shadowing; they may have no distal effect or even be associated with acoustic enhancement. Sometime, the tumors associated with distal acoustic enhancement tend to be designated high-grade at subsequence histological examination.

The purpose of this study was to demonstrate mammographic findings, ultrasound characteristic of invasive ductal carcinoma of breast in King Chulalongkorn Memorial Hospital's patients.

MATERIAL AND METHODS

Institutional ethics approval was obtained for this study.

Between January 1, 2004-December 31, 2005, 378 patients pathological proved to be invasive ductal carcinoma of the breast with Modified Bloom-Richardson histological grading system of histological grade, who admited in KCMH.* Available prediagnostic mammography and/or ultrasonographic studies of 263 patients were reviewed.

Mammography was performed with dedicated equipment (Senography 2000D full field digital mammography, GE healthcare Waukesha UI, USA). Standard craniocaudal and mediolateral oblique views were routinely obtained and additonal views such as magnification view were also obtained for better delineation of a mass or microcalcifications.

Mammographic findings were assessed for malignant features of breast cancer including soft tissue abnormalities both with mass or with no mass,

such as normal, asymmetric density or architectural distortion. In-group of the mass lesions, characteristics of the masses were reviewed such as shape and margin. Including presence or absence of microcalcification, type of microcalcifications and associate findings such as axillary lymphadenopathy, skin thickening and nipple retraction were also noted. All of the findings were reviewed via the same definition according to ACR BIRADS Lexicon.[11]

All cases after mammography had been performed, were sent to breast ultrasonography using high frequency (10-12 MHz) linear transducers (Philip HDI 5000, Advanced technology laboratory Bothell Wash USA and GE logic,[9] GE healthcare Waukesha UI, USA) and experienced radiologists. Ultrasonography characteristics assess size of mass, characteristics of mass (margin, attenuation, echotexture, halo, depth/width ratio, vascularity) peripheral duct extension and calcification.[12] All cases had Doppler studying performed. Vascularity of the mass was studied and divided into three groups according to the number of feeding vessels: avascular, hypovascular (one) and hypervascular (more than one). And then pattern of the feeding vessels of the tumor were characterized by inner, periphery and both inner-periphery locations.

All films were retrospective reviewed by a radiologist who has experienced in breast imaging.

RESULT

In the study period, there were 263 women with pathological proved invasive ductal carcinoma of the breast and multiple lesions in 6 patients. The histological grading according to Modified Bloom Richardson grading systems were revealed that, grade I: 29 (10.8%), grade II: 144 (53.5%), grade III: 79 (29.4%) and no recording of the histological grading in 17 patients. Associating pathological findings were the presence of axillary lymph node metastases in 80 patients (30.4%) and positive extensive intraductal component or ductal carcinoma insitu component in 36 patients (13.6%).

All 263 women underwent mammography and/or ultrasonography. The 222 women had both avaliable prediagnostic mammography and ultrasound studies. There were 30 women having only mammography and 11 women having only ultrasound study.

Their ages ranged from 24 to 80 years (mean, 51.6 years). Site and side of the lesions were shown in Table 1. There are 2 patients who have lesions in both breasts. Size of the lesions ranged from subcentimeter to more than 5 cm and correlation with histological grading were shown in Table 2.

MAMMOGRAPHIC FINDINGS

Two hundred and fifty-two mammography were reviewed, 222 masses were found in 217 patients. In five patients, there were two masses in one mammography. In 35 (13.8%) patients, the mammography showed no mass on mammography. Of these 35 patients, 5 were normal, 19 were asymmetrical density and 11 were architectural distortion.

Of the 222 masses on mammography, 22(10%) were round, 10(3.5%) were oval and 192 (86.5%) were irregular shape. Margins of these masses were spiculate (Fig.1) in 86 lesions (38.7%), indistinct (poorly defined, ill-defined) margin (Fig.2): 73 lesions (32.9%) and the least frequent margins such as obscured, microlobulated and circumscribed (well -defined) margins. Correlation between histological grading and margin of the lesions was also reviewed on Table 3.

Microcalcifications (Fig.3) in the lesions were detected on 111 patients. Most common findings are granular type microcalcifications about in 58 lesions follow by mixed type microcalcification (39 lesions) and linear (14 lesions).

Associated findings such as axillary lymphade- nopathy (Fig.4) were founded in 116

mammograms, skin thickening and retraction in 47 mammograms and nipple retraction in 67 mammograms. The criteria suggestive of axillary metastases were enlargement of axillary lymphnodes (more than 2 cm), round or irregular shape, increase nodal density with absence of radiolucent fat within (fatty hilar).[13,14] However in pathological database, nodal metastases were depicted only 80 patients. In these 80 patients, there were 55 patients who presenting with abnormal axillary lymph node appearances on mammography, another 25 patients showed normal appearances.

ULTRASONOGRAPHIC FINDINGS

Ultrasound images were available in 233 cases: of these 21 were grade 1 tumors, 123 were grade 2 tumors, 75 were grade 3 tumor and 14 had no histological grading record. There were 244 lesions in ultrasound images. The ultrasonographic findings of the mass were reviewed for size, depth/width ratio, shape, margin, echogenicity, attenuation and vascularity.

With regard to the depth/width ratio, 52 lesions (21.3%) of all tumor masses had an increased ratio representing taller than wide appearance.

Most common shape of the lesions were irregular shape, 195 lesions (80.1%). Angular margin (Fig.5) was the most common findings of the lesions, in 156 lesions (73.9%). Correlation between histological grading and margin were shown in Table 4.

In 203 lesions showed hypoechogenicity whereas 13 lesions were mixed solid-cystic echogenicity and other 18 lesions were very low echogenicity with shadowing on posterior attenuation.

Attenuation patterns of all lesions and correlation to histological grading were shown in Table 5.

Thick echogenic rim (Fig.5) was depicted in 195 lesions (80.1%).

Doppler ultrasonography available in 240 lesions were revealed for the amount of feeding vessels, location of vessels and correlation to histological grades shown in Table 6 and 7.

According to criteria of suggestive malignant lymph nodes from ultrasonography and Color doppler study in previous studies:[15-17] longitudinal/transverse ratio of abnormal lymph node less than 2, concentric or asymmetrical eccentric cortical thickening more than 2 mm, absence or abnormal echo of central fatty hilum and predominate peripheral flow were suggestive of malignant lymphnodes.[15-17] In our study, ultrasonography detected only 17 patients with abnormal axillary lymph nodes (Fig.4), while all the malignant axillary lymph nodes of all patients on mammograms. The associated findings were observed in ultrasound images such as intraductal extension 52 patients, daughter nodules 17 patients, subnipple extension in 14 patients and skin thickening in 11 patients.

In the detection of microcalcifications from ultrasound study, we depicted 58 lesions having small hyperechoic spots with acoustic shadow suggestive of microcalcifications. All of them were demonstrated on mammography.

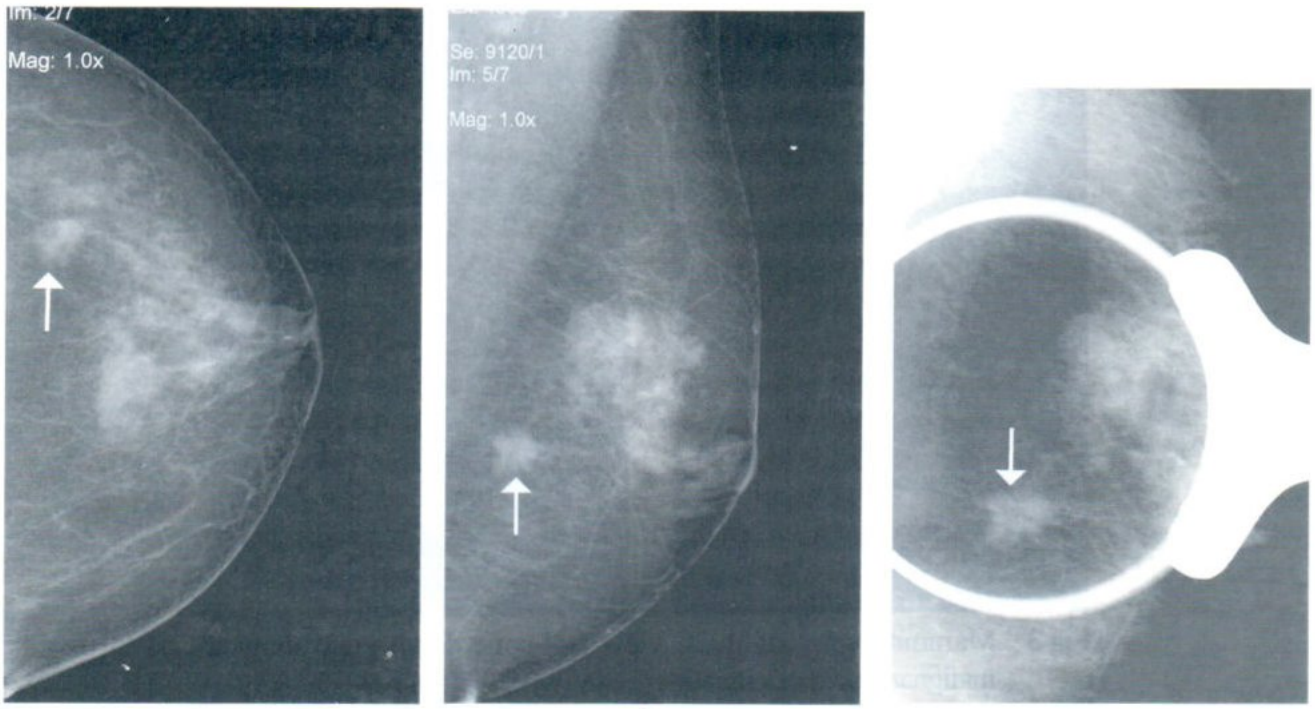

a b c

Fig.1 Mammography: left CC view (a), left MLO view (b), and cone compression (c) showed spiculated mass (white arrow) at left upper mid region.

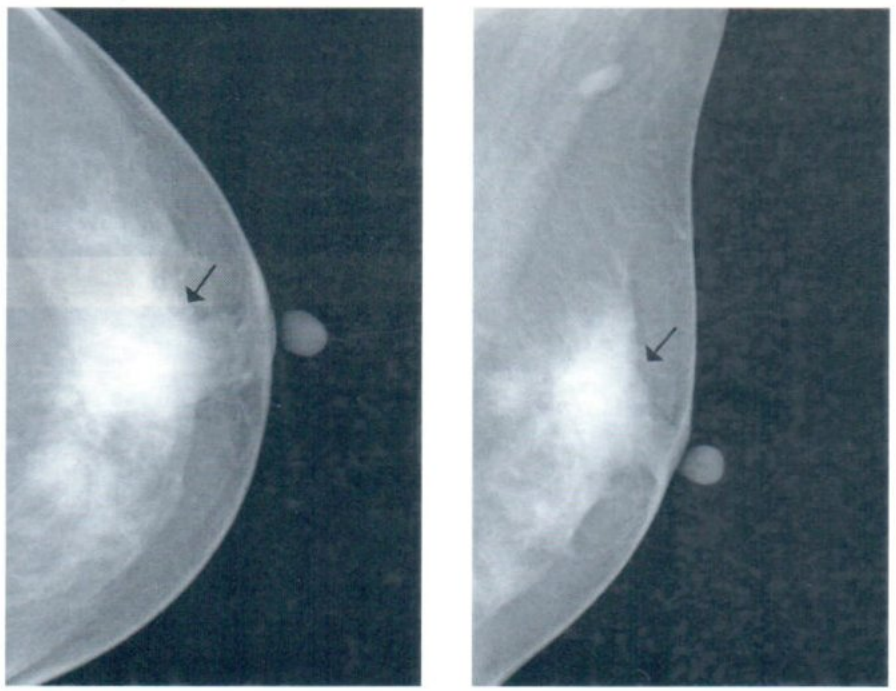

a b

Fig.2 Mammography left CC view (a), and left MLO view (b), showed an ill-defined margin mass (arrow) at left upper inner quadrant.

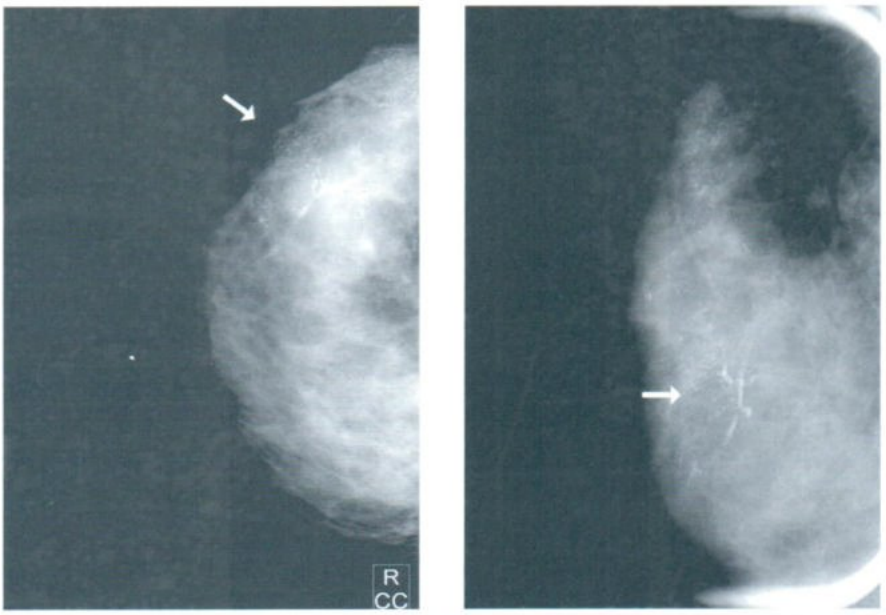

Fig.3 Mammography right CC view and cone down view showed malignant microcalcification (mixed type) white arrow;

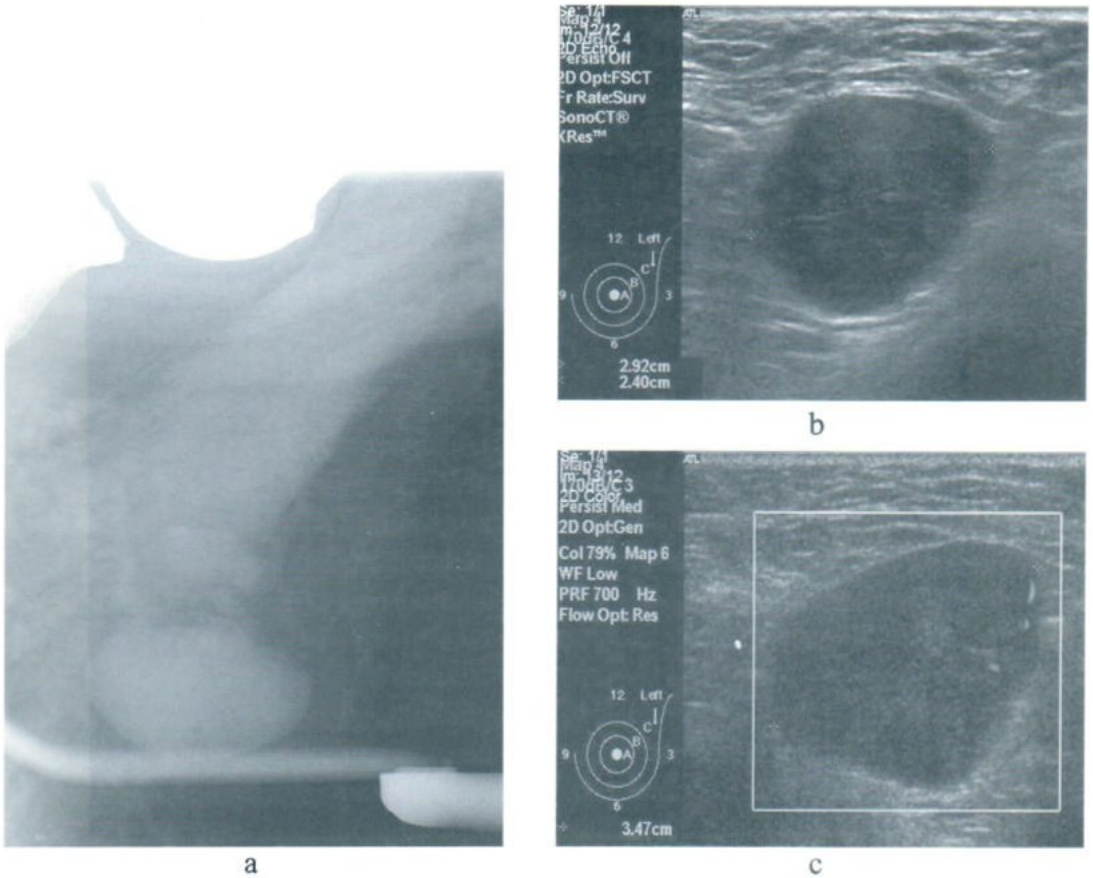

a b c

Fig.4 Enlarged dense axillary lymphadenopathy in mammography (a), and a round-shaped node form ultrasonography (b), and hypervascularity from Doppler study (c)

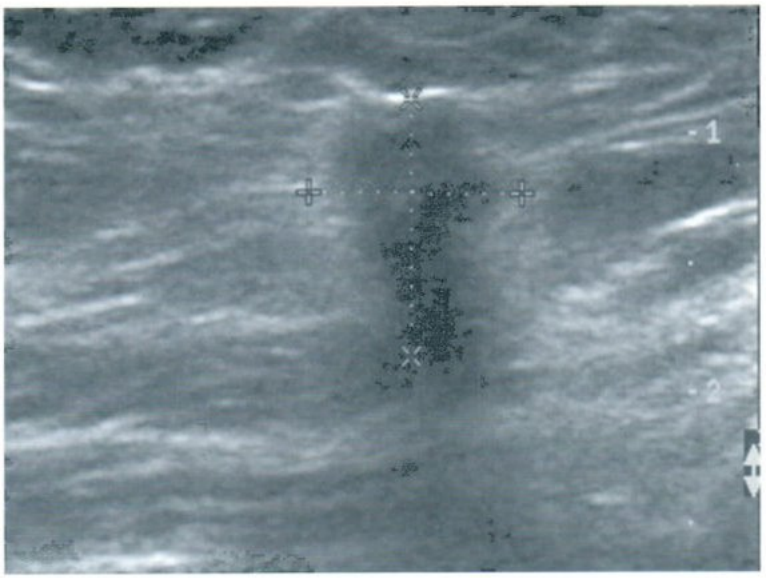

Fig.5 Ultrasonography of left breast mass showed Irregular shape, angular margin, taller than wide mass with thick echogenic rim and posterior shadowing.

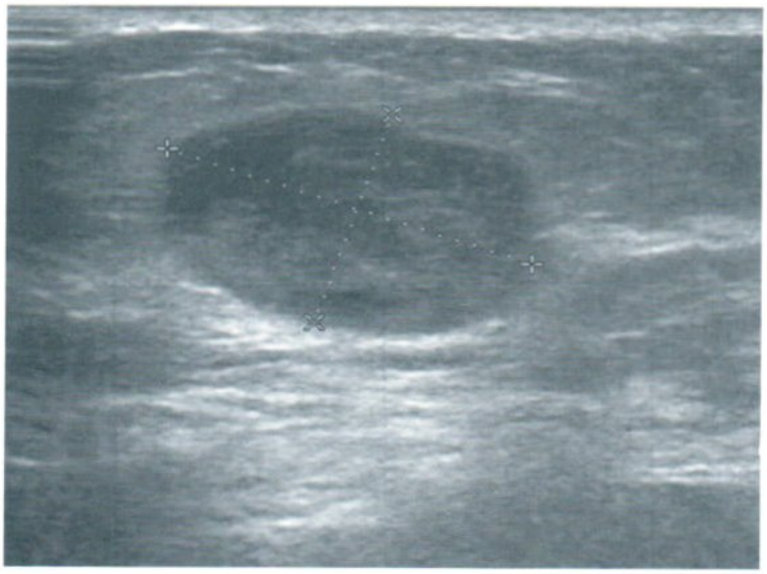

Fig.6 Ultrasonography of breast mass showed well-defined oval shaped mass with posterior enhancement, patholo gical proved to be invasive ductal carcinoma.

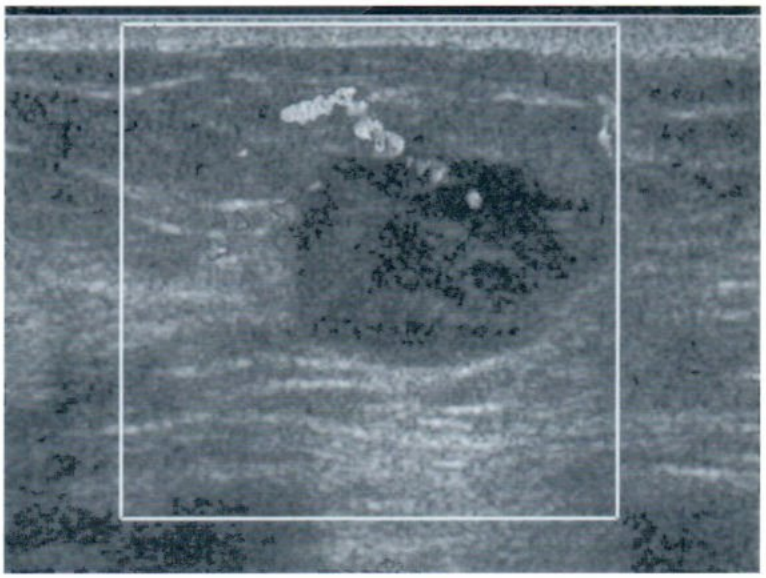

Fig.7 Color doppler study shows hypervascularity with intratumoral and peripheral location of breast mass.

Table 1 Sites of the lesions

Site	RT	LT	Total
UO (upper outer)	45	52	97 (36.6%)
MO (mid outer)	15	20	35 (13.2%)
LO (lower outer)	3	5	8 (3.0%)
ML (mid lower)	3	2	5 (1.9%)
LI (lower inner)	19	18	37 (13.9%)
MI (mid inner)	4	0	4 (1.5%)
UI (upper inner)	12	21	33 (12.5%)
MU (mid upper)	8	10	18 (6.7%)
Central	14	14	28 (10.6%)
Total	123 (46.4%)	142 (53.5%)	265

Table 2 Sizes of lesions * and histological grade

Size Histo grade	<1 cm	1-2 cm	2-5 cm	> 5 cm
No Histo grade	5	6	6	0
1	5	12	5	0
2	16	58	47	5
3	5	33	37	4
Total (244)	31 (12.7%)	109 (44.67%)	95 (38.9%)	9 (3.7%)

* Size of the lesions comes from ultrasonographic measurement in maximum diameter.

Table 3 margin of the mammographic lesions and histological grades

		Margin					Total
		Circumscribed (Well-defined)	Indistinct (Poorly or ill-defined)	Obscured	Spiculate	microlobulate	
Histological grade	No grade	0 (0%)	10(4.5%)	1(0.45%)	3(1.35%)	0(0%)	14(6.3%)
	1	1(0.45%)	7(3.15%)	5(2.25%)	11(4.95%)	0(0%)	24(10.8%)
	2	2(0.90%)	33(14.06%)	18(8.10%)	57(25.67%)	6(2.70%)	116(52%)
	3	4(1.8%)	25(11.26%)	14(6.3%)	17(7.66%)	8(3.6%)	68(30.6%)
Total		7(3.15%)	75(33.7%)	38(17.11%)	88(39.6%)	14(6.3%)	222(100%)

Table 4 margin of the ultrasound lesions and histological grade

Histological grade	Margin					Total
	Well-circumscribed	Poorly defined	Microlobulate	Angulated	Spiculate	
No grade	1(0.4%)	2(0.82%)	4(1.64%)	7(2.87%)	0(0%)	14(5.3%)
1	1(0.4%)	0(0%)	4(1.64%)	16(6.56%)	0(0%)	21(7.79%)
2	4(1.64%)	10(4.1%)	22(9.22%)	77(31.56%)	5(2.04%)	131(53.3%)
3	1(0.4%)	6(2.45%)	16(6.56%)	45(18.44%)	3(1.23%)	78(31.9%)
Total	7(2.87%)	18(7.38%)	46(18.85%)	145(59.43%)	8(3.28%)	244(100%)

Table 5 posterior attenuation of the ultrasonographic lesions and histological grade

Histological grade	Attenuation				Total
	Shadowing	Posterior enhancement	Mixed distal effect	No distal effect	
No grade	1(0.4%)	3(1.23%)	2(0.82%)	8(3.28%)	14(5.3%)
1	10(4.1%)	3(1.23%)	3(1.23%)	5(2.05%)	21(7.79%)
2	46(18.85%)	31(12.7%)	24(9.83%)	30(12.29%)	131(53.3%)
3	13(5.32%)	35(14.34%)	13(5.33%)	17(6.97%)	78(31.9%)
Total	70(28.69%)	72(29.5%)	42(17.21%)	60(24.59%)	244(100%)

Table 6 Vascularity form color doppler study of masses and histological grade

Histological grade	Attenuation				Total
	Shadowing	Posterior enhancement	Mixed distal effect	No distal effect	
No grade	1(0.4%)	3(1.23%)	2(0.82%)	8(3.28%)	14(5.3%)
1	10(4.1%)	3(1.23%)	3(1.23%)	5(2.05%)	21(7.79%)
2	46(18.85%)	31(12.7%)	24(9.83%)	30(12.29%)	131(53.3%)
3	13(5.32%)	35(14.34%)	13(5.33%)	17(6.97%)	78(31.9%)
Total	70(28.69%)	72(29.5%)	42(17.21%)	60(24.59%)	244(100%)

Table 7 Location of feeding vessels and histological grade

Histological grade	Location of feeding vessels			Total
	inner	Periphery	Both	
No grade	0 (0%)	8(4.1%)	4(2.05%)	12(6.15%)
1	4(2.05%)	7(3.59%)	9(4.61%)	20(10.25%)
2	15(7.69%)	61(31.28%)	22(11.28%)	98(50.26%)
3	8(4.1%)	38(19.49%)	19(9.74%)	65(33.33%)
Total	27(13.85%)	114(58.46%)	54(27.69%)	195(100.0%)

DISCUSSION

The role of mammography and ultrasonography in imaging of breast cancer has been accepted more over the years. The classical appearance of the breast cancer on mammography such as spiculate mass was also accepted.[8]

In this study the classical spiculate appearance of the breast cancer was found in 88 lesions (39.6%) follow by poorly defined margin in 75 lesions (33.6%). However well defined margin lesions, mostly indicate benign lesions were depicted in 7 lesions (3.15%). All of these lesions had other secondary signs[10] such as microcalcifications, axillary lymphadenopathy, skin thickening and adjunctive ultrasounds, which can help us to make diagnosis. The most common findings of the malignant breast cancer in our study were irregular shape, about 192 lesions from 222 mammographic lesions (86.5%).

The classic spiculate margin of the malignant lesions showed more than 77% is grade 1 and 2 lesions similar findings as the previous study on Lamb et al study in 2000[18] that the classical malignant appearances tend to be low grade tumor.

Malignant microcalcifications were also observed in 111 patients from mammography and only 58 patients from ultrasound study. In all 58 patients with detected microcalcifications on ultrasound study were also detected on mammograms. As we known that mammography is more sensitive to detected microcalcification.[19]

Malignant appearance of axillary lymph nodes were noted from 116 mammograms, while ultrasound detected only 17 patients with abnormal appearances and all 17 cases were detected axillary lymphadenopathy on their mammograms. There were only 80 patients having pathological approved nodal metastases. To explain this, there were some patients receiving neoadjuvant chemotheraphy and causing decrease in number of pathological detection. However to review mammography in 80 cases of pathological proved nodal metastases refered back to the mammographic findings, only 55 cases could detect malignant features of axillary lymph nodes. In other 25 cases, there were no abnormal appearances of the axillary lymph nodes. Two cases of these 25 patients, the pathological reports revealed positive nodal metastases only in the apical lymph nodes and they could not detect on mammogram. Other 6 cases, the pathological reports revealed evidence of

lymphatic vessels invasion. The rest in this group, abnormal findings of axillary lymph nodes could not be detected by mammography possible from small size of nodal metastases or micrometastases.

Ultrasound has been accepted as a role to help for the diagnostic of breast cancer especially in young patient with dense breasts.[12,19-21] Stavros A T, et al in 1995[12] showed that spiculation, angular margins and hypoehcogenicity are reliable malignant findings. There was similar finding in our study which angular margin (59.3%) and hypoechogenicity (83.2%) of the masses were the most common findings. Thick echogenic rim was the most common sign of malignant lesions in out study, about 195 lesions similar to the study on 2005.[22] In our study, only 52 lesions (21.3%) showed taller than wide appearances, similar to Stavros study. This sign is low sensitivity but high positive predictive value. According to Rahbar's study on 1999,[19] the width-AP dimension ratio more than 1.4 seem to be benignity criteria, however in over study about 90 lesions (36.8%) had width-AP ratio more than 1.4. This sign seem to be less specificity in our study.

Posterior shadowing is a sign of the malignant lesions.[12] And in later several previous studies[18,22] revealed posterior shadowing more likely to represent low or intermediate grade tumor and posterior acoustic enhancement of the mass more likely found to be high-grade tumor. Similar to our study, it was found that about 70 lesions (28.69%) had posterior shadowing most by in histological grade 1 and 2. Another 72 lesions (29.5%) having posterior acoustic enhancement, about 48.9% in this group were histological grade 3.

Hypothesis of angiogenesis can represent malignant process. In our study, about 195 lesions had one or more feeding vessels and only 45 lesions shown no detectable feeding vessels from color Doppler sonography.

We also recognized some limitations of our study. These included the fact that the evaluation of the cases were retrospectives, that there was unavoidable case-selection bias, and no case of benign study included. For example some cases have only mammography without ultrasound or some imaging findings could be found in both benign and malignant processes.

CONCLUSION

Most common malignant features of invasive ductal carcinoma of the breast are spiculate margin (39.6%) and irregular shape (86.5%). However some of invasive ductal carcinoma of the breast showed benign features. Additional suggestive malignanty features such as malignant microcalcification, axillary lymphadenopathy, skin thickening should be use to increase the confidence of the diagnostic. Adjunctive ultrasound images are recommended to increase the confidence in the diagnostic too. Most common malignant features of breast cancer on ultrasonography such as irregular mass, angular margin, thick echogenic rim and color Doppler for feeding vessels searching are detected. Posterior shadowing of the mass are mostly found in low and intermediate grade tumors, whereas posterior acoustic enhancement mostly found in intermediate and high-grade tumors. To evaluate axillary adenopathy, mammography and ultrasonography still has limitation for those metastatic nodes locating in high level, being small size or micrometastases.

ACKNOWLEDGEMENTS

The researchers wish to thank the Medical Records and Statistical Department of KCMH for providing the patients' data. Thanks also to Mr. Athipan Nonthasin for providing the imaging pictures.

REFERENCES

1. Centers for Disease Control and Prevention National Cancer Data: **http://www.cdc.gov/cancer/natlcancerdata.html**

2. American Cancer Society Breast cancer Facts & Figures: **http://www.cancer.org/statistics /index.html**
3. Sriplung H, Sontipong S, Martin N et al. Cancer in Thailand, vol. 3, 1995-1997; 47.
4. Berg WA, Gutierrez L, Ness M, Aiver MS et al. Accuracy of mammography, clinical examination, ultrasonography and MR Imaging in preoperative assessment of breast cancer: Radiology 2004 Dec; 233(3): 830-49. Epub 2004 Oct 14.
5. Tohno E, Chapter 9 malignant breast lesions, In: Cosgrove DO, Sloane JP. Ultrasound Diagnosis of Breast Diseases. Edinburgh: Churchill Livingstone; 1994.
6. Tucker AK, Chapter 9 diagnostic mammography, In: Tucker AK. Textbook of Mammography. 1st ed. Churchill Livingstone, 1993.
7. Zonderland HN Coerkamp EG, Hermans J, van de Vijver MJ, van Voorthusien AE. Diagnosis of breast cancer: contribution of ultrasonography as an adjunct to mammography: Radiology 1999; 213; 413-422.
8. Andersson I. Radiographic screening for breast carcinoma III: appearance of carcinoma and number of projections to be used at screening. Acta Radiol Diagn 1981;22:407-420.
9. Cotran RS, Kumar V, Robbins SL, The breast, In: Schoen FJ, Cotran RS, Kumar V, Robbins SL. Robbins : Pathologic Basis of Disease. 5th ed. WB Saunders 1994.
10. Gershon-Cohen J, Schorr S. The diagnostic problems of isolated, circumscribed breast tumors: AJR 1969; 106: 863-870.
11. Breast imaging lexicon, In D'Orsi CJ, Bassett LW, Berg WA, Feig SA et al. American College of Radiology (ACR). Illustrated breast imaging reporting and data system (BI-RADS TM). 4th ed. Reston, VA: American Collage of Radiology 2003.
12. Stavros T, Thickman D, Rapp C, Dennis M, Parker S, Sisney G. Solid Breast Nodules: Use of Sonography to distinguish berween Benign and Malignant Lesions: Radiology 1995:196(1); 123-134.
13. Fu KL, Fu YS, Bassett L W, Cardall SY and Lopez JK. Invasive malignancies, In Bassett LW, Jackson VP, Fu KL and Fu YS; Diagnosis of diseases of the breast. 2nd ed. Elsever Saunders,Pen 2005.
14. Lim E T, O' Doherty A, Hill A D, Quinn C M. Pathological axillary lymph nodes detected at mammographic screening: Clinical Radiology 2004; 5: 86-91
15. Yang T W, Chang J and Metreweli C. Patient with breast cancer: Differences in coler doppler flow and grey-scale US features of benign and malignant lymph nodes: Radiology 2000; 215: 568-573.
16. Esen G, Gurses B, Yilmaz MH et al. Gray scale and power Doppler US in the preoperative evaluation of axiallary metastases in breast cancer patients with no palpable lymph nodes: Eur Radiol 2005; 15: 1215-1233.
17. Mobbs L M, Jannicky E A S, Weaver D L, Harvey S C. The Accuracy of Sonography in Detecting Abnormal Axillary Lymph Nodes When Breast Cancer Is Present: Journal of Diagnostic Medical Sonography; 21:297-303
18. Lamb P M, Perry N M, Vinnicombe S J, Wells C A. Correlation Between Ultrasound Characteristics, Mammographic Findings and Histological Grade in Patients with Invasive Ductal Carcinoma of the Breast: Clinical Radiology 55, 40-44.
19. Rahbar G, Sie AC, Hansen GC et al. Benign versus malignant solid breast masses: US differentiation: Radiology 1999; 213(3): 889-94.
20. Samardar P, De Paredes ES, Grimes MM. Focal Asymmetric Densities Seen at Mammography: US and Pathologic Correlation concluded that mammographic findings of the breast cancer: RadioGraphics 2002; 22: 19-33

21. Houssami N, Irwig L, Simpson JM, McKessar M, Blome S, Noakes J. Sydney Breast Imaging Accuracy Study: Comparative sensitivity and specificity of mammography and sonography in young women with symptoms: AJR 2003 Apr; 180(4):935-40

22. Rotstient AH, Neerhut PK. Ultrasound characteristics of histologically proven grade 3 invasive ductal breast: Australas Radiol 2005 Dec; 49(6): 476-9.

REVERSING SIGN ON COMPUTED TOMOGRAPHY OF HYPOXIC ISCHEMIC CEREBRAL INJURY IN TWO CHILDREN.

Chanya CHAISIRAT M.D.[1]

ABSTRACT

An anoxic ischemic cerebral injury may cause a variety of neuropathologic abnormalities, which depend on the age of onset, duration and intensity. Reversing sign is an uncommon radiological finding on computed tomography. It is seen mainly in cases of severe pediatric hypoxia.

The purpose of this study was to present and describe the reversing sign on computed tomography of two cases of hypoxic children.

We reviewed the clinical features, etiologies, outcome and the reversal sign on computed tomography in two interested children. They have severe developmental delay due to prolonged hypoxia in different ages at the time of on set, the one was birth asphyxia and the other was cardiopulmonary arrest after seizures. They were underwent computed tomographic examination next 1-2 months after the anoxic events to evaluate the outcome.

The reversing signs on computed tomography of our two pediatric cases were defined by reversal of the normal gray and white matter density, a relative increase density of preserved thalami, brain stem and cerebellum, some decrease volume of the white matter mantle and some ventricular dilatation. The different degrees of the decrease cerebral density, white matter volume loss and atrophic ventricular enlargement were observed. They represented various degrees of periventricular leukomalacia and cystic encephalomalacia on chronic state.

As our result and reviewed relevant literatures, we presumed that the reversing sign is an uncommon classic computed tomographic findings which are divided into acute, intermediate and chronic reversing groups. They occur following diffuse anoxic ischemic injury in any age groups. It usually represents severe brain injury, irreversible brain damage and carries a poor outcome.

Key Words: Reversing sign, computed tomography, hypoxic ischemic encephalopathy (HIE).

INTRODUCTION

If cerebral circulation is interrupted for several seconds or longer, brain oxygen is rapidly depleted. Following successful resuscitation, complete recovery may occur, however in other cases, cerebral hypoxia causes edema, ischemic and hypoxic ischemic encephalopathy.[1]

[1] Department of radiology, Kamphaengphet Hospital, Kamphaengphet 62000, Thailand

An anoxic ischemic insult may cause a variety of neuropathologic abnormalities, including neuronal necrosis, marmoration of basal ganglia and thalami, watershed infarction, parasagittal cerebral injury, periventricular leukomalacia, focal and multifocal ischemic brain necrosis.[2,5] The pattern of neuropathologic alteration depends on the patient's age at the time of insult and the duration of the anoxic episode.[3]

When cerebral blood flow was interrupted completely, a small percentage of patients who suffer a global cerebral hypoxic ischemic injury develop distinctive computed tomography finding which termed as a reversal sign.

In the past and until now, CT still has been utilized in detection of the neuropathologic changes in patient who survived from this episode particularly in the rural hospital where MRI is not available.

The reversal sign expressed (1) just diffusely decreased density of cerebral cortical gray and white matter with reduced or lost gray, white matter differentiation or (2) less frequently, reversal of the normal gray white matter density. The density of thalami, brainstem and cerebellum were usually preserved and relatively increased in density.[4,5,6,12,14]

Reversal sign on computed tomography is seen mainly in cases of pediatric hypoxia. However, now the reversal sign has been described for adult who has prolonged anoxic ischemic injury in scattered literatures.[6,8]

The reversal sign has been described for anoxic ischemic states due to variety of causes, including birth asphyxia, drowning, status epilepticus, meningitis, and degenerative encephalitis.[5,6,9] It can occur following other causes such as child abuse, cardiac arrest, electrocution and accidental injury.[5,6,9] This sign has been mainly seen as either an early sign or sequel of hypoxic ischemic insult.

The aim of this report was to show the two classic reversal signs on computed tomography, which resulted from prolonged hypoxic ischemic cerebral injury of two pediatric cases who presented CT appearance as chronic reversal signs. We also discussed the clinical features, etiologies and outcome; and also reviewed the relevant literature.

MATERIALS AND METHODS

We retrospectively analyzed the clinical features and the reversal sign on computed tomography images of two hypoxic children who have severe developmental delay, one was due to birth asphyxia and the other was due to cardiopulmonary arrest. We reviewed its possible causes, and also discussed the relevant literatures.

Patient 1, A 6 month-old child born at 37 weeks gestational age by C/S. He was healthy term infant and had normal Apgar Scores at birth ~ 9, 10 and10 in 1, 5 and 10 minutes, respectively. Next 6 months later, he was brought to emergency services with unconscious after seizures, he was E1V1M1 and then he rapidly developed cardiopulmonary arrest. On arrival at the hospital he had no detectable pulse and respiration. On examination the child was comatose, cyanosis and unresponsive to noxious stimuli. Few minutes after cardiopulmonary arrest, an emergency nasotracheal intubation was performed and mechanical ventilation was initiated.

The initial computed tomography was obtained 2 hours after resuscitation. There were small right frontal intracerebral hematoma and chronic bilateral frontal convexity subdural hemorrhage (not shown).

He was referred to intensive care unit for conservative treatment, after unsuccessful cardiopulmonary resuscitation. After that, he has survived but developed clinical signs of cerebral hypoxia including spastic diplegia and seizures.

Follow up 2 months non-contrast computed

tomography after the anoxic event demonstrated diffusely decreased density of gray matter and striking increased density of white matter, it was reversal of the normal gray and white matter densities. There were slightly decrease amount of white matter mantle and mildly dilated all ventricles. Relatively increased density of the preserved thalami, brainstem and cerebellum were detected. All findings are typical features of chronic reversal sign (Fig.1 A-D). Bilateral chronic subdural hemorrhages were also detected.

Patient 2, A 2 month-old child, who had prior history of 38 weeks term infant, severe fetal distress and birth asphyxia is presented. The infant had low Apgar Scores at birth ~ 2, 4 and 5 in 1, 5 and 10 minutes, respectively. He required resuscitation and ventilatory assistance at birth. After that, he developed hypoglycemia and seizures. For long term, he survived. The clinical sign of hypoxic ischemic encephalopathy (HIE) were detected as major motor disabilities, including spastic diplegia, abnormal neuromuscular tone and reflexes. Seizures, altered consciousness and developmental delay were also observed.

One month after birth, initial plain computed tomography was performed to evaluate the clinical prognosis. His plain computed tomography scans demonstrated reversal of normal gray and white matter density which were seen as generalized CSF like hypodensity throughout the cerebral gray matter representing cystic encephalomalacia. Volume of white matter is markedly decreased, and accompanying reversal increase white mater density is seen. Relative hyperdensity are seen in thalami, brainstem and cerebellum. All findings are characteristic CT appearance of chronic form of reversal sign (Fig.2 A-D).

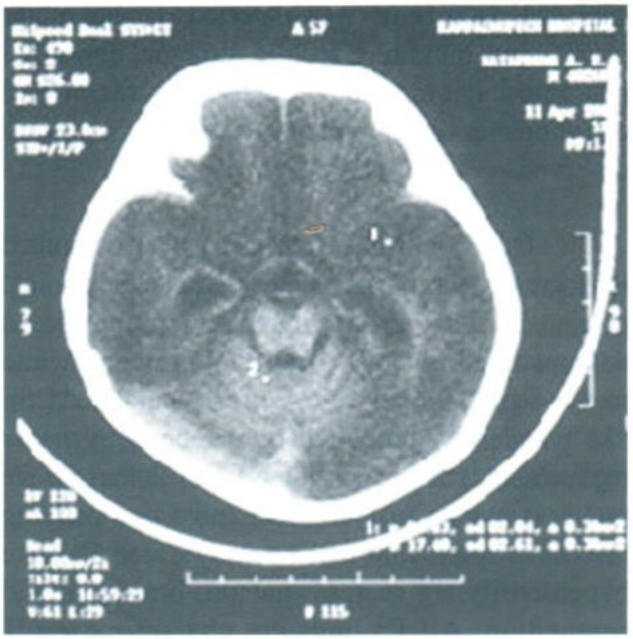

Fig. 1A

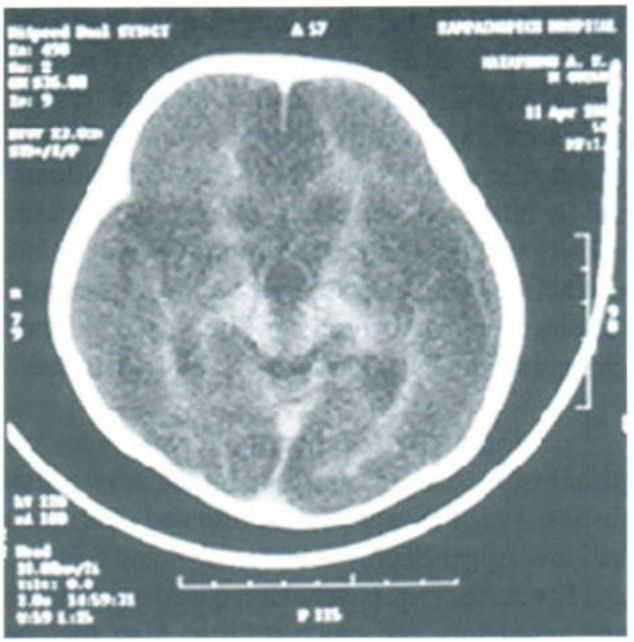

Fig. 1B

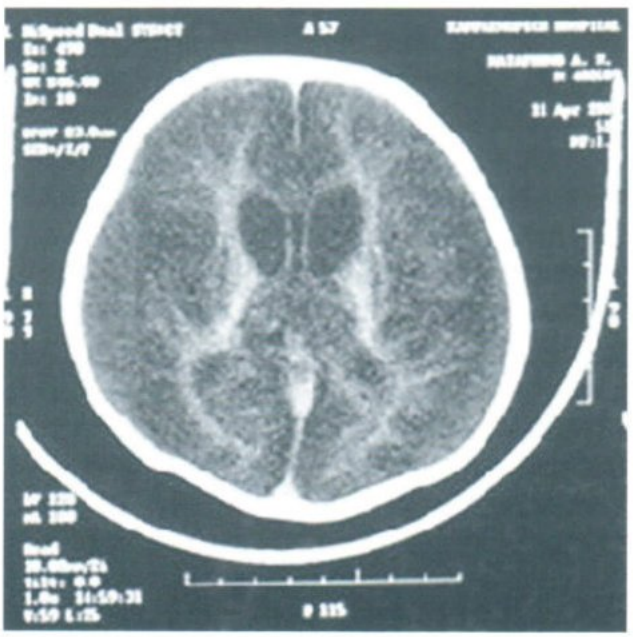

Fig. 1C

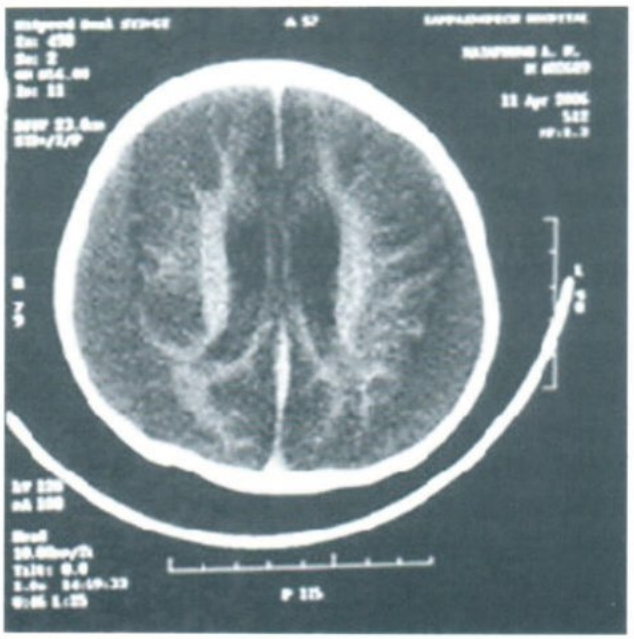

Fig. 1D

Fig.1 A-D Chronic reversal sign in 8 month-old child with history of post resuscitation for 2 months, secondary to cardiopulmonary arrest.

Plain CT scans reveal decrease density of cortical gray matter and increase density of subcortical white matter, causing reversal of the normal gray and white matter densities, some decrease amount of white matter is seen. Relative increase density of thalami, brainstem and cerebellum are observed. All ventricles are mildly dilated.

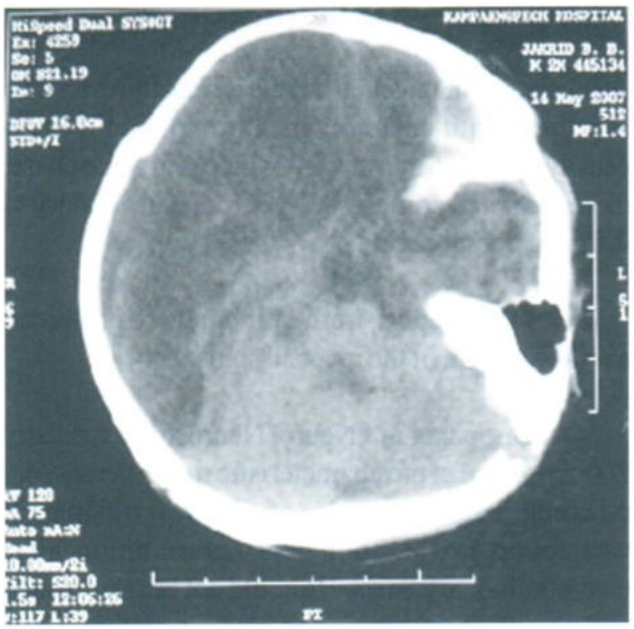

Fig. 2 A

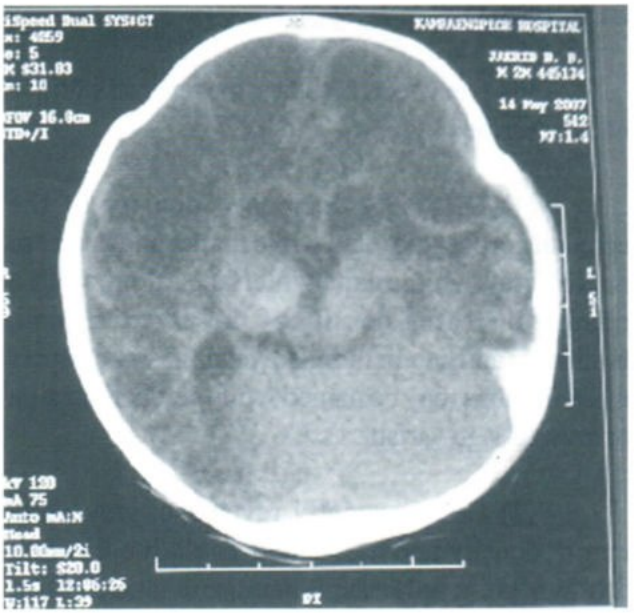

Fig. 2 B

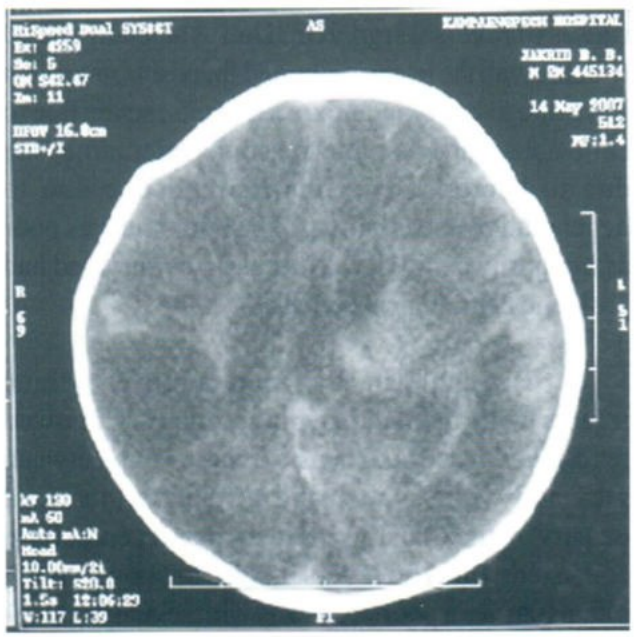

Fig. 2C

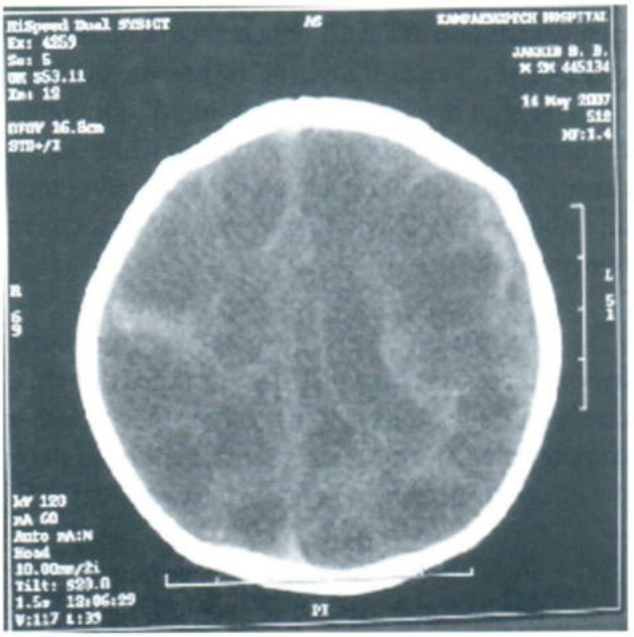

Fig. 2D

Fig.2 A-D Chronic reversal sign in 2 month-old child with previous history of fetal distress and severe birth asphyxia

Plain axial CT show generalized CSF like hypodensity throughout both cerebral hemisphere representing cystic encephalomalacia, increase density of subcortical white matter, reversal of normal gray white matter density. Markedly decreased volume of white matter and all ventricular dilatation are seen. Relative hyperdensity is seen in thalami, brain stem and cerebellum.

DISCUSSION

In several recent studies, the reversal sign has been described by;

(1) Diffusely decreased density of the cerebral cortical gray and white matter and decrease or lost gray white matter interface, along with a relative increased density of preserved thalami, brainstem and cerebellum, however in some papers these findings may be named white cerebellum sign or reversal sign variant.

(2) Less frequently, reversal of gray white matter density and associated a relative increase density of preserved thalami, brainstem and cerebellum, these findings may be named true reversal sign.

Some texts and literatures are confusing in their description of the CT appearance of theses two patterns of reversal sign. In some papers, the term reversal sign has been mainly limited to imaging findings of reversal of gray matter and white matter densities of the cerebral hemispheres, as mentioned on cathegory (2). CT findings of our two cases were true reversal signs.[12]

S. Moosa et al. presented two pediatric hypoxic cases, one of which demonstrated the white cerebellum sign, (reversal sign variant) and the other demonstrated the true reversal sign, in order to show the imaging differences between the two patterns.[12]

Actually, the reversal sign has been mainly seen as either an early sign or sequel of hypoxic ischemic insult, its recognition may be early or delayed. B. Kim Han et al. divided CT findings of reversal sign into three groups, including (1) acute within 24 hours at presentation, (2) intermediate, 2-22 days and (3) chronic reversal sign.[5]

In chronic reversal group, associated atrophic brain, atrophic ventricular enlargement and/or cystic encephalomalacia were detected and the attenuation of the cerebral mantle is visually lower than in patient with acute reversal group, and it has a density similar to that of CSF, whereas in acute phase, there are small compressed ventricles secondary to diffuse cerebral edema.

In our report, both of them were presented as chronic form of the reversal signs.

One paper in J Neurol Neurosurg Psychiatry 2000 reported acute characteristic true reversal sign on computed tomography of a 70 year old man; it was found just 1 hour post resuscitation after cardiopulmonary arrest. He could not be resuscitated and was declared brain dead, one hour later.[8]

By reviewed literatures, there are numerous causes of reversal sign. Kim Han et al. analyzed 20 children with the reversal sign and found that nine cases were due to hypoxia/anoxia incidents, seven due to child abuse, and two due to accidental trauma, one due to bacterial encephalitis and one due to degenerative encephalitis.[5] The outcome was poor as a majority expired, while those who survived had profound neurological deficits.[5]

H. Schulman et al. reported seven of nine infants with neonatal hypothermia, CT showed reversal of the normal density relationship between grey and white matter and a relative increased density of the thalami, brainstem and cerebellum consistent with the reversal sign. In six surviving infants carries a poor prognosis with severe developmental delay.[7]

We found that the reversal sign was seen mainly in cases of pediatric hypoxia but there are scattered reports describing in adult with severe anoxic ischemic injury. G. Vergote et al. reported a 36-year-old woman with bacterial meningitis. CT after resuscitation showed a striking reversal sign, it indicates serious brain damage and carries a poor

outcome.[15]

B. Nail et al. retrospectively examined the computed tomography of 9 adult patients in vegetative state due to prolonged anoxia, range of age 21-67 years and they thought that the reversal sign was a characteristic finding of the ischemic vegetative state of the adult brain.[6]

Cho Jey Min et al. evaluated prognosis -related CT findings in 28 children with a clinical history and CT findings suggestive of hypoxic ischemic encephalopathy (HIE). They found that the CT appearances including poor differentiation of gray and white matter, reversal sign, obliteration of perimesencephalic cistern, high density on tentorial edge indicate severe anoxic ischemic brain injury and carries a poor prognosis.[13] Because of CT findings showed distinct differences between groups in whom prognosis was good, and in whom it was poor. An awareness of poor prognostic, CT findings may be clinically helpful in the evaluation of patients with hypoxic ischemic cerebral injury.[13]

CONCLUSION

As a result, our study confirmed that the pattern of brain injury from prolonged hypoxic ischemic insult in neonates differed from that seen in children after the neonatal period.

The reversal sign is a classic uncommon characteristic radiological finding, secondary to hypoxic ischemic cerebral injury and can occur in any age.

The reversal sign has been mainly seen as either an early sign or sequel of hypoxic ischemic insult, dividing into acute, intermediate and chronic reversal signs.

There are numerous causes of the reversal sign, including (1) severe hypoxia particularly birth asphyxia, cardiac arrest, drowning, status epilepticus (2) trauma such as abused child, less frequently accidental injury (3) infection especially meningitis and degenerative encephalitis (4) others such as electrocution, smoke inhalation and neonatal hypothermia.

Reversal sign usually represents severe hypoxic ischemic brain injury, also indicates irreversible devastating brain damage and carries a poor prognosis. The prognosis and outcome for reversal sign were poor as a majority expired, while those who survived had profound neurological deficit and permanent impairment.

An awareness of poor outcome, CT is the most useful modality and has been use as the primary imaging method to evaluate the prognosis of patient with anoxic ischemic cerebral injury.

ACKNOWLEDGEMENT

The author acknowledges Dr. Kamchai Rangsimunpaiboon, the chief of Kamphaengphet provincial Hospital, for his supports, and also acknowledges pediatric attending clinicians who gave me the patient details and useful comments.

The author would like to thank Mrs. Jiraporn Maneeprai for her help with this project about reference papers, patient's profiles and manuscript preparation.

REFERENCES

1. Leon Weisberg, Charles Nice. Cerebral computed Tomography: Cerebral Anoxi and Brain Death. A Text Atlas, 3rd Edn, 1989 : 272-273
2. R.G. Grainger, D.J. Allison, A. Adam, A.K. Dixon. Diagnostic Radiology A Textbook of Medical Imaging, Fourth Edn,Chapter Elsevir; 2001. p. 2472.
3. S. Haward Lee, Krishna C.V.G. Rao, Robert A. Zimmerman. Atrophy secondary to anoxia. Cranial MRI and CT, third Edn, 1992: 277-281.

4. Osborn AG. Craniocerebral Trauma: In Osborn AG (editor) Diagnostic Neuroradiology, 1st Edn, Chapter: Elsevier; 1994. p. 199- 247.
5. Han BK, Towbin RB, De Courten-Myers G, McLaurin RL, Ball WS Jr. Reversal sign in CT: Effect of Anoxia / Ischemic cerebral injury in children. AJR 1990; Feb 154:361-8.
6. B. Nail, P. Yuksel, K.H. Kermal, T. Cem. T. Mustafa, U. Taner. Result of Acute Cerebral Anoxia in Adults: is it a reversal sign. Turk J Med Sci 2000; 571-577.
7. H. Schulman, L. Laufer, Julia Berginer, E. Hershkowitz, Tamar Berenstein, Shaul Sofer, Esther Maor, Yancu Hertzanu. CT findings in neonatal hypothermia. Peadiatric Radiology 1998; June 28; 6: 414-417
8. Reversal sign after cardiopulmonary arrest. J Neuron Neurosurg Psychiatry 2000; April 68: 525
9. Cohen RA, Kaufman RA,Myers PA, Towbin RB. Cranial Computed Tomography in the Abused Child with Head Injury. AJNR 1985; 6: 883-8
10. Dwarakanath S, Bansal A, Rudrappa S, Gopal S, Venkataramana NK. White cerebellum sign-A case report and review of literature. Journal of Peadiatric Neurosciences 2006; 1: 322-23.
11. A.-C. Duhaime, C. W. Christian, L. B. Rorke, and R. A. Zimmerman Nonaccidental Head Injury in Infants -- The "Shaken-Baby Syndrome" N. Engl. J. Med., June 18, 1998; 338(25): 1822-1829.
12. S. Moosa, S. Andronikou. Case Report: Hypoxic-ischaemic injury-the 'white cerebellum sign' versus the true 'reversal sign. South African Journal of Radiology Vol.9(1) 2005: 32-33
13. Cho Jay Min, Kim OH, Kang DK, Suh JH, Il YB. Hypoxic Ischemic Encephalopathy in Children: CT Findings Related to Prognosis. J Korean Radiol Soc. 1997 Jul; 37(1):167 -172. Korean.
14. (2006) Medcyclopaedia. Pediatric imaging: Reversal sign. GE healthcare Medical diagnosis. Medcyclopaedia.com.
15. G. Vergote, H. Vandeperre and R. de Man. The reversal sign. Neuroradiology 1992 ; 34: 215-216

ULTRASOUND OF FOREIGN BODY (PADDY) IN VAGINA OF A GIRL OF 2 YEARS.

Dr. M. A. Taher,[1]

A girl 2 years of age, jumped on a stack of paddy and started crying due to accidental insertion of paddy into her vagina. Her mother tried to pull it out by her finger, but it did not come out, rather impacted further upwards. Abdominal ultrasound could locate the paddy through the full urinary bladder (Fig. 1). It was pulled out in the hospital under general anesthesia (GA), to avoid the risk of sloughing by the sharp corners of the paddy resulting in vesicovaginal fistula (VVF).

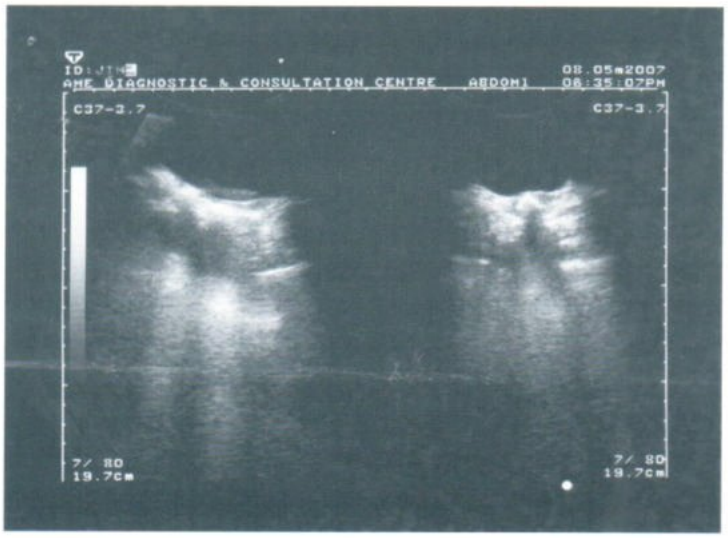

Fig. 1 Paddy Vagina

[1] Director, Centre for Nuclear Medicine & Ultrasound, Rangpur, Bangladesh

PELVIC KIDNEY CALCULI MIMICKING APPENDICITIS: A CASE REPORT

Dr. Shakila Zaman Rima,[1]
Dr. Muhammad Abu Taher[2]

INTRODUCTION

Congenital anomalies were the 7th leading cause of disability over the world in 1990, numbering 13.5 millions (2.9% of total disability) and 9th leading cause of disease burden over developing world in 1990 numbering 29.4 millions (2.4% of total disease). But however, the incidence of major congenital urinary tract anomalies has been reported as 0.14%, minor asymptomatic anomalies may occur in 10% of all life-birth.[1] Ectopia, or displacement, of a kidney is a common renal anomaly. The pelvic kidney, in which, cephalad "migration" of the kidney does not occur, is the simplest form of renal ectopy.[2]

CASE REPORT

A young unmarried female, 16yrs. Old came to CNMU Rangpur, with the complains of lower abdominal pain of 3 days. According to her statement, she suffered same type of lower abdominal pain for 3 times in the last 1 yr. Some of the physicians suspected it as acute appendicitis. This time her physician asked for ultrasonography (USG) of KUB region. USG reveals normal right kidney, but left kidney is not seen in the normal position, but found in lower abdomen in midline near the urinary bladder. There are multiple tiny bright calculi seen (Fig. 1) in the pelvic kidney with mild pelvicalyceal dilatation. We advised the patient for DMSA-Scan, but unfortunately the patient did not come.

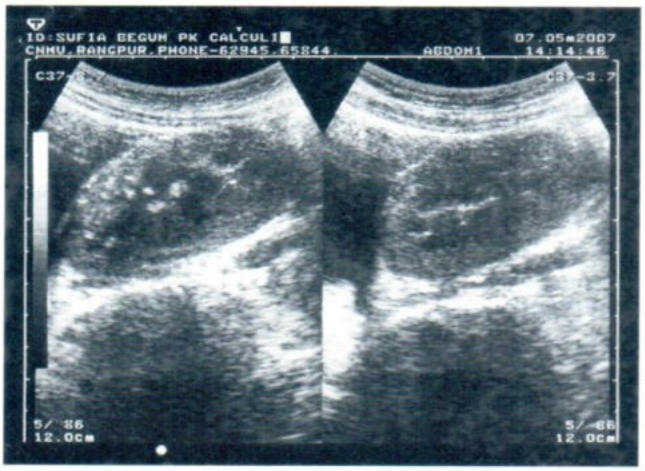

Fig. 1 Tiny calculi in pelvic kidney seen in ultrasound scan

CNMU = Centre for Nuclear Medicine & Ultrasound, Rangpur 5400, Bangladesh.

[1] Medical Officer,
[2] CMO & Director, Centre for Nuclear Medicine & Ultrasound, Box 16 Rangpur-5400, Bangladesh.

DISCUSSION

The initial stages of kidney development occur within the fetal pelvis. Through the process of differential growth, the developing kidneys ascend into the abdomen and eventually achieve their adult location, at the approximate level of the first lumber vertebra. Except for being displaced, most pelvic kidneys are normal developmentally, and these normal kidneys are easily recognised with ultrasound.

In this congenital random anomaly, the kidney remains, in on the proper side of the body, but is positioned lower than normal, either in the iliac fossa or in the pelvis. The displaced kidney may be asymptomatic and detected incidentally by physical examination during an imaging procedure. Occasionally, however, a pelvic kidney is grossly abnormal in appearance, because it is affected by dysplasia, duplication anomalies, vesico-ureteral reflux, and/or hydronephrosis. These abnormal kidneys are easily mistaken for cystic of solid masses or abnormal segments of bowel. Diagnostic error may be avoided of the ipsilateral renal fossa is examined routinely in patients with pelvic, pathology. The empty renal fossa should be a significant clue as to the nature of the pelvic mass.[2] Ectopic kidneys, for example, pelvic kidney can usually be more easily identified and investigated by radiopharmaceutical as a whole body search can be undertaken if necessary, whereas a small pelvic kidney, especially if it is poorly functioning, can not always be seen against the background of the pelvic bone.[3]

In 1970.s two excellent renal agents DTPA (diethylene triamine penta acetic acid) and DMSA (dimarcepto succinic acid) have been developed.[4] To detect a missing kidney DMSA is better than DTPA as DMSA is bound to the cortex and only a smaller fraction is excreted into the urine. Even if there is a small amount of renal tissue, it will concentrate the agent and will show the presence of a kidney wherever located. The principal advantage of DMSA is its relatively prolonged and stable retention in the kidney.[4] DTPA is a glomerular agent and shows both anatomical and functional status of kidney.[3] Nahar et al. reported a case of ectopic functioning left kidney which was missed by both USG and intravenous urography (IVU), but both DMAS and DTPA radionuclide techniques ware successful in detecting the kidney.

REFERENCES

1. Taher MA. Urogenital anomalies: case reports. Bangladesh J Nucl Med 1999; 2(2): 38-41
2. Zwiebel WJ. Normal variants and developmental anomalies of the urinary tract. In Zwiebel WJ, Sohaey (eds.) : Introduction to Ultrasound 1998 W. B. Saunders Company, Philadelphia.
3. Britton KE, Maisey MN, Hilson AJW. Renal radionuclide studies. In Maisey MN. Brittion KE, Gilday DL. (eds.): clinical Medicine. 1983, Chapmen and Hall, London.
4. Nahar N, Hasan M, Alam F, Haque M, Islam N. Superiority of radionuclide technique over IVU in the diagnosis of missing kidney-a case report. Bangladesh J Nucl Med 1999; 2(1): 19-21

CHOLEDOCHAL CYST: A CASE REPORT

Dr.Shakila Zaman Rima,[1]
Dr. M. A. Taher[2]

INTRODUCTION

Choledochal Cyst may be defined as a rare congenital dilatation of the common bile duct that is associated not infrequently with a congenital or acquired dilatation of the intrahepatic ducts. The condition predisposes to cholangitis, gallstones and carcinma, as well as to jaundice and portal hypertention. Without surgical treatment, it is universally fatal.[1]

CASE REPORT

A boy 3 yrs of age came to CNMU Rangpur, with the complaints of intermittent jaundice & upper abdominal pain. According to his parent's statement he was suffering from this problem for the last 1 year. Ultrasonographyt (USG) reveals cysic dilatation of the common bile duct (choledochal cyst) with non-dilated intrahepatic ducts (Fig-1). Then isotope scan of the hepatobiliary system was done in this centre. Which revealed choledchal chst with poor hepatobiliary excretion (Fig-2).

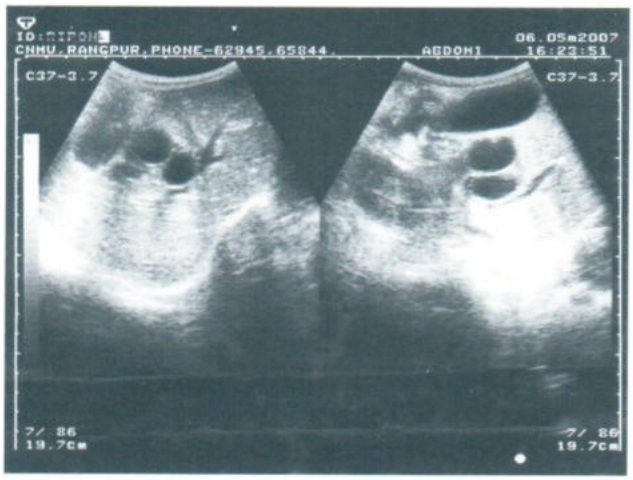

Fig. 1 Ultrasonography of the cystic lesion in upper abdomen.

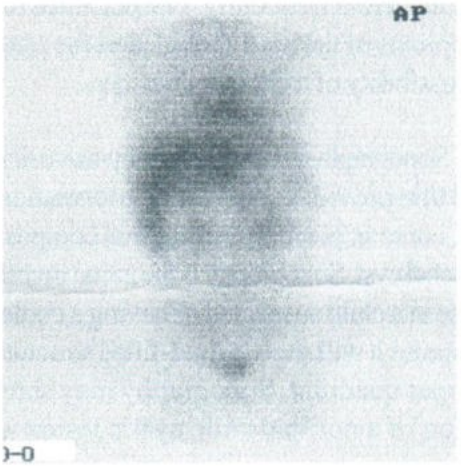

Fig. 2 Isotope scan of hepatobiliary system of the same patient showing choledochal cyst.

DISCUSSION

Choledochal cysts can be divided into four types-type-1, the most common form, consists of a fusiform dilatation of the common bile duct; type-2, the next common, consists of an eccentric diverticulum of the common bile duct; type-3, Choledococele and type-4, Caroli discase are very rare and are probably of different etiology.

[1] Medical Officer,
[2] CMO & Director, Centre for Nuclear Medicine & Ultrasound, Box 16 Rangpur-5400, Bangladesh.

The incidence of choledochal cysts in females is four to five time greater than it is in males. Most cases of choledochal cysts present in childern less than 10 yrs. Old ; 30 percent, in infants under 1 year of age, a further 50 percent in children under 10 years of age, and most of the others in chidren between 10 and 16 yrs. of age.[2] Rarely, choledochal cyst is seen in fetal abdomen as early as 19 weeks of gestational age.[3]

The classic triad of episodic abdominal pain, jaundice, and a palpable right-sided abdominal mass may occur in 17 to 25 percent of patients, but some have found it less frequently. The persence of any of the symptoms of the triad should alert the physicians to the possibility of a choledochal cyst.

Sonography is a simple, noninvasive diagnostic method that provides substantial information about the size, contour, position and internal composition of choledochal cyst. Sonography is the intital investigation of choice in a child suspected of having a choledochal cyst, because it will show a fluid-filled structure in the right upper quadrant. Sonography may show deep extension of a non-pulsatile cystic lesion into the porta-hepatis with apparent separation of the right and left lobes of the liver. This finding is the most specific for large & small choledochal cysts.[2]

Hepatobiliary scintigraphy with 99^m technetium iminodiacetic acid (IDA) provides good images and is considered by some to be the investigation of choice. An initial filling defect in the liver followed by a gradual increase in the concentraiton of radioactivity in the cyst on serial scans is pathognomonic. Scintigaphy is also useful for demonstrating the patency of bile duct-bowel anastomosis after surgery.[1]

REFERENCES

1. Tan K.C. and Howard E.R., Congenital cysic dilatation of the biliary, In Wilkins R.A. & Nunnerley H.B. (eds.), Imaging of the liver, pancereas and spllen. Blackwell, London, 1990.
2. Stringer D. A., Pediatric gastro-intestinal imaging. Decker Inc. B. C. Philadelphia 1989.
3. Metreweli C., Obstetric imaging. In Pettersson H (ed.) A Global Textbook of Radiology 1995, Oslo.

ABDOMINAL MESENTERIC CYSTIC LYMPHANGIOMA, A CASE REPORT WITH REVISION OF LITERATURES.

Chanya CHAISIRAT M.D.[1]

ABSTRACT

Abdominal mesenteric cystic lymphangioma is a rare congenital benign tumor, that can be misdiagnosed with others cystic intra-abdominal tumors. The etiology is thought to be related with the congenital malformation of lymphatics.

We presented a case of a 4 year old male child with a cystic lymphangioma, arising from lymphatics of small bowel in the mesentery and occupying nearly the entire abdominal cavity. Focal bulging of anterior abdominal wall was observed. Plain film and computed tomography confirmed the intrabdominal septated cystic tumor. Radical surgical treatment was done, according to international guide-lines. The cystic tumor, attached mesentery and 45 cm. in length of the engulfed small intestine were completely excised and then primary end to end anastomosis was done. Histological diagnosis was chylous cystic mesenteric lymphangioma. The patient had an uneventful post operative course and had no evidence of recent post operative complication. No early relapse was recorded.

INTRODUCTION

Lymphangiomas are benign congenital lymphatic malformations with a proliferation of dilated lymphatic spaces lined by thin attenuated endothelial cells. They are frequently found in children, and comprised 5.6% of all benign lesions of infancy and childhood.1 The acquired form may be detected in middle aged adults. They have no predilection for either sex or any race.[1]

Lymphangioma has been classified into three groups: (1) lymphangioma simplex; (2) cavernous lymphangioma; and (3) cystic lymphangioma.

Cystic lymphangioma is an uncommon congenital benign neoplasm, which can occur throughout the body, but are most common in the neck of children and are called cystic hygroma. They usually appears in the axillary region, and rarely occur in the mediastinum. The remainders are found in the omentum, mesentery, retroperitoneum and bone.

Intraabdominal lymphangiomas are rare. Most of them are known to be cystic lymphangioma in pathology. The majorities are presented in patients younger than 5 years of age, but occasionally these tumors do not produce symptoms until adult life. Within the abdomen, the most common site for lymphangioma is the bowel mesentery, following by omentum, mesocolon and retroperitoneum.

The clinical symptoms of mesenteric lymphangioma seem to be related with the size and site of tumor, including an abdominal mass or an acute abdomen. Usually, the cases are asymptomatic but may present with acute or chronic intestinal obstruction.

[1] Department of radiology, Kamphaengphet Hospital, Kamphaengphet 62000, Thailand

Most common complications are volvulus, intestinal obstruction, infarction, perforation, and hemorrhage.

The diagnosis of abdominal mesenteric lymphangioma can be made by multiple radiologic studies, including plain radiograph, ultrasonography, MRI and arteriography.

The aim of our study was to show the rarely huge chylous type, mesenteric cystic lymphangioma, which found in children who had presenting symptom as abdominal pain, increasing abdominal girth, abdominal distension and chronic intermittent intestinal obstruction.

CASE REPORT

On February 02, 2007, a 4 year old boy first presented to our hospital with chronic abdominal fullness, vague abdominal pain and nonbilious vomiting. He had been healthy until then with an unremarkable medical and surgical history. The initial clinical diagnosis at the first presentation was acute gastritis.

Next over 4 months later, on June 26, 2007, he came back to our emergency services again with a history of nonbilious vomiting of increasing frequency, increase abdominal girth, progressive abdominal distension and acute abdominal pain. On examination, the patient was in stable condition, but a small right abdominal movable mass was palpated with firm consistency. It was painful on palpation. He had mild tenderness in the right lower abdominal region. There was no hepatomegaly, splenomegaly or clinical lymphadenopathy. Auscultation of the abdomen revealed normal bowel sounds. Laboratory data were within normal limits.

Preoperative radiographic studies were performed, including plain radiograph and computed tomography (CT). The plain abdominal radiograph (Figure 1) showed a large radiopaque right abdominal soft tissue mass with mass effect to the nearby structures and displacement of bowel loops.

An abdominal CT (Figure 2 A-D) confirmed a large thin walled, bilobed cystic mass and few internal septations which producing multiloculated cysts. It occupied nearly the entire abdomen, right side predominance. The mass extended from the level of left subhepatic region to the pelvic cavity, just above the bladder. The mass caused pressure effect to the intraabdominal structures, strikinly compressed and stretched the adjacent bowel loops. There is no complicated hemorrhage, volvulus or leakage.

Notably, some dilated gastric cavity caused mass effect to the gastric outlet, seen in both plain radiograph and CT. In conjunction with clinical nonbilious vomiting, so partial gastric outlet obstruction should be considered.

Due to progressive worsening and increasing frequency of vomiting, the child was underwent standard preoperative preparation for a laparotomy. This included inserting a nasogastric tube, retained Foley's catheter, initiating intravenous fluid therapy, and starting prophylactic antibiotics. Then patient was taken to the operating room and an urgency surgical treatment was performed, 2 days after admission on June 28, 2007.

The provisional diagnosis was intrabdominal cystic mass with partial gut obstruction. Cystic teratoma, lymphangioma, omental / mesenteric cyst, duplication cyst, pseudocyst, loculated ascites were listed in the differential diagnosis.

At operation, midline vertical incision was done. After opening the peritoneum, the cyst was seen popping out of the abdominal incision (Figure 3). A giant gray-yellowish spongy mutiloculated cystic tumor and relative soft consistency within the root of small bowel mesentery was exposed. It occupied the majority of abdominal cavity. In order to mobilize the tumor, it was necessary to extend the incision cavity

in both directions. It was then noticed that the tumor was apparently involved the adjacent small bowel and infiltrated its mesentery. The rest of bowel and other abdominal structures appeared normal; there was no any dilatation, ischemia or inflammatory change of the intestine and mesentery.

Due to part of small intestine plastered the lateral border of the mass, in a way that the mass could not be enucleated. Extensive resection of the mass, including the mesentery and the part of the engulf small intestine was done. Therefore about 22-23 cm. long segment of gut on either sides of the tumor were radically resected with the mass and then a primary end to end anastomosis was done. With careful dissection of the mesenteric arteries, the tumor was removed completely with accompanying adjacent small bowel and mesenteric resection. No ascites was seen in the peritoneal cavity.

Post operative details, he was maintained NPO with intravenous fluids and nasogastric suction until bowel function returns. Prophylactic antibiotics can be discontinued after 7 postoperative days. He had an uneventful post operative course, and had no evidence of recent post operative complication.

The patient was discharged at the 9th postoperative day. He was followed up 2-3 weeks after being discharged from the hospital and found out to have no problem. At the present time, 2 months after operation the patient is healthy, his condition is normal.

The mass with the attached small intestine was sent to the pathology department for evaluation.

The gross specimen consisted of a large lobulated gray-yellowish multicystic mass in the small bowel mesentery with soft consistency, measured approximately 20 x 20 x 17 cm., contiguous long segment of small intestine plastered to its surfaces about 22-23 cm. of each sided (Figure 4). Serial sections show numerous small and large cysts which were filled with turbid and milky odorless fluid soluble (chylous cysts).

Microscopic description shows numerous dilated lymphatic channels with varying in sizes within loose fibroconnective tissue and a few disorganized bundles of smooth muscle presented in the wall of the larger channels, these findings were consistent with cystic lymphangioma.

Finally, the diagnosis was mesenteric chylous cyst, histologically cystic mesenteric lymphangioma.

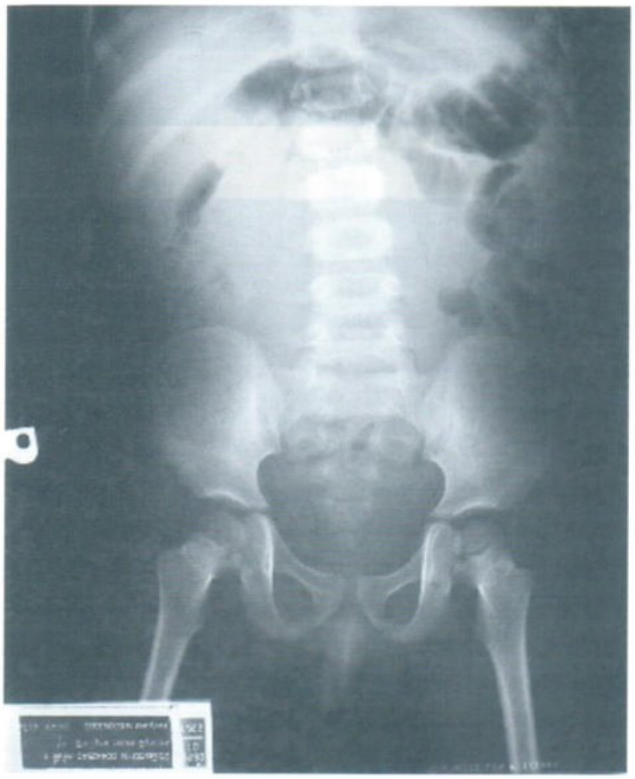

Fig.1 Supine radiographs of the abdomen show a soft-tissue mass within the right hemiabdomen that displacement of bowel loops, upward and laterally. Some dilated stomach and transverse colon due to mass effect.

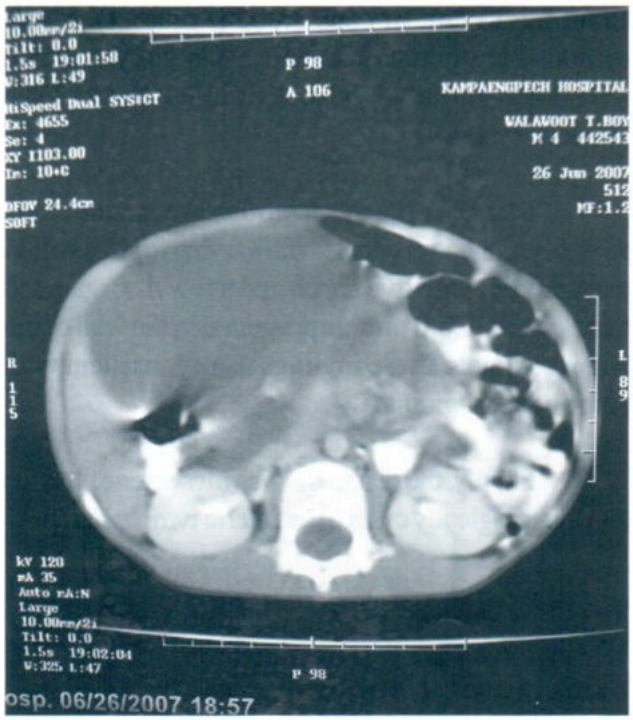

Fig.2A

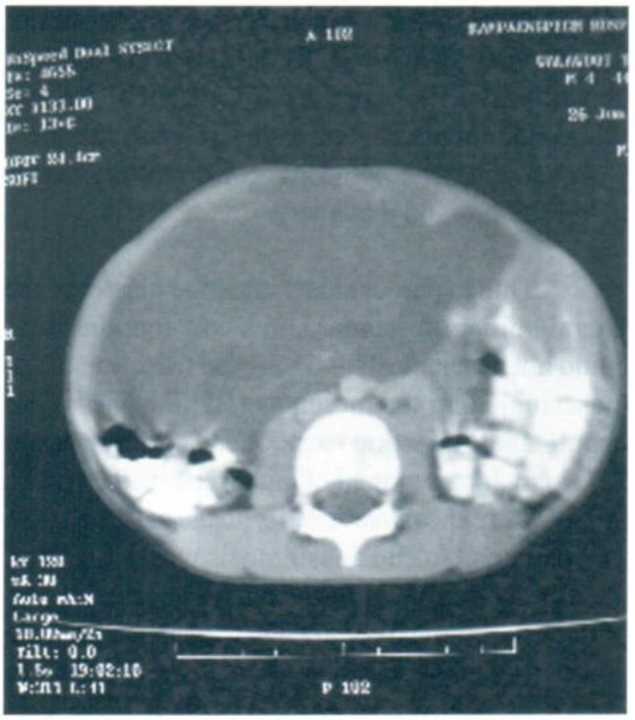

Fig.2B

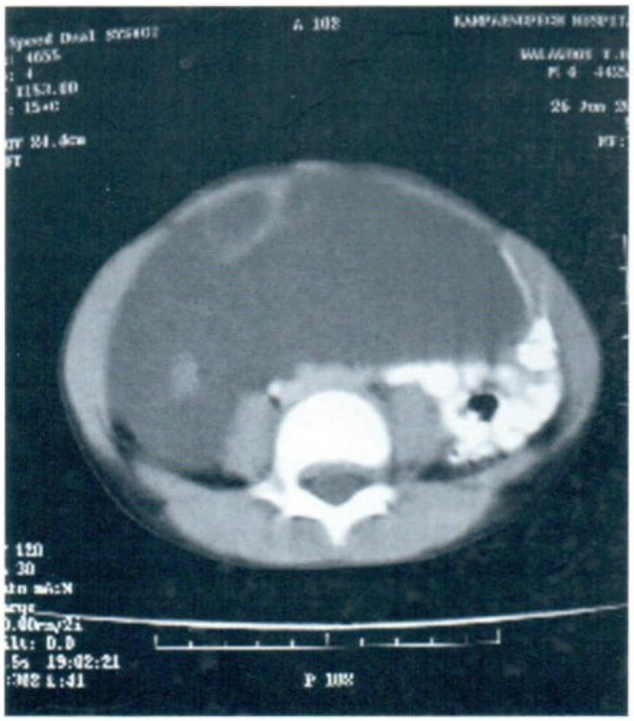

Fig.2C

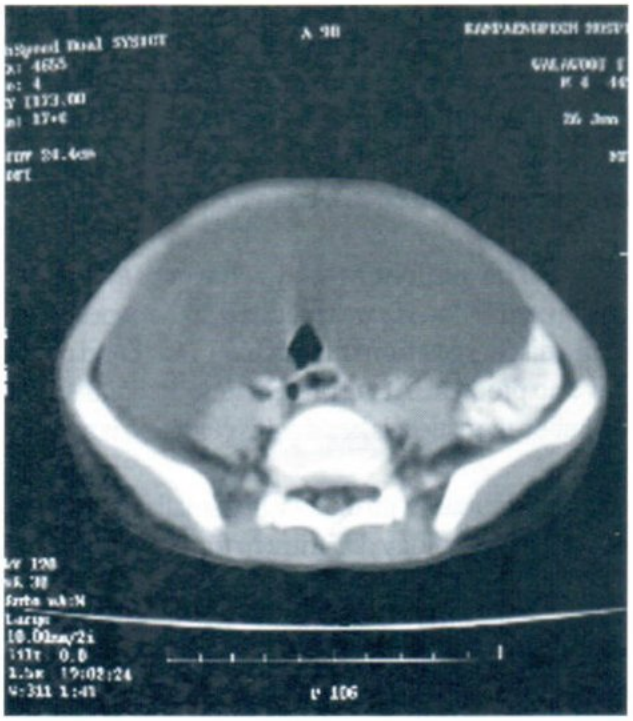

Fig.2D

Fig.2A-D CT images obtained with intravenously administered contrast material show huge bilobed nonenhancing cystic mass occupying nearly entired abdomen and pelvic cavity, with associated thin wall, well encapsulation, and poor enhancing faint internal septations.

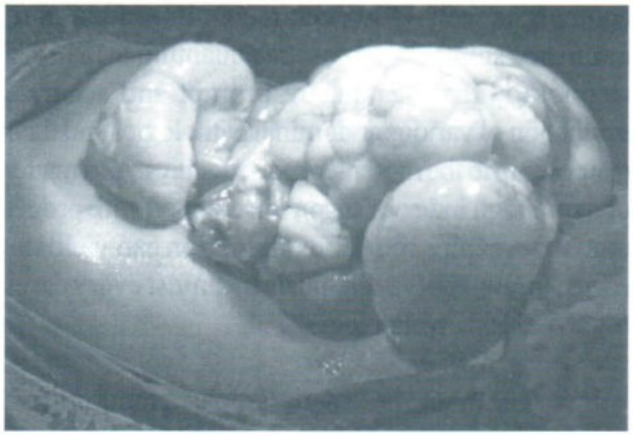

Fig.3 Operative photograph shows bunches of lymphangioma in the mesentery of small bowel, which was seen popping out of abdominal incision.

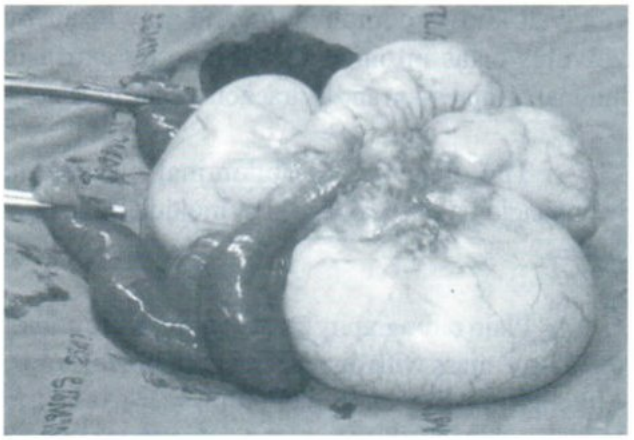

Fig.4 Photograph of the gross specimen shows that the cyst is multiloculated with a long segment of small intestine plastered to its surface. There is no communication between the intestine and the cyst. This picture of mass shows good correlation with CT appearances.

DISCUSSION

Lymphangioma has been classified into three groups: (1) lymphangioma simplex; (2) cavernous lymphangioma; and (3) most frequency, cystic lymphangioma, or cystic hygroma.

Histologically, a lymphangioma can be well circumscribed lesion composed of one or multiple large cysts which can interconnect. These are typically called cavernous lymphangioma. A lymphangioma can also be composed of microscopic cysts, producing an ill defined, compressible, spongelike lesion, known as a cystic lymphangioma. The walls of lymphatic spaces are thin and contain fibrous tissue, smooth muscles and aggregates lymphoid tissue. The lymphatic spaces and channels are lined by one row of the flat endothelial cells. There is no discrete capsule. In the small bowel mesentery, the spaces may be filled with chyle and are called chylous lymphangioma or may be occasionally filled with hemorrhage.

Intrabdominal cystic lymphangioma of the mesentery is a rare congenital lesion with a relative low growth potential. It typically found in young adult and present with chronic features.10 In younger children as in our patient, the lymphatic malformations usually are aggressive with rapid growth. Actually mesenteric cystic lymphangioma is a rare cause of bowel obstruction and preoperative diagnosis is difficult due to silent clinical course.

Most common presenting symptoms are abdominal distention with a palpable mass, followed by abdominal pain. However, the lesion may not be palpable due to its flaccid and mobile nature. Symptoms were presented in all patients including abdominal pain, bilious or nonbilious vomiting and diarrhea.

Our reported case was a chylous cystic mesenteric lymphangoma in a young child which presented as a diagnostic dilemma. Our patient's symptoms include abdominal distention, palpable mass and small bowel obstruction.

Complications are volvulus, intestinal obstruction, infarction, perforation and intracystic hemorrhage. Perforation and hemorrhage may be spontaneous and may be caused by trauma or minor trauma. Partial or complete small-bowel obstruction

is a well known complication and may occur by volvulus or as in our reported case by extrinsic luminal compression and by traction on the mesentery.

The diagnosis of abdominal mesenteric lymphangioma can be deduced by multiple radiologic studies.

Plain radiography most commonly reveals a soft-tissue mass with displacement of bowel loops. Although not diagnostic, plain films help to identify complications such as bowel displacement and/or intestinal obstruction.

The typical US appearance is a large well -circumscribed anechoic cystic or multicystic mass, often with thin wall, multiple thin septations and posterior acoustic enhancement. They also showed variable internal echogenicity, which is accounted for by the various contents that are possible. Occasionally, some solid echogenicity with a honeycomb pattern have also been described. However, the exact origin of the mass may not be ascertained on ultrasonography.

The CT findings demonstrated multiloculated or bilobed fluid-filled masses. The attenuation of the fluid ranged from that of fluid to that of fat, again according to the different content. Lymphangiomas have also been characterized as being well defined with a thin wall and occasionally with septa. The mass usually show no enhancement on IV contrast administration, but the thin septae inside the mass may enhanced faintly. The lesion may be distinguished from ascites by the absence of bowel loop separation or fluid in the typical sites, such as the cul-de-sac, or the presence of focal septa.

The magnetic resonance (MR) imaging can also be used to demonstrate the relationship of the mass and surrounding structures. Actually MR has been considered superior to CT in determining both the exact origin of a cyst and in assessing its exact extent due to the ability of viewing the lesion in multiple planes. MR helps in characterizing its contents as well. However, recent introduction of multislice spiral CT represent a quantum leap in CT technology that has ensure prompt and accurate evaluation of various abdominal pathologies and their relationship to the mesenteric vasculatures. As a matter of fact, a high index of suspicion coupled with proper ultrasonography and CT examination can yield the correct preoperative diagnosis in almost every cases using multislice technology.

The cystic mesenteric lymphangioma is a rare benign tumor and its diagnosis should be included in the differential diagnosis of cystic intra-abdominal neoplasias. The most common type of mesenteric or omental cystic tumor is the lymphangioma, followed by a nonpancreatic pseudocyst, duplication cyst, mesothelial cyst, and enteric cyst. The differential diagnosis includes the other histologic types of mesenteric and omental cysts mentioned earlier, and there are no specific radiologic features. Another consideration is a cystic leiomyoma or leiomyosarcoma, and again differentiation requires histologic evaluation. A cystic teratoma should also be included, but one would expect fat content with one or more clusters of calcifications. Nevertheless, a mesenteric lymphangioma with peripherally calcified caseous material has been documented. Mesotheliomas may also appear cystic, thus requiring a histologic diagnosis, but these usually occur in middle-aged women.

Due to the tumor's location, as in the our patient, the surgeon should plan the appropriate surgery as to avoid morbidity, since the objective of such treatment is curative. The goal of surgical therapy is complete excision of the mass. Mesenteric cystic lymphangioma can be removed without endangering the adjacent bowel. The preferred treatment of benign well encapsulated mesenteric lyphangioma is (1) first option, enucleation, although intestinal resection is frequently required to ensure that the remaining bowel is viable. (2) Second option, involved mesentery and bowel resection may be required in cases of infiltrative lymphangioma. Any resulting mesenteric defect must be closed to prevent an

internal hernia. If enucleation or resection is not possible because of the size of the cyst or because of its location deep within the root of the mesentery, (3) the third option is partial excision with marsupialization of the remaining cyst into the abdominal cavity. Approximately 10% of patients require this form of therapy. If marsupialization is performed, the cyst lining should be sclerosed with 10% glucose solution, electrocautery or tincture of iodine to minimize recurrence. Partial excision alone with or without drainage is not indicated because of the high recurrence rate associated with this procedure.[11] Lymphangioma has an unsatisfactory therapeutic outcome due to its invasive nature.

Other modalities of treatment for unresectable intrabdominal lymphangioma include sclerotherapy with doxycicline, alcohol, bleomycin, Picibanil (OK -432). More recently, new attempts to sclerose these lesions, scerotherapy is now being performed with increasing frequency, and have met with more success than in the past.[6,8]

In our patient, a small-bowel loop engulfed to the mesenteric lymphangioma and had to be excised with the the mass lesion (second option). After surgery, our patient was alright and well-tolerated, and he was discharged without complications or further incidents.

CONCLUSION

In conclusion, mesenteric cystic lymphangioma is a rare congenital benign tumor. The most common presenting symptoms are abdominal pain, abdominal distension, palpable mass, followed by intestinal obstruction and increasing abdominal girth.

Although mesenteric lymphangiomas are rare tumor, they should be considered as a possible cause of acute abdomen especially in children.

Mesenteric cysts must be considered when evaluating children with abdominal pain and mass, associated clinical findings of small-bowel obstruction should prompt suspicion of complicated midgut volvulus.

Cystic teratoma, cavernous hemangioma, pancreatic/nonpancreatic pseudocyst, duplication cyst, mesothelial cyst, mesenteric cyst and enteric cyst, all should be kept in mind in the differential diagnosis of mesenteric cystic lymphagioma.

We thought that proper abdominal ultrasonography complemented by multislice spiral CT can yield the correct preoperative diagnosis in almost every case, but histological examination will confirm the diagnosis.

Complete resection is the treatment of choice and has an excellent prognosis. Although an abdominal lymphangioma is considered benign, it may become locally invasive. Therefore any involved organ must also be resected. Incomplete resection may lead to recurrence. Hence, a rapid and accurate preoperative localization of the lesion is critical and important for facilitating proper management.

Follow-up imaging, therefore, is advised, with ultrasound as the modality of choice.[12]

The effectiveness of radical surgical excision is higher than that of sclerosing therapy, but the risk of complication with surgery was greater, may be three times in paper of Hiki Saori et al.[6,8]

As tumor was diffuse, total excision may require resection of involved abdominal organ and bowel to prevent recurrence.

Early recognition and appropriate treatment of these lesions are associated with a good outcome, provided that, if the tumor is completely excised, a good prognosis could be archived.

Although the lesions tend to surrounds and sometime invades normal anatomic structures it

presumably have no malignant potential, but it has been described in few literatures that malignant degeneration is usually to a low-grade sarcoma, but this very rarely occurs.

ACKNOWLEDGEMENT

I would like to thank Mrs. Jiraporn Maneeprai for her help with this project about reference papers, patient's profiles and manuscript preparation.

REFERENCES

1. Peter M. Som, Hugh D. Curtin. Congenital Malformations of the cervical lymphatic system. Head and Neck Imaging 4th Edn. 2002: 1847 -1852
2. Eric M. Chand, Timothy W. McNeely, Lawrence J. Freant. Pathologic Quiz Case: Mail with increasing abdominal girth. Collage of Americal Pathologist. Archives of Pathology and Labatory Medicine 2000; 124(11): 1723 -1724
3. Colin R. Mar, MD, Chitra Pushpanathan, MD, David Price, MD and Benvon Cramer, MD. Omental Lymphangioma with Small-Bowel Volvulus. Radiographics. RSNA 2003; 23: 847-851
4. Chen CW, Hsu SD, Lin CH, Cheng MF, Yu JC. Cystic lymphangioma of the jejunal mesentery in an adult, a case report. World J Gastroenteral 2005; 11(32): 5084-5086
5. Yoshikawa Yoshinobu et al. A case of adult mesenteric chylous cyst with volvulus. Japanese Journal of Gastroenterological Surgery 2004; 37(8): 1475-1479
6. Hiki Satori et al. Treatment of lymphangioma in children: a report of 105 cases. Juntendo Medical Journal 2003; 48(4): 476-483
7. Jain S, Upreti L, Bhargava SK, Gupta R, Gupta PK. Mesenteric lyphangioma: diagnosis by multislices spiral CT. Indian J Radol Imaging 2002; 12: 580-582
8. Kang PS, Jung PM. Clinical Manifestation and Treatment of Lymphangioma in Children: a Review of 117 cases. J Korean Assoc Pediatr Surg 2002; 8(2): 95-100
9. Kim SY, Park HJ, Choi SW, Lee SI, Kim KW, Choi SH. A case of lymphangioma in the jejunal mesentery preoperatively diagnosed by lipoprotein electrophoresis. Korean J Med 2003; 64(1) 101-104
10. Lt Col R Handa,Col R Kale, Lt Col MM Karjai, Col V dutta. Intrabdominal lymphangioma: A Case Report. MJAFI 2007 63: 80-81
11. Amulya K saxena. Mesenteric and Omental cysts. eMedline from WEbMD 2006: eMedline > specialists > Pediatrics > General Surgery
12. Hakan Uncu, Erhan Erdem, Ercument Kuterdem. Lymphangioma of the ileum: A report of two cases and a review of the literature. Journal surgery Today 1007 27(6) 542-545
13. Moni Stein et al. Alcohol Ablation of a Mesenteric lymphangioma. AJNR 2000; 11: 247-250
14. Erkan Y, Koray D, Tevfix K, Unal S. Cystic lymphangioma: report of two atypical cases. CardioVasc Thrac Surg 2004; 3: 63-65
15. De Perrot M, Rostan O, Morel P, Le Coultre C. Abdominal lymphangioma in adult and children. Br J Surg 1998; 85(3): 395
16. Merrot T et al. Abdominal cystic lymphagioma in children. Clinical and therapeutic aspect: apropos of 21 cases. Ann Chir 1999; 53(6) : 494-499
17. Prashant N Monhite et al. A huge Omental Lymphangioma with extension into Labia Majorae: A case report. MNC Surgery 2006; 6(18) 1471-1482

MANAGEMENT OF HEPATOCELLULAR CARCINOMA USING RADIONUCLIDE METHODS WITH SPECIAL EMPHASIS ON TRANSARTERIAL RADIOCONJUGATE THERAPY AND INTERNAL DOSIMETRY IN THAILAND

Krisdee PRABHASAVAT,[1] Sathaporn MANASATID,[1] Pawana PUSUWAN,[1] Sathaporn MANASATID,[2] Pachee CHAUDAKSHETRIN,[1] Malulee TANTAWIROON,[1] Anintita SURARAKHIRUN.

Purpose: To study therapeutic efficacy of 188 Re-HDD lipiodol in the treatment of unresectable hepatocellular carcinoma (HCC) The study was coordinated by IAEA in Vienna Austria.

Material and method: Patients had histopathologically proven HCC. Radioconjugate was prepared by using an HDD kit developed in Korea and lipiodol. 188 Rhenium was eluted from 188 W/188 Rhenium generator at OAP in Thailand. Total 13 patients (12 males and1 female) mean age 55 years old (36-78 years).

Results: There was no serious side effect or major complication. Median survival rate was 11 months, survival rate at 6 months and 1 year were 54% and 48% respectively.

Conclusion: 188 Re-HDD lipiodol can be used for the treatment of unresectable HCC in Child class A,B. In this study we found good result and minimal adverse effect after treatment.

Hepatocellular carcinoma (HCC) is a malignant tumor arising from parenchymatous liver cell. It is a common malignancy worldwide causing almost one million deaths annually.[1,2] Asia is a high risk area, the disease being particularly highly prevalent in China, Vietnam, Japan, Mongolia, Singapore and Korea.

HCC is one of the most common cancer in Thailand, male predominance with a male-to-female ratio of approximately 6:1.[3] Various risk factors have been associated with the development of HCC, among them exposure to certain toxin and infection with hepatitis virus, in particular HBV, as well as HCV in areas non-endemic for HBV infection.

Early HCC is typically clinically silent and the disease is often already well advanced with the first manifestation. Without treatment, there is a 5-years survival rate of less than 5 %.[4] Complete surgical resection followed by hepatic transplantation offers the best long term survival, but few patients are eligible for this therapy. All other therapies are palliative. Many treatment options have been developed to improve the quality and duration of life for patients with unresectable HCC. Presently, commonly used palliative therapies include systemic therapies, radiofrequency (RF) ablation, transarterial chemoembolization (TACE), and selective internal radiotherapy.

HDD	=	4-Hexadecyl 1-2,9,9-tetramethy l-4,7-Diaza-1,10 -Decanethiol
HCC	=	Hepatocellular Carcinoma
HBV	=	Hepatitis B Virus
HCV	=	Hepatitis C Virus
TACE	=	Transarterial Chemoembolization
RF	=	Radiofrequency
OPA	=	Office of atomic energy for peace
TACE	=	Transarterial chemoembolization
AFP	=	Alpha-fetoprotein

[1] Department of Radiology and Nuclear Medicine,
[2] Department of Medicine, Siriraj Hospital Faculty of Medicine, Mahidol University Bangkok, 10700, Thailand.

For unresectable HCC, selective internal radiation therapy usually involves the delivery of a radioactive material into the arterial blood supply of a tumor after directed catheterization with fluoroscopic guidance.

In this study used radioconjugate, namely rhenium-188 HDD lipiodol (188 Re-lipiodol).

The objective of this study were to establish the safety of delivering transarterial rhenium-188 lipiodol in patients with unresectable HCC and determine the adverse effect and response rate for this radioconjugated treatment in a small group of patients.

MATERIALS AND METHODS

A multi center study was sponsored by the International Atomic Energy Agency (Vienna), Austria. Patients were informed of potential risks of hepatic angiography and proposed radioconjugate treatment and consent were obtained. This study was approved by Siriraj ethics committees. This study was done during August 2003 to May 2005.

Rhenium-188 is a radionuclide with a physical half-life of 16.9 hours. It has an energetic and potentially cytotoxic beta-minus emission, as well as a gamma emission that may be imaged using external imaging techniques such as gamma cameras. The mean energy of β-rays is 795 keV and γ-rays with an energy of 155 keV in 15 % abundance. The maximum tissue penetration of the β-rays is 11 mm, with the mean being 3.8 mm.

Rhenium -188 is eluded from a 188W/188 Re generator (Oak Ridge National Laboratory, Oak, USA), which has a long useful shelf-life of several months and provides a good yield of carrier-free ^{188}Re on a routine basis.[5]

The radioconjugate was prepared by using an HDD(4-hexadecyl 1-2,9,9-tetramethyl-4,7-diaza -1, 10-decanethiol) kits developed in Korea and lipiodol.

The concentrated eluded from the W-Re generator is heated with the HDD in water bath for 1 hour to produce Re-HDD complex. Then lipiodol is added and centrifugation is performed to extract the Re-HDD into lipiodol. This processes were prepared at OAP (Office of Atoms for Peace.) in Thailand. The ^{188}Re-HDD lipiodol radioconjugate is stable for at least 4 hours.

Patients selection: HCC is defined in this population by histopathology or cirrhotic patients with liver mass who have consistently elevated serum alpha-fetoprotein levels (>320 IU/ml) with one imaging study or two in four studies demonstrated hypervascular mass(1. Ultrasound, 2. CT, 3. MRI, 4. Angiography).

Eligibility criteria were as follows:

1. Patients had to be at least 18 years of age, and not pregnant.
2. Patients had to have bidimensionally measurable HCC by CT, which had to be demonstrated to have a solitary lesion > 5 cm in greatest diameter, or ≤ 3 lesions ≤ 3 cm in greatest diameter, or an inoperable solitary lesion < 5 cm in greatest diameter in a patient not fit for surgery owing to co-existing severe medical illness.
3. All patients had to have been off chemotherapy or immunotherapy for at least 4 weeks, and off bronchodilators and/ or steroids for at least 8 weeks, prior to entry into the study.
4. All patients had to be ambulatory with Karnofsky status of ≤ 70%.
5. Serum creatinine ≤ 2 mg/dl.
6. Absolute neutrophil count (ANC) μ1, 500/μl, platelet count ≤ 100,000/ μl.
7. Prothrombin time ≤ 1.3 x control, and/or an international normalized ratio(INR) ≤ 1.5.
8. Patients had to sign an informed consent form for participation in this study.

Exclusion criteria were :

1. Child 's C status
2. Clinically significant cardiac disease (New York Heart Association class III/ VI)
3. Pulmonary disease, e.g. asthma/chronic obstructive pulmonary disease, requiring bronchodilators
4. FEV1/ diffusion capacity < 70% of normal.
5. Serious infection requiring antibiotic treatment, or other serious illness
6. Pregnancy or lactation
7. Survival expectancy of least than 1 month
8. Evidence of extrahepatic spread
9. Allergy of intravenous contrast.
10. Rupture HCC

Subjects: 13 Patients were treated (12 male and 1female). The mean age was 55 years (range 36-78).

A CT scans of liver were performed to assess pre-treatment size of the tumor and liver and tumor volume(s) (Fig.1, 2, 3).

Patients were admitted for hepatic angiography and treatment after injected radioconjugate. The consent had been obtained. The gamma camera dosimetry studies are performed the next day after admission. Pre-treatment day: the patients were sent to the Nuclear Medicine Department for flood source transmission scans to obtain attenuation correction factors for lung and liver to use dosimetry calculations the following day (Fig.4).

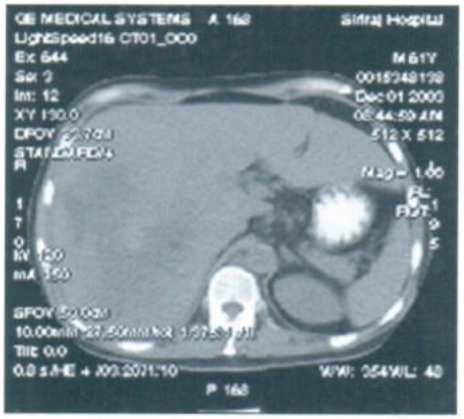

a.

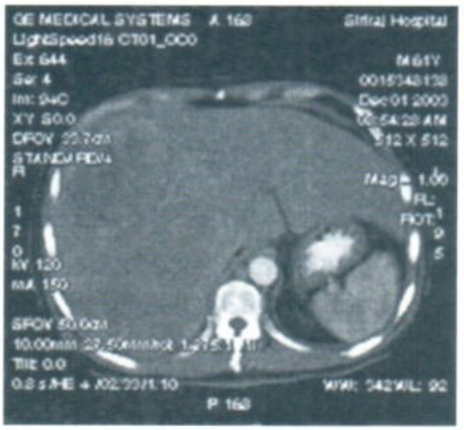

b.

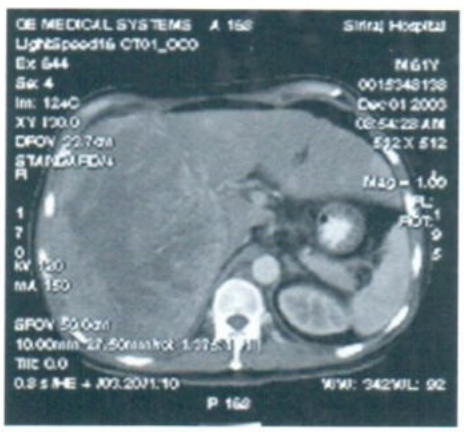

c.

Fig.1 CT scans liver of male patient with large HCC at right lobe of liver (a) non contrast phase large heterogeneous mass and enhancement on arterial phase (b), portal phase (c) showed central necrosis.

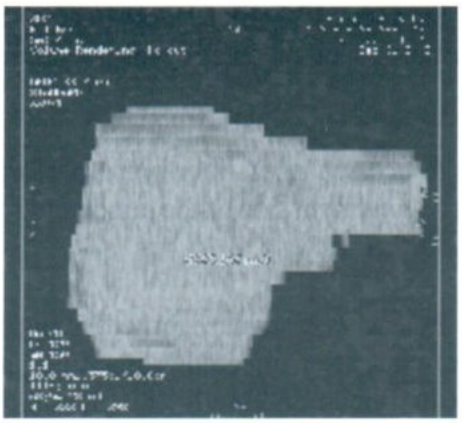

Fig.2 liver volume

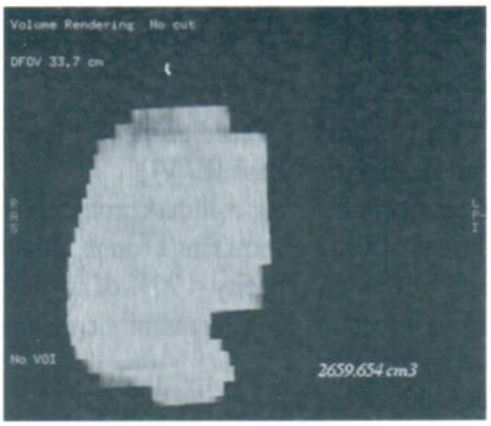

Fig.3 tumor volume

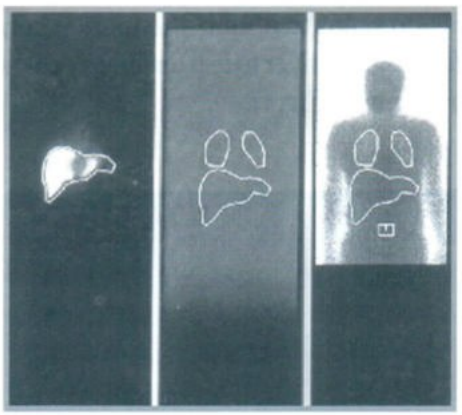

Fig.4 Pretreatment day. Patient was sent to the Nuclear Medicine Department for 99m Tc-phytate liver scan(a) and flood source transmission scans.

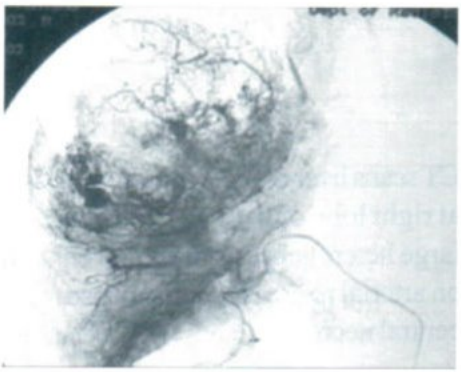

a.

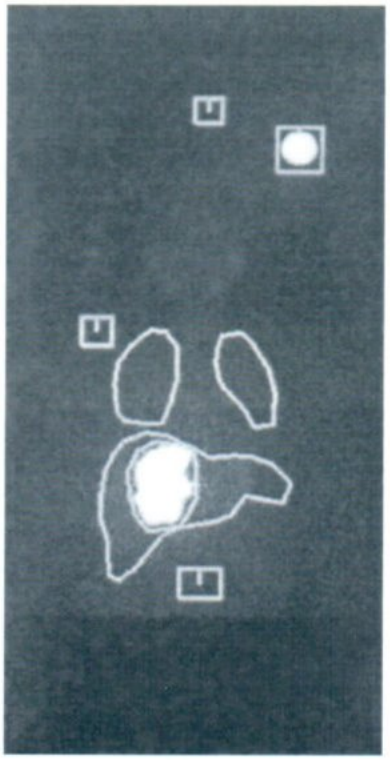

b.

Fig.5 Right lobe HCC, angiography was performed (a) in treatment day for scout dose injection (b).

Treatment day:

At Radiology Department (DSA room) hepatic angiography was performed via femoral artery by using 5 French vascular sheath. Then tumor and vascular supply were accessed by selective arterial supply close to feeding artery. After that initial transarterial infusion of radioconjugate was performed (scout dose) about 5 mCi (200 MBq), avoiding reflux of the gastroduodenal artery which risk to radiation complications. The tip of catheter was placed at the feeding artery, then patients were transported to the Nuclear Medicine Department by using sterile technique. Imaging of the scout dose in the liver was performed in static mode, both anterior and posterior images were obtained to calculate the geometric counts.(Fig.5)

Region of interest (ROI) were placed over lung, liver and tumor and calculated maximum tolerated activity (MTA), which were defined as the amount of radioactivity calculated to deliver no more than 1Gy to lungs, or 30Gy to liver, or 1.5Gy to bone marrow using Excel spreadsheet.

Then the patients were sent back to the Radiology Department (DSA room) for injection of the calculated treatment dose (reaching to MTD as much as possible) by nuclear physician and catheter position was checked by interventional radiologist within an hour of the scout dose.

After treatment dose were injected the patient was sent back to a single room in the ward for monitoring symptoms and adverse events. The patient can be discharged usually on the third or fourth days after admission.

Post treatment evaluation: A successful course of the therapy was defined as completion of one therapeutic dose of radioconjugate.

End of therapy was defined on 12 weeks after therapy administration. End of study was defined as death or progression of disease, defined as: increase in size or number of lesions or extrahepatic spread, or decrease in Child's status to C, or worsening of Karnofsky status.

Response parameter were evaluated as follows:

1. Complete response: disappearance of all measurable disease.
2. Partial response: 50% or greater reduction in the product of two perpendicular diameters of any measurable lesion and no new lesion.
3. Stable disease: no change in the size of lesion but less than a partial response; no new lesions.
4. Progression: appearance of new lesions, or increase by 25 % or more in the size of any measurable lesion Toxicity. Toxicity was graded in accordance with the Common Toxicity Scale developed by National Cancer Institute of the USA.

Adverse events: An adverse event was any new undesirable medical experience or change of an existing condition that occurred during or after administration of the investigational agent, whether or not it was considered agent related. Abnormal laboratory findings considered to be clinically significant were also considered adverse events.

RESULTS

Thirteen patients (12 males and 1 female) were treated. Eight cases has liver cirrhosis (61.5%). Six cases (46%) showed portal vein invasion and 4 cases (31%) showed portal hypertension. The mean treatment dose activity was 59.7 mCi (21.2-97.6 mCi). Mean maximum tolerate dose activity was 281.8mCi (48.5-777mCi). Treatment dose per maximum tolerated dose activity was 31.2% (Fig.6). The treatment dose was not up to MTD activity due to decay radioacitivity.

MTD were calculated to limiting organs, lung 8 cases (57%), liver 6 cases (45%). A biodistribution image is shown in figure 4. There is uptake of radioconjugate in lung on scout images, probably due

to arteriovenous shunt.

Median survival rate was 11 months, survival 6 months was 54%, 1 year survival rate was 46% (Fig.7). Five patients (38.4%) had stable disease at 3 months, and eight patients showed stable disease (table1). Only one patient received two radioconjugate dose and showed stable disease at 3 months. Alpha-fetoprotein (AFP) levels were stable in 12 patients (90%) and elevation in 1 patient (7.7%).

There were no significant changes in white cell counts, ANC or platelet count at 24 hours, 1 month of follow up. There were slightly elevation of ALT and AST at 24 hours (69%) but no significant change of liver function test at 2 weeks after treatment (table 2). Seven patients demonstrated mild abdominal discomfort and 3 patients showed low grade fever. Some patients have had more than one symptom.

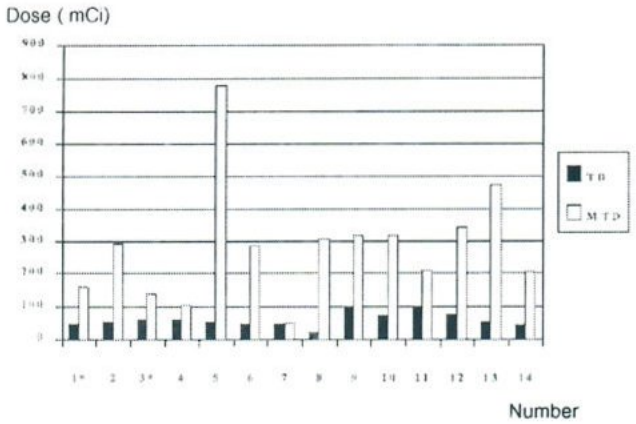

Fig.6 Treatment activity and maximum tolerated dose.
Number 1and 3 are same patient,
TD= treatment activity,
MTD=maximum tolerated dose

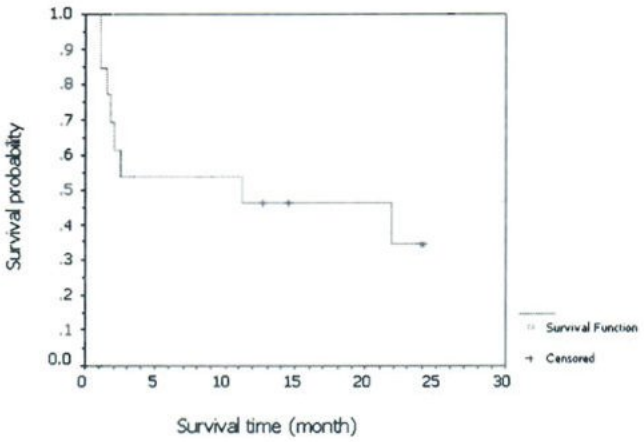

Fig.7 Kaplan-Meier survival curve

Table 1 Response at 12 weeks

	No.
Stable disease	5
Progressive disease	8

Table2 adverse effect
Some patients have had more than one adverse effect.

Adverse effect	No.	%
Mild abdominal discomfort	7	53%
Low grade fever	3	23%
Elevation of hepatic enzyme	9	69%

DISCUSSION

Hepatocellular carcinoma is often advanced at first manifestation. Many treatment options have been developed for treatment of advanced stages of HCC, that many patients are ineligible to a cure for HCC.

Radiofrequency ablation is the preferred method for managing unresectable HCC which are few in numbers. More widespread diseases are treated with percutaneous therapies such as chemoembolization and selective internal radiation therapy. Systemic administration of biologic and chemotherapeutic agents are minimally successful in slowing the growth of HCC and typically are used to control symptoms in patients with overwhelming disease.

Transarterial chemoembolization (TACE), various protocol for pharmaceutical infusion and/or arterial emolization via catheter have been developed to help patients who are ineligible for more definite treatment of hepatic neoplastic disease. TACE has been widely used for the palliative treatment of unresectable HCC. Side effects at TACE including abdominal pain, fever, nausea, jaundice, abscess and encephalopathy, were noted.

There have been many reports on the use of radionuclide therapy for the treatment of HCC such as Iodine131 (131 I-lipiodol), Yttrium90 (90 Y)and radiolabeled monoclonal antibodies.[6] Radionuclide methods can be used in the presence of portal vein thrombosis.[7]

At the 2003 annual meeting of the Radiological Society of North America, Lewandowski et al reported their experience with ^{90}Y in the management of unresectable HCC in 85 patient.[8] They found a median survival rate of 23.3 months and 16.6 months for the patients, Okuda stage 1 disease and Okuda stage 2 disease respectively. Steel et al[9] found that patients with HCC who underwent treatment with ^{90}Y -bearing glass microspheres (TheraSphere; MDS Nordion, Ottawa, Ontario, Canada) had a higher level of functional well-being than did those who received a hepatic arterial infusion of cisplatin.

Both ^{131}I-lipiodol and ^{90}Y microspheres are rather expensive. ^{188}Re-lipodol offers a convenient alternative for developing countries (Vietnam, Thailand). The short half-life of ^{188}Re avoids prolong hospital stays and reduced radiation exposure of the critical healthy organs. ^{188}Re-lipiodol showed minor adverse effect such as mild abdominal discomfort, low grade fever and slightly elevation of hepatic enzyme at 24 hours after treatment but no significant changes of liver function test at 2 weeks after treatment. Patients with HCCs without treatment, the 5-year survival rate is less than 5%. At the 2003 annual meeting of the Radiological Society of North America, Lewandowski et al found the median survival rate of patients, untreated HCCs at Okuda stage 1, to be 8.1 months and Okuda stage 2 to be 2.1 months, having significant shorter life expectancy.[8] In this study, we found a median survival rate in patients with unresectable HCCs with ^{188}Re-lipiodol treatment to be 11 months, but 6 months survival rate being 54% and 1 year survival rate being 46%.

There are few limitations of the study, such as difficulties in obtaining adequate activity of radiochemically pure ^{188}Re-lipiodol due to problem of concentrating elude from the generator and in obtaining good labeling. Another problem was the transportation of ^{188}W/ ^{188}Re generator to Thailand taking about 1 month and only obtainable one generator per year. Treatment dose activity available was less than maximum treatment activity levels.

During the procedure a small accidental leakage of tracer dose during injection due to uncontrolled tracer dose, was detected.

CONCLUSION

^{188}Re-lipiodol is as easily available

radioconjugate for transarterial treatment of HCC. The short half-life of ^{188}Re avoids prolonged hospital administra- tion and reduces radiation exposure of critical healthy organs. ^{188}Re-lipiodol can be used for treatment of unresectable HCC in Child Pugh A, B and portal vein thrombosis. In this study showed minimal adverse effect of ^{188}Re-lipiodol treatment. There appears to be some response to treatment, ^{188}Re needs to be confirmed in a larger number of patients in phase 3 study including comparison with TACE.

REFERENCES

1. Parkin DM, Bray F, Ferlay J, Pisani P. Estimating the world cancer burden: Globocan 2000. Int J Cancer 2001; 94: 153-156.
2. Akriviadis EA, Llvovel JM, Efremidis SC, et al. Hepatocellular carcinoma. Br J Surg 1998; 85: 1319-1331.
3. Sriamporn H, Prakin DM, Ferlay J. cancer in Thailand. Cancer Epidermiol Biomarkers PreV. 1995; 4: 475-483.
4. Ulmer SC. Hepatocellular carcinoma: a concise guide to its status and management. Postgard Med 2000; 107(5): 117-124.
5. Knapp FF Jr, Beets AL, Guhulke S, Zamora PO, Bender H, Palmedo H, Biersack HJ. Develpement the alumina-based tungsten -188/rhenium-188 generator and use of rhenium-188 labeled radiopharmaceuticals for cancer treatment. Anticancer Res 1997; 17: 1783-1796.
6. Yoo HS, Park CH, Suk JH, et al. Radioiodinated fatty acid ester in the management of hepatocellular carcinoma: preliminary findings. Cancer Chemother Parmacol 1989; 23 (Suppl 1): S54-S58.
7. Raoul JL, Guyader D, Bretagne JF, et al. Randomised controlled trial for hepatocellular with portal vein thrombosis: intra-arterial iodine-131 iodised oil versus medical support. J Nucl Med 1994; 35: 1782-1787.
8. Lewandowski R, Salem R, Oman B, Margolis J, Gates V, Sergie Z. 90Y microspheres (TheraSphere) for the treatment of unresectable hepatocellular carcinoma: mid-term clinical results(abstr). In: Radiological Society of North America scientific assembly and annual meeting program. Oak Brook, Ill: Radiological Society of North America, 2003; 328.
9. Steel J, Baum A, Carr B. Quality of life in patients diagnosed with primary hepatocellular carcinoma: hepatic arterial infusion of cisplatin versus 90-yttrium microspheres (TheraShere). Psychooncology 2004; 13: 73-79.

HIGH-DOSE I-131 THERAPY FOR VARIED ASPECTS OF WELL-DIFFERENTIATED THYROID CARCINOMA

Tanyaluck THIENTUNYAKIT, M.D.[1] Teerapon PREMPRAPHA, M.D.[1]
Suchitra THONGMAK, M.D.[1]

ABSTRACT

Purpose: This study aimed to evaluate the response to high-dose RAI (100-200 mCi) in three groups of patients: with a thyroid remnant, high Tg/negative WBS, and with metastasis.

Materials and methods: We retrospectively chart-reviewed 159 patients who had been admitted and received high-dose RAI from October 1999 until August 2004 at our tertiary treatment center in southern Thailand. The indications for treatment included 1) a thyroid remnant after at least 2 OPD ablative doses, 2) high serum Tg with negative diagnostic WBS, and 3) I-131 avid metastasis.

Results: 45 of 79 patients receiving high-dose I-131 for thyroid remnant ablation were successfully ablated. 12 of 24 patients with high Tg/negative WBS showed I-131 uptake on post-therapy WBS, while 3 showed no uptake on subsequent WBS; none returned to a normalized Tg level. Of 54 patients who had I-131 uptake in their metastases, 24 achieved complete response.
There was no statistical difference in age, sex, histologic type, pre-treatment Tg level or accumulated small dose RAI between good and poor response groups.

Conclusions: 1)A thyroid remnant (after surgery and small dose RAI) could not be ablated with up to 250 mCi in 34/79 patients (43%). 2) In high Tg/negative WBS, high-dose RAI might improve sensitivity but without obvious benefit in therapeutic outcome. 3) 24 out of 54 metastases (44%) showed a positive response to high-dose RAI, particularly those exhibiting RAI uptake at a single site

WBS = Whole body Scan

[1] Division of Nuclear Medicine, Department of Radiology, Songklanagarind Hospital, Faculty of Medicine, Prince of Songkla University, Hatyai, Songkla, Thailand 90110
For correspondence or reprints contact: Tanyaluck Thientunyakit, MD, Division of Nuclear Medicine, Department of Radiology, Songklanagarind Hospital, Faculty of Medicine, Prince of Songkla University, Hatyai, Songkla, Thailand 90110
E-mail : stanyalu@hotmail.com

INTRODUCTION

I-131 is routinely used in the treatment of well -differentiated thyroid carcinoma (WDTC), however, there is no current consensus on many aspects.[1-4] Many previous studies have reported on the results of radioiodine (RAI) treatment, but they do not really present a coherent picture of the treatment due to differing details such as patient status, staging of disease, dosages of I-131 treatment and criteria for successful treatment. In this study, we retrospectively reviewed the data of 157 well-differentiated thyroid carcinoma patients who underwent high-dose RAI treatment at Songklanagarind Hospital to review the response to treatment for one of three indications: thyroid remnant, high Tg/negative WBS, and I-131 metastasis.

MATERIALS AND METHODS

From October 1999 to August 2004, 296 thyroid carcinoma patients received primary treatment (thyroid surgery and OPD ablative doses of RAI) and were admitted to an isolation room for high-dose RAI treatment. All patients were followed up at Songklanagarind Hospital in Hatyai, Thailand. We retrospectively chart-reviewed 157 patients who had undergone high-dose RAI for thyroid remnant ablation (n=79), diagnosis and therapy in the case of high Tg but negative WBS (n=24) and treatment of I-131 avid distant metastases (n=54). All patients had undergone a thyroidectomy with or without neck dissection and received at least 1 small OPD dose (30-50 mCi) of post-operative I-131 therapy. The first I-131 ablation was performed four to six weeks after surgery, with no thyroid hormone treatment given in the interim. Post-therapy I-131 WBS was performed 5-7 days after the I-131 treatment using a single-head gamma camera system (GCA-901 A/HG, Toshiba Corperation,® Japan). A follow up diagnostic WBS (3-10 mCi) was performed 6 months after each I-131 treatment. Each patient was instructed to cease taking thyroxine for 4 weeks before the I-131 administration for scanning or treatment. Long-term thyroxine replacement using levothyroxine was given after post-therapy scanning. Patients were asked to commence a low iodine diet 1 week prior to the scan.

Thyroid function tests, including TSH, serum thyroglobulin (Tg), anti-thyroglobulin antibody (anti-Tg Ab) and a chest radiograph, were performed prior to I-131 administration. I-131 was administered when the serum TSH level was at least 30 mIU/L. Serum Tg under TSH stimulation of 20 ng/ml or above was considered to be high and when found, was followed until normalized.

High-dose RAI therapy was considered if the radioiodine uptake was found within the thyroid bed or areas suggesting metastasis on the follow up diagnostic scan after at least 1 small OPD dose. The treatments administered ranged from 100-150 mCi for thyroid remnant ablation to 150-200 mCi for high Tg/negative WBS or distant metastases. The patients were admitted to an isolation room for 2 days and discharged after the exposure radiation at 1 m was below 5 mRem/hour.

Further radioiodine therapy was considered if radioiodine uptake could still be detected on the follow-up scan 6 months after the high-dose therapy. In some patients with very intense metastatic uptake and very high Tg, further high-dose therapy 4-6 months later was given unless a diagnostic WBS was done. In the high Tg/negative WBS group, if post-therapy WBS showed no uptake, there was no further I-131 treatment or follow up scanning.

Hospital records were reviewed and the following data were stored in the computer: age, gender, extent of surgery, histopathological type, primary tumor size, operative findings, pre-treatment Tg levels and anti-thyroglobulin antibody levels,

WDTC = Well-differentiated Thyroid Carcinoma
WBS = Whole body Scan

accumulated small I-131 doses, pre- and post-therapy WBS results and radiographic findings.

Data analysis was performed using SPSS version 11.0 and the results are presented as mean ± SD. A two-tailed unpaired t test was used to evaluate statistical significance.

DEFINITIONS

- **thyroid remnant:** positive I-131 uptake at thyroid bed in diagnostic WBS after receiving at least 2 doses of small OPD I-131 ablation
- **Tg0-max:** Pre-treatment serum Tg under TSH stimulation (TSH 30 mIU/L or above)
- **high Tg-max:** Serum Tg under TSH stimulation 20 ng/ml or above
- **complete response:** negative I-131 uptake at the primary lesion on subsequent diagnostic or post -therapy WBS after RAI treatment
- **partial response:** decrease in number or extent of I-131 uptake on subsequent diagnostic or post -therapy WBS after RAI treatment
- **no response:** unchanged or progressive I-131 uptake lesion on subsequent diagnostic or post -therapy WBS after RAI treatment
- **response by Tg:**
- **complete response:** at least 50% reduction of Tg-max compared to the pre-treatment level

no response: less than 50% reduction or increased level of Tg-max compared to the pre-treatment level

RESULTS

Among the 157 patients with thyroid cancer, there were 94 papillary carcinomas, 45 follicular carcinomas and 18 mixed papillary-follicular carcinomas. 112 patients were female with a mean age of 42 (± 15) years and 45 patients were male with a mean age of 43 (± 16) years at the time of diagnosis. Mean follow up period since the first high-dose RAI was 34 (range 7-116) months. The results of high-dose RAI treatment were evaluated in 3 groups according to the by indications for treatment.

Group 1) Thyroid remnant after OPD small ablative doses (n=79)

Following a post-operative small ablative dose, 79 patients, 58 females and 21 males, underwent high-dose I-131 treatment for thyroid remnant ablation. The mean ages of the complete response and no response groups were 44 (± 12) and 40 (± 12), respectively. Of the 79 patients who received a dose of 100-150 mCi for remnant ablation, 45 (57%) were successfully ablated with one or two doses of I-131. Of these 45, 27 were papillary (56% of all papillary carcinomas), 14 were follicular (64% of all follicular carcinomas) and 4 were mixed type (44% of all mixed papillary-follicular carcinomas). Table 1 shows the characteristics and successful rates of thyroid remnant ablation in these patients. There were no statistically significant differences in the success rates between the different ages ($p = 0.909$), sexes ($p = 0.593$), histological cell types ($p = 0.493$), pre-treatment Tg max's ($p = 0.167$) and accumulated small I-131 doses ($p = 0.681$).

Table 1 Characteristics and success rates of thyroid remnant ablation of well-differentiated thyroid cancer patients after high-dose I-131 therapy

	Complete response (N = 45)	No response (N = 34)	p value
Sex			
- Female (%)	32 (71%)	26 (76%)	0.593
- Male (%)	13 (29%)	8 (24%)	
Age at diagnosis (years)	44 ± 12	40 ± 12	0.909
Cell type			0.493
- Papillary	27 (60%)	21 (62%)	
- Follicular	14 (31%)	8 (23%)	
- Mixed papillary – follicular	4 (9%)	5 (15%)	
Tg0 max, ng/ml	71 ± 190	139 ± 238	0.167
Range	0-823	0-862	
Median	1.4	10	
Accumulated small dose	106 ± 91	119 ± 168	0.681
Number of treatment (median)	1	2	
other site uptake	11	14	0.085
- mediastinum	9	9	
- lung	1	2	
- mediastinum & lung	1	2	
- bone	-	1	
Number of surviving patients	45	34	-

Group 2) High serum Tg with negative WBS (n=24)

This group included 24 patients with persistently high serum Tg-max levels was based on a cut-off point of 20 ng/ml and a negative diagnostic I-131 WBS study. Patients with positive anti -thyroglobulin antibodies were excluded. Almost half of these patients still showed a negative WBS after administration of up to 50 mCi. Then an initial high-dose I-131 treatment of 150 mCi was administered to detect any I-131 uptake lesion. Follow up treatment results with a further post-therapy scan (in cases with positive uptake) and Tg-max response using the previously mentioned criteria were obtained.

Among the 24 patients who received high-dose I-131 for their high Tg level only, 10 showed I-131 uptake on the post-therapy scan and 2 showed questionable uptake. The sites of uptake on the post -therapy WBS are listed in Table 2. Further high-dose RAI treatment was administered in 9 patients of whom 4 showed complete resolution on a subsequent post-therapy scan. The remaining 5 patients still had unchanged uptake, although 3 of them received an accumulated I-131 dose of more than 1 Ci. There was no follow up WBS in 3 patients who had minimally positive uptake on the first high-dose WBS.

Table 2 The sites of I-131 uptake on the post-therapy scan of 12 patients with high Tg negative diagnostic WBS

Site of uptake at the 1st post therapy WBS	Uptake on high-dose RAI		Tg post therapy	
	Uptake	No uptake	Unchanged	Increase
Thyroid bed, n = 3	Possibly = 1 Not F/U = 1	0	1	2
Lung, n = 3	2	1	1	2
Questionable uptake at mediastinum, n = 2	Not FU = 1	1	0	2
Thyroid + mediastinum, n = 3	Not FU = 1	2	0	3
Mediastinum + LN, n = 1	1	0	1	0

Only 1 of these 12 patients (8.3%) showed significant reduction of the Tg-max level after one or more high-dose RAI treatments. The responses as indicated by I-131 uptake and Tg max level using a cut-off ? 50% reduction from pre-treatment levels is shown in Table 3. There was no significant difference of I-131 uptake on the first post-therapy WBS among different age groups (p = 0.124), sexes (p = 0.673), histological cell types (p= 0.165) or pre-treatment Tg-max levels (p = 0.781).

Table 3 Patient characteristics between those with positive and negative uptake on the first post-therapy WBS

	Uptake (N = 12)	No uptake (N = 12)	p value
Sex			
- Female (%)	7 (58%)	8 (67%)	0.673
- Male (%)	5 (42%)	4 (33%)	
Age at diagnosis (years)	38 ±14	43±16	0.124
Cell type			0.165
- Papillary	9 (75%)	6 (50%)	
- Follicular	1 (8%)	5 (42%)	
- Mixed papillary – follicular	2 (17%)	1 (8%)	
Tg max, ng/ml, mean ± SD	255±248	283±238	0.781
Range	44-697	15-708	
Median	127	235	
Accumulated small dose	191±362	220±126	0.798
High-dose RAI range	150-1024	150-660	0.192
Response of post-treatment Tg	1(8.3%)	0	-
Number of surviving patients	12	10	-

Group 3) Iodine-131 avid metastasis (n =54)

Among the 54 patients with positive I-131 uptake at their metastatic sites, 39 were female and 15 were male. 45 patients had single organ metastasis, in lung (n = 25), mediastinum (n = 10) or bone (n =

10) (Table 4). One patient with bony metastasis had multiple bones involvement, while the other 9 also had multiple organ metastases.

Complete response using resolution of uptake at the primary lesion(s) on follow up WBS was achieved in 24 patients. Of these 24, 17 were papillary carcinomas (55% of all papillary carcinomas), 5 were follicular carcinomas (29% of all follicular carcinomas, and 2 were mixed (33% of all mixed papillary-follicular carcinomas). There were no statistically significant differences in the rates of successful treatment between different sexes ($p = 0.422$) histological types ($p = 0.474$), or Tg max's (0.183), but older age ($p = 0.018$) and higher accumulated small dose RAI ($p = 0.043$) were noted in patients with poor response to high-dose RAI treatment.

Among the 24 patients with good response to high-dose RAI treatment, 22 (92%) had single organ metastasis. Of 9 patients with multiple organ metastases, 2 showed complete response, 4 partial response and 1 no response. Of 26 patients with no response to RAI, 6 with co-existent lung and bony metastases died from cancer.

The responses to high-dose RAI in all 3 subgroups of 157 well-differentiated thyroid carcinoma patients are summarized in Table 5.

Table 4 Clinical features of WDTC patients with I-131 avid metastasis and responses to high-dose RAI

	Complete response (N = 24)	Partial response (N = 4)	No response (N = 26)	p value
Age at diagnosis (years)	36±16	40±14	45±15	0.018
Sex				0.422
- Female (%)	17	4	18	
- Male (%)	7	0	8	
Histology				0.474
- Papillary	17	1	13	
- Follicular	5	3	9	
- Mixed papillary – follicular	2	0	4	
Site of metastasis				
- Lung	11 (3)*	-	14 (3)*	
- Mediastinum	5 (0) *	-	5 (0) *	
- Bone	6 (1) *	-	4 (1)*	
- Multiple organs	2 (0) *	4 (1)*	3 (3)*	
Tg0 max, mean ± SD	143±214	282±208	366±308	0.183
range	0-711	92-490	0-837	
Median, ng/ml	12.5	273	490	
Accumulated small dose	432±286	104±228	662±338	0.043
Number of surviving patients	24	4	20	-

NB : ( )* = number of patients with newly detected I-131 uptake lesion on subsequent WBS after high-dose RAI therapy

Table 5 Summery of responses to high-dose RAI in all 3 subgroups of 157 well-differentiated thyroid carcinoma patients

Group	N Subjects	RAI dose, mCi	Tg range (mean) Ng/ml	Response		
				Complete	Partial	None
Remnant	79	98-1,401	0-862 (105)	45 (11)*	-	34 (14)*
High Tg	24	150-1,024	15-708 (269)	-	-	24 (12)*
Metastasis	54	135-1,330	0-837 (263)	24 (4)*	4 (1)*	26 (7)*

NB : ( )* = number of patients with newly detected I-131 uptake lesion on subsequent WBS after high-dose RAI therapy

DISCUSSION

Radioactive iodine-131 is used for post -operative thyroid remnant ablation and also for treatment of distant metastases in papillary and follicular thyroid cancer patients.[1-4] Although it is well known that I-131 plays a role in the treatment of thyroid cancer, there are still several controversial aspects to its use.[5-7]

I-131 therapy is given post-operatively for three reasons. First, it destroys any remaining normal thyroid tissue. Secondly, it increases the sensitivity of subsequent I-131 whole-body scanning and the specificity of measurement of the serum thyroglobulin for the detection of persistent or recurrent disease. Third, the use of a large amount of I-131 for therapy permits I-131 WBS, a sensitive test for detecting persistent carcinoma.[8]

One study reported that the remaining thyroid tissue can be destroyed with a single dose of I-131 in about 80% of patients, as defined by a diagnostic scan using 2 to 3 mCi of I-131 several months after the initial treatment, provided that the surgeon has left only a relatively small thyroid remnant. In this study, the first dose abolished thyroid uptake in 81% of patients given 30 mCi and 84% of those given 100 mCi.[9-11] The size of the thyroid remnant is also important. For example, in one study an average dose of 87 mCi was more effective in destroying the thyroid remnant after near-total thyroidectomy than less extensive surgery (90% vs. 22%). The remnant was destroyed successfully with I-131 in 94% of patients when the surgeon left less than 2 gm of thyroid tissue but in only 68% of patients in whom the remnant was larger.[11] Unfortunately, in our study the surgical data was incompletely recorded in many patients and an analysis of this parameter on response to treatment could not be carried out.

In the present series, 79 of 157 thyroid cancer patients underwent high-dose (100-150 mCi) RAI therapy for thyroid remnant ablation after at least two small ablative doses. The thyroid remnant of 57% (45/79) of these patients could be ablated by giving one or two doses of high-dose RAI. Only 37% (29/79) of these patients with a thyroid remnant could be cured with a single dose of RAI and another 20% with a double doses.

The successful rate of thyroid remnant ablation in our series was much lower than earlier reports. One important difference in our study was the smaller dose of RAI. Our patients had persistent thyroid remnant after receiving at least two small doses

I-131 (mean accumulated dose = 110 mCi). We hypothesize that small doses I-131 given previously might have had some effect on the biochemical properties of the thyrocyte, resulting in decreasing the ability of the radioiodine trapping mechanism and so negatively affecting the treatment response. This defect of thyrocyte ability should not have been the 'thyroid stunning' effect because all patients had an interval of at least 4-6 months between each I-131 administration. However, there was no significant difference of accumulated small dose I-131 between those who were successfully ablated and those who were not ($p = 0.681$).

In one study in 2001 by Arslan et al.,[9] the total I-131 dose needed for successful ablation was significantly higher in males ($p = 0.003$). This finding suggested that sex might play a role in successful I-131 ablation. In our series, however, we found no significant difference in the sexes between the two response groups, and our findings are similar to a study of 544 patients performed by Lin et al.[11] In their study, factors identified as influencing response to I-131 therapy included age, clinical stage, survival, recurrence, extent of surgery and the post operative serum Tg level; sex was not a factor in this study. In our study, patients who were successfully ablated had lower pre-treatment Tg level (mean 71 ±190) in comparison with those who were not (mean 139±238). However, there was no statistically significant difference ($p = 0.167$), possibly due to the relatively wide range of Tg levels. Further study on significance of high Tg level and response to RAI treatment might be important in the management, e.g. selecting early high-dose RAI treatment instead of waiting until no response after 2 small doses in patients with initially high Tg.

Arslan et al.[9] also reported that 19 of 218 patients (7.8%) showed metastasis on a post-therapy scan and successful treatment was achieved in 11 of the 19 (57.8%). 25 of 79 (32%) thyroid remnant patients which in our study showed metastasis on their subsequent post-therapy scan, most commonly at the mediastinum. This high rate could be due to the initial small dose of I-131 treatment destroying some of the residual thyrocyte and increasing the ability of I-131 uptake at the metastatic site. The pre-treatment Tg level in these patients was significantly higher than in those without metastasis (179 vs. 69 ng/ml, $p = 0.051$). The successful rate of treatment in these patients was 71% (17/19).

In 10-15% of the patients, detectable increase in serum Tg levels were found despite a negative WBS.[12] This discrepancy was mainly due to a metastasis being able to produce Tg but having iodine uptake too low to be visualized on a diagnostic WBS, either because the mechanism of iodine trapping was defective or the mass of neoplastic tissue was small. However, false negative WBS's can be caused by technical factors such as an excessive iodine pool, poor instrumentation, or inadequate serum TSH elevation.[12] We are confident that our patients did not represent false negative WBS's, because more than 50% of the diagnostic WBS's remained negative with I-131 dose up to 50 mCi.

There is still considerable controversy concerning the use of I-131 therapy in patients with true negative scans and a high serum Tg level. Some reports have suggested a benefit from empiric therapy for scan-negative, Tg-positive WDTC patients. Positive I-131 uptake on post-therapy scan could be detected 10-50% of these patients. Reduction in Tg level and disappearance of I-131 uptake in subsequent post-therapy scan could be achieved after treatment.[11, 13-15] However, many studies do not support benefits of empiric high-dose I-131 therapy in these patients.[7, 12, 17-19]

In a review article in 2001, Mazzaferri and Kloos[20] reported on 10 Tg-positive, diagnostic WBS -negative patients with serum Tg levels more than 15 ng/ml. Eight of these patients had evidence of metastasis on their post-therapy scan and 3 had a

WDTC = Well-differentiated Thyroid Carcinoma

subsequent negative post-therapy scan, with reduction of serum Tg to 5 ng/ml. A more recent report by Pacini et al.[12] compared the results of 28 untreated patients with 42 treated patients. The authors found a positive post-therapy WBS in 71% with reduction in Tg and disappearance of lung uptake with repeated therapy. They recommended treating all Tg-positive, WBS-negative cases once with 100 mCi of I-131 and continuing therapy until post-therapy WBS becomes negative.

In our present study of 24 patients treated with RAI who had detectable Tg and negative diagnostic WBS, 10 showed definite positive uptake on the post-therapy scan and 2 showed suspected I-131 uptake at the mediastinum. On a subsequent post-therapy scan, 4 of 9 (44%) who had a follow up post-therapy WBS showed complete remission. However, only 1 of these 12 patients with positive uptake on their post-therapy scan showed significant reduction of Tg level during the follow up period (based on at least a 50% reduction from the pre-treatment level). Our results suggest that in patients with a positive post-therapy scan, high-dose radioiodine treatment can be used as a diagnostic tool to identify tumor location. However, the beneficial therapeutic effect of this therapy remains unclear and has no obvious effect on survival. We would not advise the continuation of radioiodine therapy in patients with negative post-therapeutic WBS, unless a positive response is observed in individual cases, to prevent unnecessary radiation exposure to the patients.

I-131 therapy has been used to control distant metastasis from WDTC for more than 50 years.[21,22] In our series, the most common distant metastatic sites were lung, bone and mediastinum. A previous report by Brown et al.[23] on 235 patients who were treated for WDTC, of whom 42 had distant metastases and received I-131 therapy. 54% of the patients whose metastasis was confined to the lungs were alive without disease at a 10 year-follow up. Similar findings were reported by Schlumberger et al.,[24] who found that 46% of 394 patients with distant metastases who were treated with I-131 had complete resolution of uptake and excellent long-term survival.

In our series, the success rate based on complete resolution of uptake after high-dose treatment in patients whose metastasis was confined to either the mediastinum or a single bone was 50% for both, and only slightly lower in patients with lung metastasis (44%). The rate of successful treatment was significantly lower in those with multiple organ metastases, as only 2 of 9 patients (22%) showed successful treatment. Of 54 patients with metastasis, 2 with co-existing lung and bony metastases which had not responded to RAI treatment died from cancer.

The successful treatment rate in our patients was possibly false high, however, as based on the criteria we used to define success. The response to treatment was assessed based on the resolution of uptake at the primary detected lesion only, not all uptake of which some may appear on a subsequent scan. However, we nonetheless feel that a successful response to I-131 treatment can be achieved in as many as 40-50% of patients with single organ metastasis, with a poorer outcome in patients with multiple organ metastases.

CONCLUSION

I-131 has a major impact on the progressive control and cure of thyroid carcinoma, however it is not a panacea. The rate of unsuccessful thyroid remnant ablation with high-dose RAI is as high as 50%, depending on negative I-131 uptake at thyroid bed on post-therapeutic scan. In high Tg/negative WBS, high-dose RAI might improve sensitivity but without obvious benefit in therapeutic outcome. High-dose RAI therapy has some benefit in controlling metastasis, though there is lesser response where there is multiple organs involvement. Pre -treatment Tg level is not a significant factor in

predicting response to RAI, and further investigation is needed on the factors predicting response to treatment.

ACKNOWLEDGEMENTS

We would like to express our deep appreciation to our project consultant, Professor Tada Yiptinsoi, for his comment and Mr. David Patterson for reviewing the manuscript.

The data in this paper were originally presented in part at the 44th Annual Scientific Meeting of The Royal College of Radiologists of Thailand and the Radiological Society of Thailand, 29-31 March 2005.

This research methodology has been approved by the Ethics Committee on Human Research, Faculty of Medicine, Prince of Songkla University.

REFERENCES

1. Harmer CL, McCready VR. Thyroid Cancer: differentiated carcinoma. Cancer Treat Rev. 1996; 22: 161-77.
2. Mazzaferri EL. Treating differentiated thyroid carcinoma: where do we draw the line? Mayo Clin Proc. 1991;66:101-11.
3. Goolden AW. The indications for ablating normal thyroid tissue with 131 I in differentiated thyroid cancer. Clin Endocrinol. 1985; 23: 81-6.
4. Davis NL,Gordon M, Germann E, McGregor GI, Robins RE. Efficacy of 131 I ablation following thyroidectomy in patients with invasive follicular thyroid cancer. Am J Surg. 1992; 163: 472-5.
5. Creutzig H. High or low dose radioiodine ablation of thyroid remnants ? Eur J Nucl Med. 1987; 12: 500-2.
6. Maxon HR 3rd, Englaro EE, Thomas SR, et al. Radioiodine-131 therapy for well differentiated thyroid cancer - a quantitative radiation dosimetric approach: outcome and validation in 85 patients. J Nucl Med. 1992; 33: 1332-6.
7. Mazzafern EL. Treating high thyroglobulin with radioiodine: a magic bullet or a shot in the dark? J Clin Endocrinol Metab. 1995; 80: 1485 - 7.
8. Robbins J, Schlumberger M. The evolving role of 131I for the treatment of differentiated thyroid carcinoma. J Nucl Med. 2005; 46: 28s-37s.
9. Arslan N, Ilgan S, Serdengecti M, Ozguven MA, Bayhan H, Okuyucu K, et al. Post -surgical ablation of thyroid remnants with high dose (131)I in patients with differentiated thyroid carcinoma. Nucl Med Commun. 2001; 22: 1021-7.
10. de Klerk JM, de Keizer B, Zelissen PM, Lips CM, Koppeschaar HP. Fixed dosage of 131I for remnant 131I scintigraphy. Nucl Med Commun. 2000; 21: 529 - 32.
11. Lin JD, Kao PF, Chao TC. The effects of radioactive iodine in thyroid remnant ablation and treatment of well differentiated thyroid carcinoma. The Brit J Rad. 1998; 71: 307-13.
12. Pacini F, Agate L, Elisei R, Capezzone M, Ceccarelli C, Lippi F, et al. Outcome of differentiated thyroid cancer with detectable serum Tg and negative diagnostic (131) I whole body scan: comparison of patients treated with high (131) I activities versus untreated patients. J Clin Endocrinol Metab. 2001; 86: 4092 - 97.
13. Schlumberger M, Mancusi F, Baudin E, Pacini F. 131I therapy for elevated thyroglobulin levels. Thyroid. 1997; 7: 273 - 6.
14. Pineda JD, Lee T, Ain K, Reynolds JC and Robbins J. Iodine - 131 therapy for thyroid cancer patients with elevated thyroglobulin and negative diagnostic scan. J clin Endocrinol Metab.1995.;80:1488-92.

15. Kabasakal L, Selcuk NA, Shafipour H, Ozmen O, Onsel C, Uslu I. Treatment of iodine-negative thyroglobulin-positive thyroid cancer: differences in outcome in patients with macrometastases and patients with micrometastases. Eur J Nucl Med Mol Imaging. 2004 ; 31: 1500-4.
16. Koh JM, Kim ES, Ryu JS, Hong SJ, Kim WB, Shong YK. Effects of therapeutic doses of 131 I whole - body scan: comparative study. Clin Endocrinol (oxf). 2003; 58: 421-7.
17. Alexander C, Bader JB, Schaefer A, Fink C and Kirsch CM. Intermediate and long- term side effects of high - dose radioiodine therapy for thyroid carcinoma. J Nucl Med.1998; 39: 1551-4.
18. McDougall IR. 131 I treatment of 131 I negative whole body scan, and positive thyroglobulin in differentiated thyroid carcinoma: what is being treated ? Thyroid. 1997; 7: 669-72.
19. Fatourechi V, Hay ID, Javedan H, Wiseman GA, Mullan BP and Gorman CA. Lack of impact of radioiodine therapy in Tg-positive, diagnostic whole-body scan-negative patients with follicular cell-derived thyroid cancer. J Clin Endocrinol Metab. 2002; 87: 1521 - 6.
20. Mazzaferri EL, Kloos RT. Clinical review 128: current approaches to primary therapy for papillary and follicular thyroid cancer. J Clin Endocrinol Metab. 2001; 86: 1147-1463.
21. Mazzaferri EL. Carcinoma of follicular epithelium: radioiodine and other treatment outcomes. In: Braver man LE, Utiger Rd, RD, eds. Werner and Ingbar's The Thyroid: A fundamental and Clinical Text.7th ed. Philadelphia: Lippincott - Raven,1996: 922-945.
22. Maxon HR 3rd, Smith HS. Radioiodine-131 in the diagnosis and treatment of metastatic well differentiated thyroid cancer. Endocrinol Metab Clin North Am. 1990; 19: 685-718.
23. Brown AP, Greening WP, McCready VR, Shaw HJ and Harmer CL. Radioiodine treatment of metastatic thyroid carcinoma: the Royal Marsden hospital experience. Br J Radiol. 1984; 57: 323-7.
24. Schlumberger M, Challeton C, De Vathaire F, Travagli JP, Gardet P, Lumbroso JD, et al. Radioactive iodine treatment and external radiotherapy for lung and bone metastases from thyroid carcinoma. J Nucl Med. 1996; 37: 598-605.

SONOGRAPHICALLY GUIDED HYDROSTATIC REDUCTION OF CHILDHOOD INTUSSUSCEPTION IN UTTARADIT HOSPITAL [1]

Kanda SAKSORNCHAI, MD.[2]

ABSTRACT

Over 10-year period, real-time ultrasound (US) were performed in 33 intussusceptions (32 cases). 21 cases were undergone immediate reduction procedure after the diagnosis. The reductions were performed under US-guided using normal saline as enema fluid under pressure control of 80-110 mmHg. The height of the enema bag is about 3feet above the table top as usual. 4 cases were successfully reduced. Complete reductions could not be confirmed in another 3 cases but follow up revealed complete recovery. 14 cases were operated. 12/14 operated cases underwent manual reductions and 2/14 got bowel resections. Surgical findings were as followed: 1 gangrenous bowel,1 polyp in the terminal ileum,1 inflamed appendix, 3 ileo-ileocolic intussusceptions, 3 ischemic changes, 4 long intussusceptions, 4 small residual intussusceptions and 1 negative for intussusception (more than one findings in one case).

Success rate of reduction is 19.05% (n=21). Factors influencing incomplete reductions were poor general conditions, massive rectal bleeding, small bowel obstruction and rectal-sealed problem.

Potential improvement can be made to achieve better result. The seal problem can be avoided by inflation of the Foley's balloon and controlling the reduction time not longer than 15 minutes. The poor general conditions should be improved prior reduction attempted. Although this method has not yet been shown to be as good as those conventional ones, the obvious benefits are radiation free effect and being more friendly to the atmosphere. Sonogram is operator dependent and the US-guided saline enema reduction needs time for learning curve to become more accepted procedure.

Index term: Children intussusception, hydrostatic reduction, US-guided.

INTRODUCTION

Intussusception is one of the most common causes of the acute abdomen in early childhood. Intussusception occurs when a portion or the digestive tract becomes telescoped into the adjacent bowel segment. This condition usually occurs in children between 6 months and 2 years of age.[1]

In the past, intussusception could be a severe condition with high morbidity and mortality rates. Currently, prompt diagnosis and effective treatment lead to favorable outcomes in most cases. In fact, there are mild cases that may reduced spontaneously.[2,3]

[1] Regional Hospital, Ministry of Public Health, Thailand.
[2] X-ray department,Uttaradit Hospital, Naresuan University, Thailand.

Radiologists play roles in the diagnosis and therapy of the suspected intussusception. US has been reported to achieve a sensitivity of 98.5-100% in the diagnosis of intussusception.[15-16] Several studies have emphasized the value of sonography as an initial screening procedure in patients with suspected intussusception.[12-13] Some authors do not recommend US as a routine screening method because US signs, most commonly used as diagnostic criteria of intussusception, are not pathognomonic.[12,14-17] Fluoroscopy guided barium enema and pneumatic reduction techniques are widely used. However, both methods are under ionizing radiation. There is no consensus as to which technique is superior.[4] Recently, sonographically guided hydrostatic reduction has been used with different types of enema fluid.[5-10]

This article describes the author experience of US-guided hydrostatic reduction of intussusception. The purpose of the article is to first report of this technique in Thailand and to encourage the procedure usage.

MATERIALS AND METHODS

Over a period of 10 years (May 1997-Apr 2007) 33 intussusceptions (including 1 case of recurrence) were diagnosed with sonogram study.[21] consecutive unselected patients underwent hydrostatic reduction with US monitoring. The procedure as well as the equipment followed those of the Queen Sirikit National Institute of Child Health (Children Hospital) Bangkok Thailand with addition of enema bag to the system11 (Fig.1). They were 10 boys and 11 girls ranging in age from 2 to 39 months(average 13.6 months). 12/33 intussusceptions were excluded due to incomplete information (6 cases) and reduction by other techniques (6 cases). US examinations were performed with 5-8 MHz convex and linear transducers (Aloka 650, BK 3535 and BK 2000 Panther advanced imaging). All cases were diagnosed upon sonographic findings. The signs of intussusception including target sign, pseudokidney sign and multiconcentric ring sign were demonstrated (Fig.2). The reduction attempts upon agreement of attending physician and surgeon immediately followed the diagnosis of intususception. All cases showed no sign of peritonitis. Those cases with leading points demonstrated were proceeded for surgery. Plain films of abdomen were performed in some cases. Reduction was performed without sedation, antispasmodic nor intentional external pressure on the abdomen. The process of reduction demonstrated by ultrasonography was shown in figures 3a-3f (Fig.3). There is warm, friendly atmosphere in the US room with parents, clinicians, nurses, circulating personals as well surgeons. Patient vital signs and general appearance were easy to access during the procedure than under the fluoroscopic screen that overshadowed the small patient.

The reduction started with insertion of a Foley's catheter, as largest diameter as possible, into the rectum. Two years experience with sealing problem has led to the use of balloon-type catheter to provide an effective airtight seal. The patient's arms and buttocks were held closely together with cloth and adhesive tape. The buttocks also pressed together manually during the procedure. The enema fluid (normal saline 400 to 1000 ml) at body temperature was introduced (controlling pressure between 80-100 mmHg) via Y tube connection by inflated rubber bulb of a sphygmomanometer (Fig.2a). Some authors place the enema bag at 80-100 cm above the supine patient to create hydrostatic pressure of 83-104 cm water which is equivalent to 61-77 mmHg (A 1cm water column is equivalent to a 0.74 mm mercury column).[6]

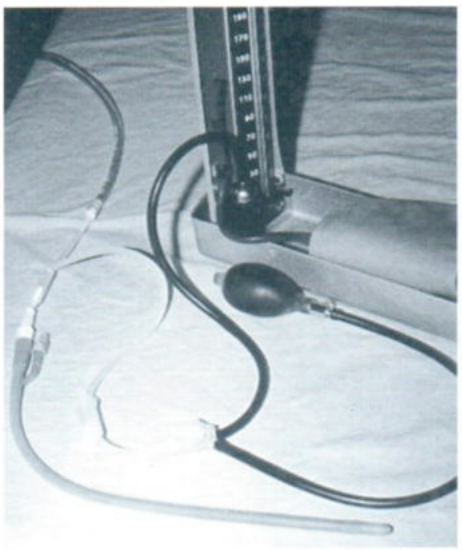

a

b

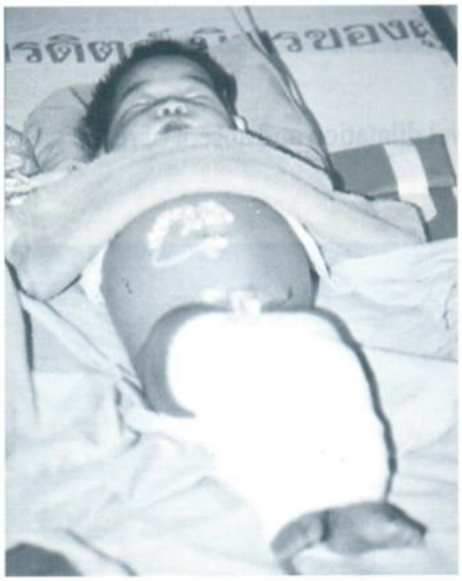

c

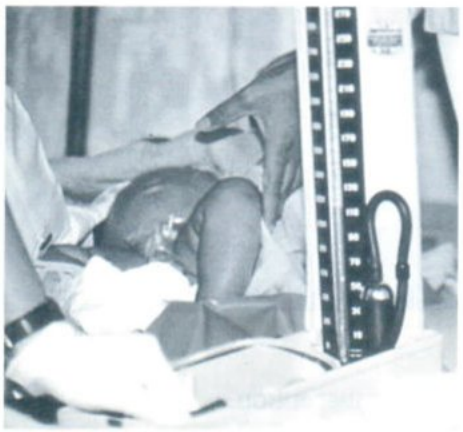

d

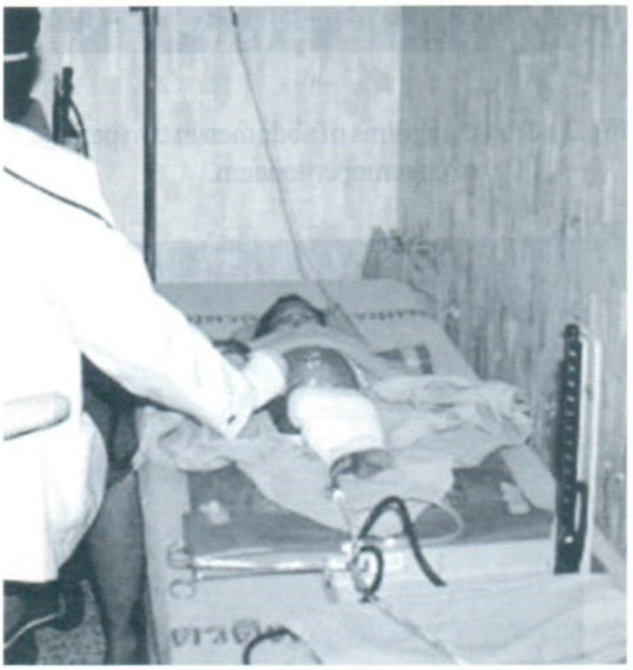

e

Fig.1 a & b system of rectal catheter sphygmomanometer and saline enema bag;

Fig.1c & d the patient hands and knees were wrapped with clothes; fig.1e reduction was monitored under ultrasound by radiologist.

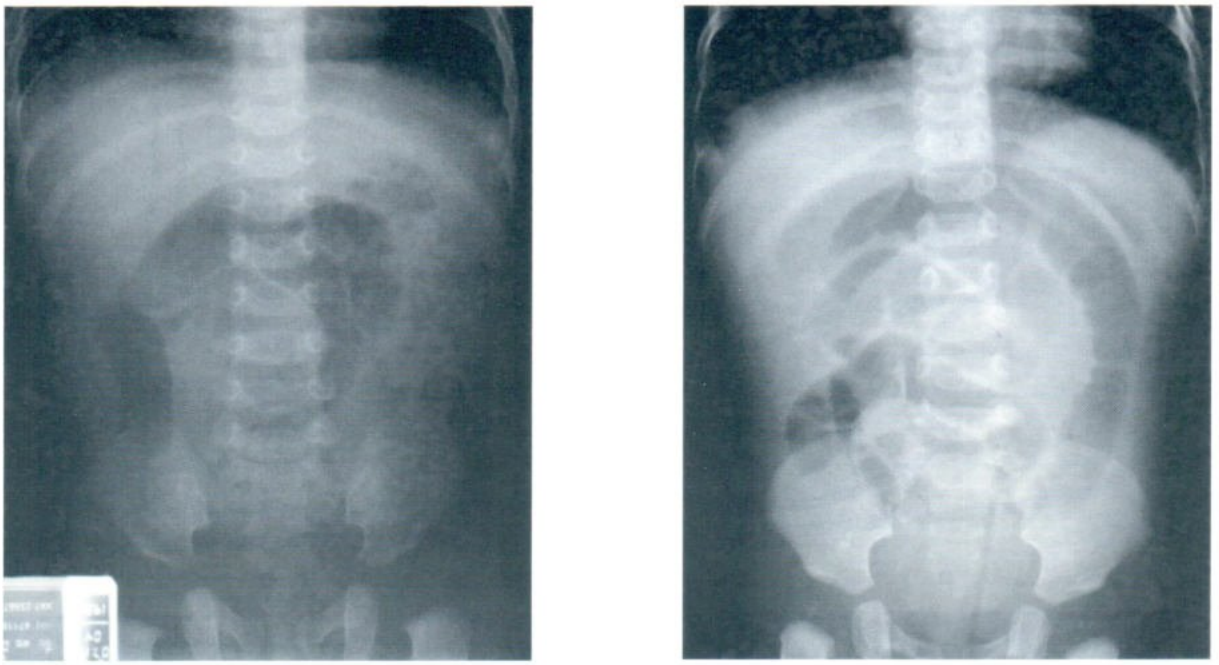

a b

Fig.2 a&b plain films of abdomen in two patients showing bowel dilatation and absent of rectal gas. No sign of pneumoperitoneum.

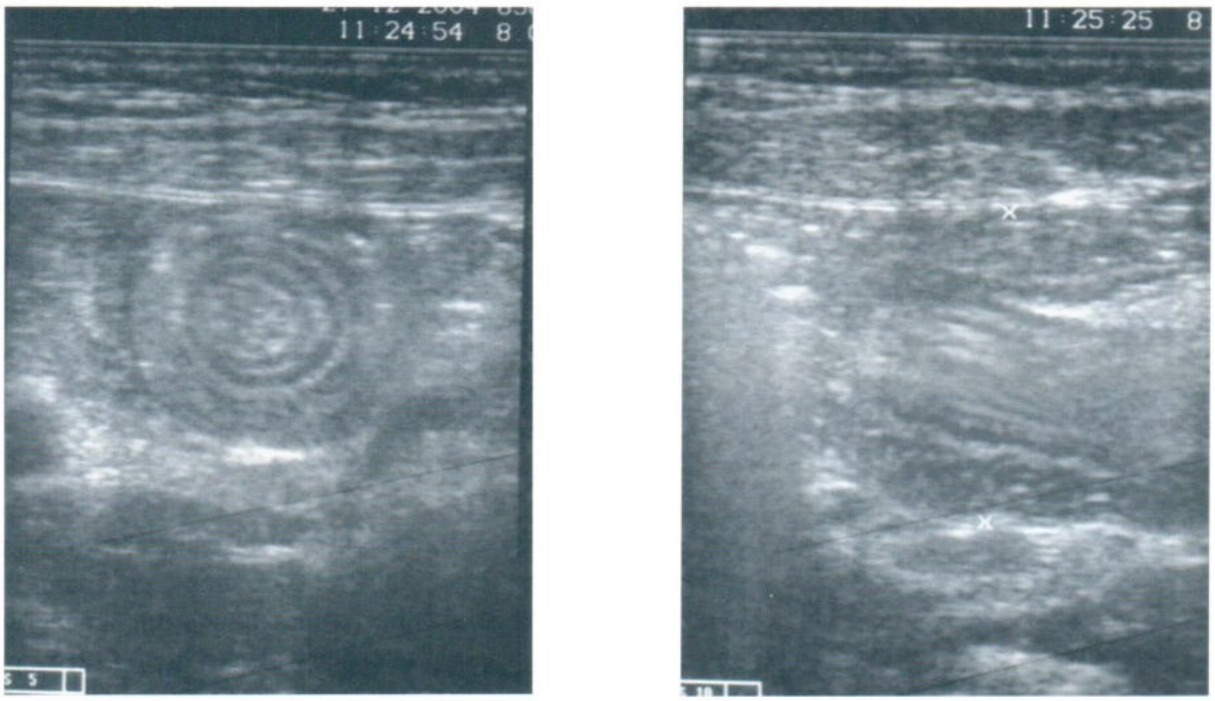

a **b**

Fig.3 a&b sonogram shows the target and pseudokidney signs of intussusception.

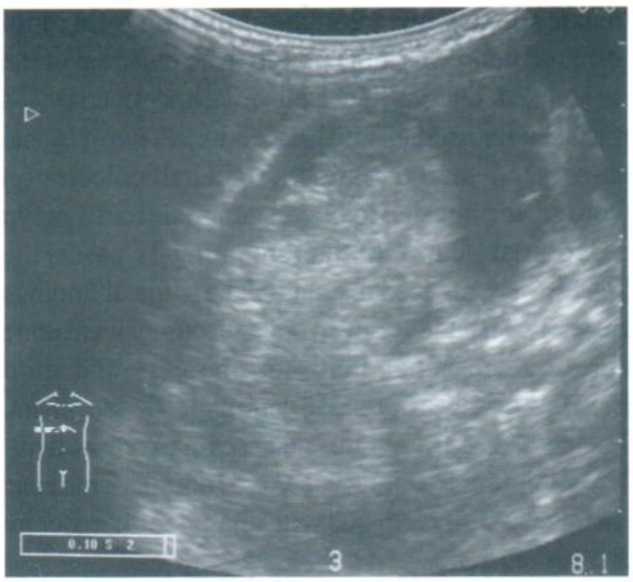

Fig 3c shows saline enema reduction with intussusceptum outlining by fluid.

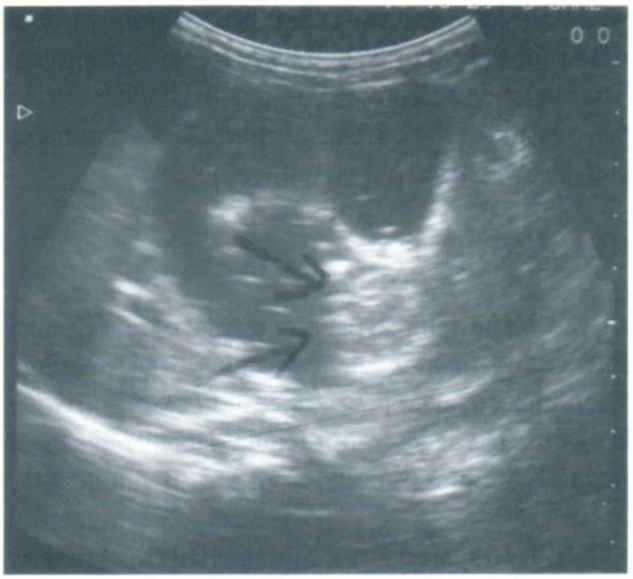

Fig 3d shows disappearance of intussusceptum from the cecum.

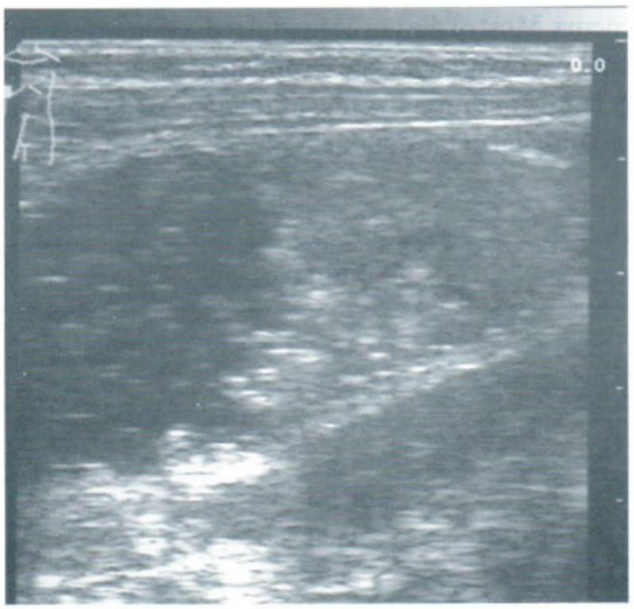

Fig.3e shows residual mucosal edema in cecum.

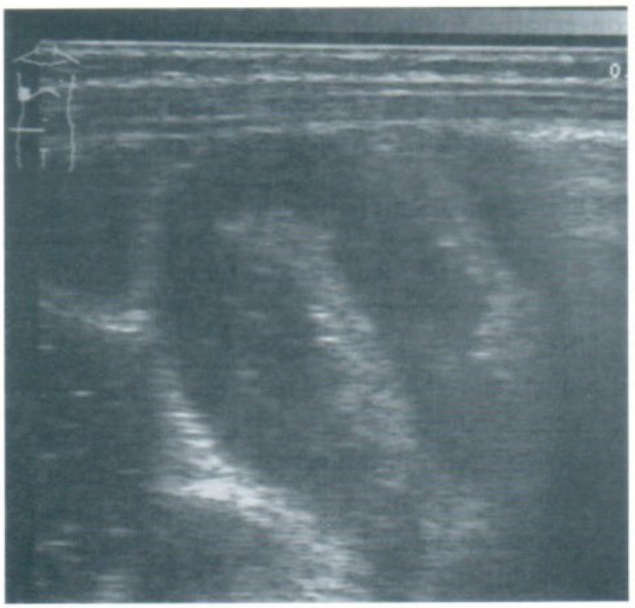

Fig.3f shows complete reduction, confirmed by unequivocal fluid filling the terminal ileum.

During reduction, the retrograde progression of the installed fluid was monitored. When the head of intussusceptum was outlined by the fluid, the contour and position change of the intussusceptum was observed while the procedure was on going until there was fluid filled terminal ileum and the intussusceptum disappeared. The peritoneal cavity was inspected intermittently for possible perforation indicated by sudden increased in fluid within the cavity or disappearance of fluid in the colonic lumen. The sonographic criteria for successful reduction are (a) complete disappearance of the intussusceptum from the large bowel and (b) unequivocal retrograde filling of the distal small bowel with fluid. Clinical recovery

was assured when the patients passed stool without mucus bloody stained and were free of symptoms. The reduction attempt was terminated if there was no progression of the intussusceptum after 3-5 minutes and the clinical status was unfavorable.

RESULTS

None of the 21patients displayed any clinical and/or radiographic contraindications to the reduction. The number of attempt was once in 17 cases and twice in 4 cases. The average time required for all reductions was 12.8 minutes (ranging from 5 to 20 minutes).

Reduction was successful in 4 cases (19.05%), as confirmed with US and the resolution of signs and symptoms of intussusception. There were 3 cases the results of which were uncertain but conservative follow up showed complete clinical recovery. Of the 14 cases underwent surgery, one also revealed no intussusception at surgery 5 hours after termination of hydrostatic reduction. These could be late spontaneous reductions or fluid reflux into terminal ileum was not enough to be detected or the residual edematous ileocecal valve and mucosa was mistaken for residual intussusception. In two surgical cases, segmental resections (right half colectomy) were performed due to bowel gangrene and a polyp in terminal ileum. In the remaining 11 cases, the bowels were reduced manually. The surgical findings are shown in table 1. Seven appendectomy were done due to acute appendicitis in one case and mild ischemic changes or mild inflammation in the others. There was recurrent intussusception in one patient. The symptom free interval was 5 months. This case was successfully reduced with air under fluoroscopy on the recurrence.

All patients have had no complication during or after hydrostatic reduction with normal saline enema. Most of the unsuccessful reduction cases who underwent surgery were terminated because of poor general conditions. A few of them were due to non progression of the intussusceptum.

Table 1 Clinical summary results

Clinical parameters	Number
US diagnosis of intussusception	33
Saline enema US-guided reduction	21
Success reduction	4
Conservative follow up	3
Surgical treatment	14
Manual reduction	11
Right half colectomy	2
- Gangrenous bowel	1
- A large polyp interminal ileum	1
appendectomy	7
No residual intussusception	1

DISCUSSION

The treatment of intussusception has long been a varied and controversial issue. Non-surgical reduction of an intussusception was first reported by Samuel Mithchell in 1836. Two years later, John Garham reported five cases treated by means of rectal insufflations of air. In 1876, Horald Hirschsprung

reported reduction of an intussusception by means of a hydrostatic enema with trans-abdominal manipulation.[19] After discovery of x-ray, radiography has been the method of choice for monitoring hydrostatic reduction of intussusception. This remains true despite the modern use of US for diagnosis. Most Thai radiologists are trained in this traditional way. In Eastern-Europe and North-America, barium sulfate suspension continues to be the contrast-enhancing enema solution used. It was only gradually and mainly in Western-Europe that barium began to be replaced by water-soluble contrast medium mixture in order to reduce complications in the event of perforation and to increase the success rate of non-surgical reduction. However, nowadays barium sulfate suspension remains the most widely used enema solution. The main reasons for this are probably conservative attitude and financial control. The retrograde insuflations of air or oxygen has been undergoing a renaissance in Western-Europe and being increasingly used in North-America for the reduction of intussusception. Although the method often requires shorter reduction time than with use of barium sulfate, the method still requires the use of fluoroscopy,

Performance of an enema with normal saline and US control for the hydrostatic reduction of childhood intussusception was first described by Kim et al in 1982. Thereafter, some authors report its efficacy in the non-operative management of intussusception with the use of saline solution or water of Hartmann solution.

However, there is continuing debate without general agreement about which is the best for reduction. The few randomized studies that have been performed did not show statistically significant differences in reduction and perforation rate between air and liquid enema.

In Thailand, reduction by air enema under fluoroscopy was introduced by Dr. Pantipa in 1982, at Queen Sirikit National Institute of Child Health (Children's Hospital) and has been performed as the standard reduction procedure at this institute until present (274 cases in 346 cases).[11] There is no report on the use of ultrasound controlled reduction of intussusception. In fact US is quite useful. Us is used not only for the diagnosis of intussusception but also for monitoring its reduction. Avoidance of ionizing radiation is the main advantage. The reduction success rate was 19.05% (4/21) with saline enema under US in this study. This result was less than the achievement of the other treatments that have shown a high reduction rate (76%-95%) with few complications (one perforation in 825 reports cases). The low success rate may be due to factors such as young experience, problem of colonic pressure control and the patient selection criteria which may have some roles in this study. The author believe that with increasing experience along the usual learning curve, it should be able to improve the success rate.

Analysis of unsuccessful 14 patients who underwent later surgery revealed that 9/14 had absolute surgical indications (table 1) while 5/14 did not. These cases without surgical indications might had been successfully reduced by non surgical reduction with improvement of technique.

The principal advantage of US-guided hydrostatic reduction is the lack of radiation exposure. As a result, there is no limitation to the procedure time allowing visualization of all components of the intussusception as well as easier recognition of leading points and residual intussusception. The evaluation of residual intussusception should be concluded with caution for beginner. There has been no report of serious complication during or after hydrostatic reduction with US guidance. Low perforation rate (0.26%) without mortality was reported. There has been no complication in our series.

Although high pressure values reported in pneumatic reductions lead to an increased success rate to more than 90% as well as offer an easy and clean technique, they need more x-ray exposure time, visualize only intraluminal contrast and produce a high rate of perforation. There is no complication in those

unselected patients in Uttaradit Hospital. Raising the instillation pressure with caution in some suitable patients together with increasing experience with the technique may result in a further increase in the success rate.

In conclusion, US is a simple and reliable modality for diagnosis and monitoring hydrostatic reduction of intussusception. New trainees and experien ced practitioners alike should be encouraged to be familiar with the usage of this new technique.[4] In the future, this radiation-free reduction method should become more widely accepted.

REFERENCES

1. John R. Sty, MD; Robert G. Wells. MD; Robert J. Starshak, MD; David C. Gregg, MD. Diagnostic Imaging of Infants and Children: Aspen Publishers, Inc 1992 P 187-190.
2. Hutchinson IF, Olayiwola B, Young DG. Intussusception in infancy and childhood. Br J Surg. 1980; 67: 209-212.
3. Ein SH, Stephens CA. Intussusception: 354 cases in 10 years, J Pediatr Surg. 1971; 6: 16-27.
4. Richard I, Markowitz, MD. James S. Meyer MD. Pneumatic versus hydrostatic Reduction of intussusceptions. Radiology 1992; 183: 623-624.
5. Seong Ku Woo, MD. Jung Sik Kim, MD. Tae Won Paik, MD. Soon Ok Choi, MD. Childhood intussusception: US-guided hydrostatic reduction Radiology 1992; 182: 77-80.
6. Thomas W. Riebel, MD. Rohangiz Nasir, MD. Kerstin Weber MD. US-guided hydrostatic Reduction of intussusception in children. Radiology 1993; 188: 513-516.
7. Kim YG, Choi BI, Yeon KM, Kim CW. Diagnosis and treatment of Childhood intussusception using real-time ultrasonography and saline enema: preliminary report. J Korean Soc Med Ultrasound 1982; 1: 66-70.
8. Bolia AA. Case report: diagnosis and hydrostatic reduction of an intussusception under ultrasound guidance. Clin Radiol 1985; 655-657.
9. Wang GD, Liu SJ. Enema reduction of intussusception by hydrostatic pressure under ultrasound guidance: a report of 377 cases. J. Pediatr Surg 1988; 23: 814-818.
10. Yoon CH, Kim HS Ultrasound guided reduction of childhood intussusception. J Korean Radiol Soc 1986; 22: 788-793.
11. Kruatrachue A, Wongtapradit L, Nithipanya N, Ratanaprakarn W. Result of Air Enema Reduction of Intussusception at Queen Sirikit National Institute of Child Health (Children's Hospital) since 1992-2001.
12. Swischuk LE, Hayden CK Jr, Boulden T. Intussusception: indications for ultrasonography and an explanation of the doughnut and pseudo -kidney sign. Pediatr Radiol 1985; 15: 388-391.
13. Tran-Minh VA, Praeros JP, Massard PE, Louis D, Pacross-Deffrenne P. Diagnosis of acute intestinal intussusception (All) by real-time ultrasonography: evaluation in 176 children with symptoms suspicious for All (Abstr). Pediatr Radiol 1985; 15: 267-268.
14. Bisset GS III, Kirks DR. Intussusception in infants and children: diagnosis and therapy. Radiology 1988; 168: 141-145.
15. Verschelden P, Filiatrault D, Garel L, et al. Intussusception in children: reliability of US in diagnosis-a prospective study. Radiology 1992; 184: 741-744.
16. Woo SK, Kim JS, Suh SJ, Paik TW, Choi SO. Childhood intussusception: US-guided hydrostatic reduction. Radiology 1992; 182: 77-80.
17. Riebel TW, Nasir R, Weber K. US-guided hydrostatic reduction of tntussusception in children. Radiology 1993; 188: 513-516.
18. Swischuk LE, John SD, Swischuk PN. Spontaneous reduction of intussusception: verification with US. Radiology 1994; 192: 269-271.
19. Gloria del-Pozo, MD., Jose C. Albillos, MD., Daniel tejedor, MD., Rosa Calero, MD., Miguel Rasero, MD., Urbano de-la-Calle, MD., Ulpiano Lopez-Pacheco, MD. Intussusception in Children: Current Concept in diagnosis and Enema Reduction. Radiographic 1999; 19: 299-319

NORMAL VALUES OF UPPER CRANIOFACIAL SKELETAL MEASUREMENTS OF THAI PATIENTS IN UDONTHANI HOSPITAL BASED ON COMPUTED TOMOGRAPHY

Khomdao BOONCHIT, M.D.[1]

ABSTRACT

This study was performed to establish normal values of the upper craniofacial skeleton of 1026 Thai patients in Udonthani hospital using CT scan. The samples were collected from july 2006 to july 2007, age ranging from newborn to 82 years. The measurement values were divided into four age groups, for those under the age of 1 year, 1 year, morethan 1 year upto 17 years and more than 17 years in the last category. No comparison between genders in this study, except in the subjects with the age of more than 24 years and these increase gradually to adult sizes. The size of these measurement increase rapidly to about 85 % of adult sizes by the age of 5 years and then increases gradually to adult sizes. The ability of Computed Tomography (CT scan) to identify bony and soft tissue features makes it particularly useful for the management of craniofacial disorders. The normal values of the upper craniofacial skeleton of Thai patients in Udonthani hospital are useful for the accurate diagnosis and reconstructive surgery planning of Thai patients in Udonthani and Northeastern Thailand.

INTRODUCTION

Knowledge of normal measurement values in the craniofacial region will help to improve diagnostic accuracy for presurgical reconstruction planning and postsurgical follow-up of patients of craniofacial anomalies such as orbital hypertelorism in Frontoethmoidal Encephalomeningocele, craniosynostosis syndrome, frontonasal dysplasia and facial clefts.

Current techniques in craniofacial surgery would benefit from objective (quantitative), as well as the current subjective (quanlitative) and radiographic assessment which are to be considered in the planning and execution of craniofacial bony reconstruction. Measurement of certain skeletal dimensions is essential for the accurate diagnosis and planning for reconstructive surgery.

Various methods have been used in the past to indirectly analyze the craniofacial region such as anthropometry[1] which is limited in its capacity to develop accurate normative standards for the craniofacial complex, because they are influenced by overlying soft tissues and is therefore unreliable in the assessment of the skull. Cephalometric radiography[2,3] and cephalometrics with multiplane and finite-element scaling analysis.[4] are inaccurate because of the enlargement and distortion of the image, structures overlapping, limited identifiable landmarks and positioning problems in the taking of the radiograph.

The other method is direct measurement in cadaveric skull.[6]

[1] Department of Radiology, Udonthani hospital, Udonthani 41000, Thailand

Quantitative CT measurement in the craniofacial region would be a useful adjunct to existing treatment methods, window setting, quality control and CT calibration error, partial-volumn effect, patient positioning, display/film distortions, spatial uniformity, resolution, scan noise and artifacts affect CT images.[7,8] However CT is now an established key modality in the diagnosis, surgical planning and follow up of craniofacial anomalies.[9] The intraobserver error, interobserver error and accuracy of CT linear measurements were all within acceptable limits (range, 0.4 to 0.9 mm.).[10] Three-dimentional CT of the craniofacial region was very accurate.[11]

The error of CT measurements of the upper craniofacial skeleton was within clinically acceptable limits (less than 5 percent) if the angle tilt was no more than ± 4 degree from 0 degree setting (baseline or orbitomeatal line).[12]

Normal values of craniofacial skeletal measurements are analyzed such as craniofacial anthropometry in Turkish population,[13] roentgen-cephalometric standards for a Swedish population,[14] growth of interorbital distance and skull thickness as observed in roetgenographic measurements,[15] bony interorbital distance,[16] CT in the evaluation of the orbit and the bony interorbital distance,[17] the study of normal interorbital distance of Oriental adults,[6] craniofacial skeletal measurements based on Computed Tomography.[12]

The purpose of this study was to provide normal values of the upper craniofacial region of Thai patients in Udonthani hospital taken from CT scans.

MATERIAL AND METHODS

The measurements in the present study were obtained from Thai population subjects of different ages who went to have CT scan in Udonthani hospital. The 1026 samples were collected from july 2006 to july 2007, ranging in age from newborn to 82 years.

CT scans in Udonthani hospital were obtained from an Elscint EXEL 2400 ELECT CT scanner. All patients were positioned by laser-light guiding for scanning in the orbitomeatal line. Head position was maintained with restraints and confirmed with a scan film.

Exclusion criterias are asymmetric scans, syndrome and diseases affecting craniofacial skeleton such as congenital anomalies, orbital and sinus diseases, fracture or previous surgery. Rotation of the subject can be determined by the distance between each orbital rim, adjacent facial bones and skull.

The growth levels gradually stop at about 13 years of age in girls and 21 years of age in boys, similar to other areas of the upper face and midface.[16] Generally, facial growth changes minimally after late adolescence (17-20 years of age).[17] So the measurement values were divided into four age groups for those under 1 year of age, 1-year age categories, from more than 1 to 17 years, and then more than 17 years in the last category.

MEASUREMENTS

A series of five parameters (table1) was obtained from the CT scan of each subject. The measurements were performed in picture archiving, with bone window setting (window width 1500 H.U. and window level 200 H.U.) The process of measurements was performed by the author (twelve-year experienced radiologist).

TABLE 1 Computed Tomographic measurements of the Craniofacial Skeleton

Measurement	Description
1. Interorbital distance	The distance between bilateral dacryons (junction of the frontal, lacrimal and maxillary bones) (Fig.1)
2. Anterior interorbital distance	The distance between a point on each lacrimal bone representing the anterior end of the medial orbital wall. (Fig.1)
3. Mid interorbital distance	The distance between a point on each medial wall of the bony orbit (ethmoid bone) midway between the lacrimal bone and the base of the optic strut. (Fig.2)
4. Lateral orbital distance	The distance between the most anterior tip of each lateral orbital wall. (Fig.2)
5. Intertemporal distance	The distance between the most medial aspect of each temporalis groove. (Fig.3)

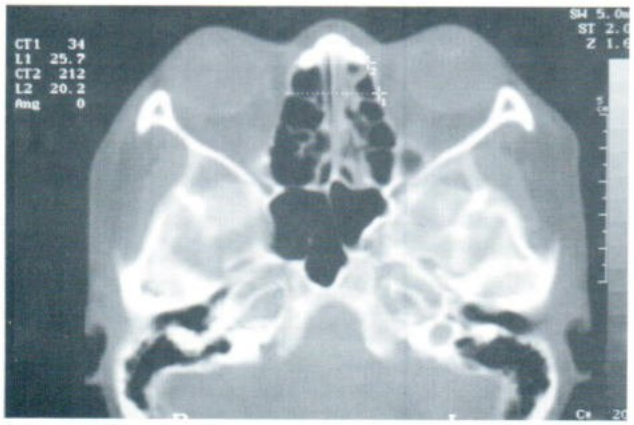

Fig. 1 1. Interorbital distance
2. Anterior interorbital distance

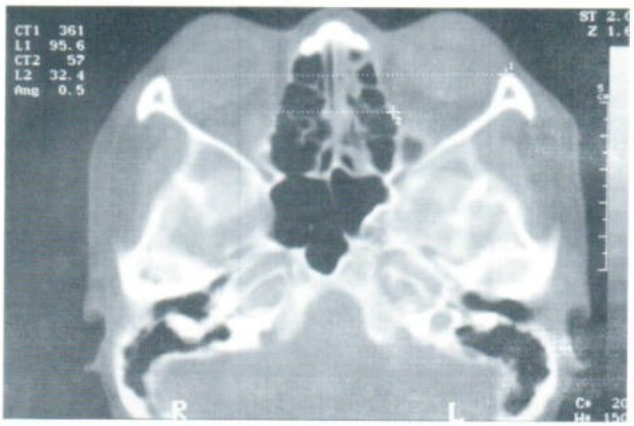

Fig.2 1. Lateral orbital distance
2. Mid interorbital distance

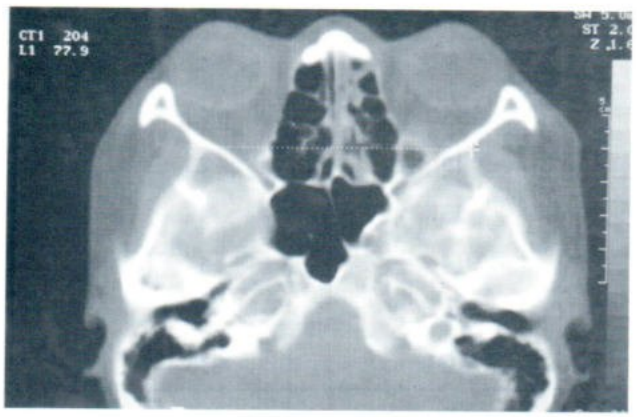

Fig.3 1. Intertemporal distance

ANALYSIS

The age and sex distribution of Thai patient population of this study is shower in Table2.

SAS statistical procedures were used for all calculations. Statistical differences between group means were tested by the Student's t-test. Group means, standard deviations and 95 % confidence intervals for individual predicted values were calculated since the purpose of this study was to produce normative values (table 3 and 4). Test statistics associated with probabilities of 0.05 or less were considered significant, and all probability (p) values quoted were two sides.

RESULTS

TABLE 2 Sex Distribution of Study Population

Age Category	Males	Females	Total
0-3 mo	2	4	6
4-6 mo.	3	3	6
7-9 mo.	4	4	8
10-11 mo.	1	2	3
1 yr.	3	3	6
2 yr.	6	2	8
3 yr.	5	4	9
4 yr.	4	3	7
5 yr.	6	2	8
6 yr.	2	4	6
7 yr.	5	6	11
8 yr.	6	2	8
9 yr.	6	3	9
10 yr.	7	2	9
11 yr.	4	4	8
12 yr.	8	4	12
13 yr.	11	4	15
14 yr.	15	2	17
15 yr.	13	4	17
16 yr.	14	5	19
17 yr.	12	7	19
>17 yr.	435	330	765
Total	622	404	1026

TABLE 3 Means, Standard deviation and Ninety-Five Percent Confidence Intervals of interorbital distance, anterior interorbital distance and mid interorbital distance (mm.)

Age	Interorbital distance			Anterior interorbital distance			Mid interorbital distance		
categories	Mean	SD	95% CI	Mean	SD	95% CI	Mean	SD	95% CI
0-3 mo.	15.66	2.20	10.19-21.13	17.63	1.98	12.70-22.56	16.03	1.87	11.37-20.69
4-6 mo.	17.63	2.13	12.32-22.93	18.23	4.61	12.32-22.93	18.05	3.54	14.32-21.77
7-9 mo.	17.21	2.55	15.07-19.34	18.46	2.51	13.56-22.30	18.36	2.13	13.06-23.67
10-11 mo.	17.51	2.50	15.35-19.79	18.56	3.30	14.52	18.51	2.89	14.39-22.66
1 yr.	17.93	2.17	15.65-20.21	18.67	3.37	15.65-20.21	18.67	3.37	15.85-21.43
2 yr.	18.46	2.21	12.95-23.97	19.23	4.45	14.55-23.90	19.20	1.72	15.68-23.04
3 yr.	18.46	2.21	12.95-23.92	19.28	2.62	17.08-21.08	19.86	3.00	12.39-27.34
4 yr.	19.20	4.84	11.15-26.24	19.60	1.95	16.23-20.96	23.08	2.25	21.20-24.97
5 yr.	21.02	1.06	19.32-22.72	20.50	3.54	14.86-26.13	24.10	0.23	23.73-24.46
6 yr.	21.60	1.97	19.95-23.24	20.73	2.91	18.29-23.17	24.01	1.42	22.81-25.20
7 yr.	24.75	2.07	20.11-25.38	21.05	3.04	15.76-26.86	26.06	4.00	16.12-36.00
8 yr.	24.03	1.92	19.24-28.82	21.27	3.61	10.36-28.30	27.40	0.98	18.50-36.29
9 yr.	24.26	1.79	22.76-25.76	21.33	3.45	18.45-24.22	29.82	1.53	28.54-31.10
10 yr.	24.80	2.70	20.06-23.53	22.06	2.49	13.86-26.26	29.93	3.76	20.58-34.28
11 yr.	24.10	1.78	21.31-26.88	22.22	0.91	20.77-23.67	28.32	3.40	22.90-33.74
12 yr.	25.77	1.84	24.22-27.32	22.45	2.33	20.49-24.40	30.27	2.27	28.37-32.17
13 yr.	26.12	2.41	24.58-27.66	22.98	3.25	19.97-25.99	32.49	2.87	30.66-34.31
14 yr.	25.72	3.37	22.60-28.85	23.97	4.60	21.04-26.90	31.57	4.02	27.84-35.29
15 yr.	24.52	5.27	21.81-27.23	21.59	2.27	20.42-22.76	31.49	1.76	30.58-31.39
16 yr.	27.76	1.85	26.34-29.19	21.31	3.37	19.68-22.94	31.66	3.38	29.06-34.26
17 yr.	26.08	2.46	24.89-27.27	24.86	2.64	22.83-26.89	31.12	2.77	29.78-32.46
> 17 yr.	26.59	2.39	24.42-28.76	23.45	2.93	23.24-23.65	31.46	4.68	26.13-31.79

SD = standard deviation, CI = confidence interval for individual predicted values

TABLE 4 Means, Standard deviation and Ninety-Five Percent Confidence Intervals of Lateral orbital distance and intertemporal distance (mm.)

Age categories	Lateral orbital distance			Intertemporal distance		
	Mean	SD	95% CI	Mean	SD	95% CI
0-3 mo.	65.32	4.90	54.18-72.19	61.16	0.25	60.54-61.79
4-6 mo.	68.36	3.83	58.82-77.90	68.26	5.25	59.28-77.25
7-9 mo.	67.86	7.34	49.60-86.12	67.46	6.73	50.72-84.20
10-11 mo.	72.05	7.07	58.67-82.63	67.69	6.01	56.52-78.87
1 yr.	73.45	6.81	67.75-79.14	67.93	6.70	62.33-73.54
2 yr.	73.60	8.44	64.73-83.46	66.30	4.45	56.38-76.21
3 yr.	78.50	4.44	67.46-89.53	68.56	3.62	59.56-77.57
4 yr.	82.16	3.87	78.92-85.40	69.66	6.00	57.30-82.02
5 yr.	82.35	1.23	80.37-84.32	72.60	3.59	66.88-78.31
6 yr.	84.81	3.54	81.85-87.77	73.08	3.67	69.84-76.32
7 yr.	86.86	0.40	85.86-87.87	73.83	5.04	69.62-78.05
8 yr.	89.77	2.02	67.79-84.55	76.17	5.26	67.79-84.55
9 yr.	89.86	1.70	85.63-94.09	76.72	4.48	72.97-80.47
10 yr.	90.51	2.43	88.47-92.55	73.73	3.32	65.46-82.00
11 yr.	91.50	4.24	73.38-109.61	77.10	3.67	64.04-90.18
12 yr.	90.88	8.04	79.41-102.34	77.07	3.11	74.18-79.95
13 yr.	92.68	3.89	89.08-96.28	78.81	4.31	76.07-81.55
14 yr.	92.82	1.97	91.16-94.48	80.33	3.17	77.67-82.99
15 yr.	97.04	3.68	95.15-98.94	80.27	3.87	78.27-82.26
16 yr.	98.06	4.98	94.23-101.89	81.31	4.59	77.77-84.84
17 yr.	95.57	4.70	93.30-97.83	79.74	5.23	77.22-82.27
>17 yr.	96.45	6.20	96.01-96.88	79.14	4.34	78.84-79.44

SD = standard deviation, CI = confidence interval for individual predicted values

DISCUSSION

1026 Thai patient population who went to have CT scan in Udonthani hospital ranging in age from newborn to 82 years from july 2006 to july 2007 and five parameters of the upper craniofacial skeleton were measured. These distances change with age which were verified in the present study (table3 and 4). The overall size of them reaches about 85 % of adult sizes by the age of 5 years and then increases gradually to adult. No comparison between males and females within each age study group of newborn, children to late adolescence because female patients in this study may have been too small. The patient ages more than 24 years old were compared between genders with also comparison between these data and the report of Mafee MF et al. (1986)[17](table 5).

TABLE 5 CT evaluation of the interorbital distance in adults (age>24 years)(mm.)

	Number of patients	Minimum		Maximum		Mean	
		Male	Female	Male	Female	Male	Female
Mafee MF et al.	400	22.9	22.9	32.1	32.0	26.7	25.6
Udonthani hospital	724	20.60	19.20	35.60	31.40	27.14	25.87

In 1992, Waitzman et.al 18 retrospectively define normal values for a series of craniofacial measurements. (table 6)

TABLE 6 Means and standard deviations of the orbital region (mm.)

	Age categories	Number of patients	Anterior interorbital distance	Mid interorbital distance	Lateral orbital distance	Intertemporal distance
Waitzman et al.	17 yr.	16	23.8±1.7	27.5±2.3	95.3±5.9	78.7±6.1
Udonthani hospital	17 yr.	19	24.86±2.64	31.12±2.77	95.57±4.70	79.74±5.23

The discrepancies between different studies may be the result of differences in race and population size used. The error of CT measurements is patient positioning. I suggest that the normal values of the upper craniofacial skeleton depend on age, sex and race which in my study, they are useful for the accurate diagnosis and reconstructive surgery planning of Thai patients in Udonthani and Northeasten Thailand.

REFERENCES

1. Farkas LG. Anthropometry of the head and face in medicine. New York:Elsevier,1981.
2. Broadbent B. A new X-ray technique and its application to orthodontia. Angle Orthod. 1931; 1:45.
3. Moyers RE., Bookstein FL. The inappropriateness of conventional cephalometrics. Am J Orthod 1979;75:599-617.
4. Grayson BH, McCarthy JG, Bookstein F. Analysis of craniofacial asymmetry by multiplane cephalometry. Am J Orthod 1983; 84: 217-24.
5. Richtsmeier J. Comparative study of normal, rouzon, and Apert craniofacial morphology using fine element scaling analysis. Am J Phys Anthropol 1987; 74: 473-93.
6. Nond Rojvachiranonda, Taom Bunaprasert, Prachya Maglin, Thawatchai Watanakajorn. The study of normal interorbital distances of oriental adults:a preliminary report. Chula Med J 1998; 42(10): 945-52.
7. McCullough EC. Factors affecting the use of quantitative information from a CT scanner. Radiology 197; 124: 99-107.
8. Baxter BS, Sorenson JA. Factors affecting the measurement of size and CT number in computed tomography. Invest Radiol 1981;16:337-41.
9. Becker M. Computed tomography in the evaluation of the craniofacial malformations. In: Converse JM, McCarthy J, Wood-Smith D, eds. Symposium on diagnosis and treatment of craniofacial anomalies. Vol 20. St. Louis: Mosby, 1979; 182.
10. Christiansen EL, Thompson JR, Kopp S. Intra - and interobserver variability and accuracy in the determination of linear and angular measurements in computed tomography. An in vitro and in situ study of human mandibles. Acta Odonto Scand 1986; 44: 221-9.
11. Matterson SR, Bechtold W, Philips , Staab E. A method for three-dimentional image reformation for quantitative cephalometric analysis. J Oral Maxillofac Surg 1989; 47: 1053-61.
12. Waitzman AA, Posnick JC, Armstrong DC, Pron GE. Craniofacial skeletal measurements based on computed tomography: Part I. Accuracy and reproducibility. Cleft Palate -Craniofacial J 1992; 29: 112-7.
13. Evereklioglu C, et al. Craniofacial Anthropometry in a Turkish Population. Cleft Palate -Craniofacial J 2002; 39: 208-18.
14. Thilander B, Persson M, Adolfsson U. Roentgen-cephalometric standards for a Swedish population. Eur J Orthod 2005; 27: 370-89.
15. Hansman CF. Growth of interorbital distance and skull thickness is observed in roentgenographic measurements. Radiology 1996; 86: 87-96.
16. Costaras M, Pruzansky S, Broadbent BH Jr. Bony interorbital distance (BIOD), head size, and level of the cribiform plate relative to orbital height: 1. Normal standarcs for age and sex. J Craniofac Genet Dev Biol 1982; 2: 5-18.
17. Mafee MF, et al. CT in the evaluation of the orbit and the bony interorbital distance. Am J Neuroradiol 1986; 7: 265-9.
18. Waitzman AA, Posnick JC, Armstrong DC, Pron GE. Craniofacial skeletal measurements based on computed tomography: Part II. Normal values and growth trends. Cleft Palate-Craniofacial J 1992;29:118-28.

THE IMAGE QUALITY AND PATIENT DOSES IN SIMPLE RADIOGRAPHIC EXAMINATIONS: ESTABLISHING GUIDANCE LEVELS AND COMPARISON WITH INTERNATIONAL STANDARDS.

Anchali KRISANACHINDA,[1] Kiat ARJHANSIRI,[1]
Petcharleeya SUWANPRADIT[2]

ABSTRACT

The International Atomic Energy Agency (IAEA) mentioned in the International Basic Safety Series Number 115 that the optimization of medical exposure should be considered in the terms of the image quality and the radiation dose the patient received. The guidance levels (GL) for medical exposure should be established as the intention to be an indication of doses for averaged size patients. It should be applied with flexibility to allow higher exposures with clinical judgments and should be revised as technology and technique improve. This study is part of IAEA Research which the data were collected at two sites with high load on simple radiographic examinations. The reject analysis was as high as seven percents and the patient skin dose was also higher than the IAEA GL for the chest examination at one site. After reviewing of the data, the education and training for the technologists were immediately scheduled. The quality control was regularly performed and the patient dose was reduced as the high kVp technique was implemented. The maximum skin dose was within the guidance level. It is recommended that the image quality, the retake analysis and the patient skin dose should be obtained and reviewed regularly. The National GL should be established by the professional societies and the National Atomic Energy Authority for the benefit of the patients.

INTRODUCTION

The International Basic Safety Standards[1] (BSS) requires attention to image quality of radiography which corrective action is considered. Poor image quality results in unnecessary radiation exposure to patients and the unjustified exposure which wastes the resource. The diagnostic requirements presented as image criteria[2] for a particular type of radiograph are those deemed necessary to produce an image of standard quality. The criteria for radiation dose to the patient are expressed in terms of a reference dose value for each type of radiograph which is based on the third quartile (75 percentile) value seen in national patient dose surveys. Its purpose, if it is exceeded, as to initiate an immediate investigation into the reasons for using relatively high dose techniques and to trigger appropriate corrective action. The reference dose value can be taken as a ceiling from which progress should be pursued to lower dose levels in line with the ALARA (as low as reasonably achievable) principle. Compliance with the image and patient dose criteria was possible when the recommended techniques were used. To encourage widespread use, the image criteria have been expressed in a manner requiring personal visual assessment rather than objective physical measurements which need sophisticated equipment unavailable to most departments. However, the assessment of compliance with the criteria for

[1] Department of Radiology, Faculty of Medicine, Chulalongkorn University
[2] Department of Radiology, King Chulalongkorn Memorial Hospital, Bangkok

radiation dose to the patient for a specific radiograph unavoidably involves some form of dose measurement. This requires representative sampling of the patient population. BSS also requires the establishment of Guidance Level (GL) for the country. These can be obtained if the national quality control program is implemented. The retake analysis is the good indicator for the image quality which should be considered closely to the patient dose.

MATERIALS

Two X-ray systems were studied at King Chulalongkorn Memorial Hospital (KCMH) in Bangkok as detail in table 1.

TABLE 1 2 X-ray systems of details of manufacture and model used in the study.

Hospital	Manufacturer	Model	Year of Installation
King Chulalongkorn Memorial Hospital	Hitachi	DR-155HM	1989
	Toshiba	KXO 80G/DST 101 A/DG 80G	2005

METHODS

The study consists of two phases. The first phase involves the image quality and the second phase involves the patient dose and guidance level. The details are as following:

Phase I The study of film retake rate and the image quality

1. Identify the radiographic site for the detail of the x-ray equipment.
2. Collect for film retake rate at the radiographer level, image quality grading in A, B and C by radiologists (A-Clearly accepted without any remark or reservation, B - accepted with some remarks or reservations, C - rejected.)
   - 2.1 Collect data within 2 weeks
   - 2.2 Daily record of film used, retake rate as in B and C.
   - 2.3 Analyze the causes of retake such as
     - 2.3.1 Over & under exposure
     - 2.3.2 Artifacts
     - 2.3.3 Field size misplacement
     - 2.3.4 Processing problem
   - 2.4 Educate radiographers in order to improve the retake rate.
   - 2.5 Redo 2.2-2.3
   - 2.6 Report the changes in retake rate and image quality.

Phase II Patient dose determination and Guidance Level (GL)

1. Perform quality control of x-ray equipment, record air kerma for patient dose calculation.
2. Record exposure parameters of kVp, mAs, for chest PA, abdomen AP, lumbar spine AP and lateral, skull and pelvis approximately 10 cases for each projection.
3. Perform patient dosimetry in terms of entrance skin air kerma, ESAK
4. Rectify the problem from QC results in 2
5. Repeat patient dosimetry to obtain the changes in patient doses
6. Compare the results with GL of BSS.

RESULTS

I. Film retake rate and image quality

This work is performed in two parts: one at the radiographer's level and the second at the radiologist's level.

1. Radiographer: Keep daily record of total number of films used and films rejected in a particular room; estimate the repeat rate at radiography room and dark room level and complete the radiographer's part of the form.
2. Radiologist: Grade the remaining radiographs using Table 2 according to:

A: radiograph clearly accepted without any remarks

B: radiograph accepted with some remarks, and
C: radiograph should be rejected

TABLE 2 Retake analysis at Out-Patient-Department (Hitachi 1989) and at Emergency Room (Toshiba 2005).

Room No.	**OPD Room 5**	
Time period of the analysis (mm.yy)	From_04,06 to __05,06__	
At the level of RADIOGRAPHER		
Number of films used during 2 weeks	**489**	
Number of films rejected by radiographer	**37**	
Percentage of films rejected by radiographer	**7.57**	
At the level of RADIOLOGIST (use Table 1)		
	Number	**Percentage**
A grade films	244	49.9
B grade films	208	42.5
C grade films	37	7.6
TOTAL	**489**	**100%**
Cause analysis (B and C graded films)		
Over- & under-exposure	2	0.82
Artefacts	5	2.04
Field size misplacement	1	0.41
Processing problems	3	1.22
Other, Positioning, etc.	234	95.5
TOTAL	**245**	**100%**

Room No.	**Emergency**	
Time period of the analysis (mm.yy)	From_04,06 to __05,06__	
At the level of RADIOGRAPHER		
Number of films used during 2 weeks	**610**	
Number of films rejected by radiographer	**44**	
Percentage of films rejected by radiographer	**7.2**	
At the level of RADIOLOGIST (use Table 1)		
	Number	**Percentage**
A grade films	255	41.8
B grade films	311	51.0
C grade films	44	7.2
TOTAL	**610**	**100%**
Cause analysis (B and C graded films)		
Over- & under-exposure	5	1.4
Artefacts	5	1.4
Field size misplacement	2	0.56
Processing problems	3	0.84
Other-Positioning	340	95.8
TOTAL	**355**	**100%**

II Quality Control of x-ray equipment and ESAK measurement

Use a suitable detector (e.g.: ionisation chamber) to measure air kerma (mGy) at 1m focus-detector-distance for different kVp settings. Divide the resulting dose by the applied mAs in order to get mGy/mAs as in Table 3 and plot these values against the kVp as in figure1. From this curve we can determine for a given kVp and mAs the air kerma at 1m AK(100cm). The ESAK can be calculated using AK (100 cm) and the focus-patient surface-distance FSD as in the following equation:

$$\mathbf{ESAK = AK(100cm)*(100/FSD,cm)^2}$$

TABLE 3 Air Kerma, AK measurement at 1 meter and AK/mAs determination at Out-Patient-Department (Hitachi 1989)

kVp	mAs	AK in 1 m (mGy)	AK/mAs (mGy/mAs)
40	25	0.245	0.0098
50	25	0.488	0.0196
60	25	0.93	0.0373
70	25	1.29	0.0518
80	25	1.75	0.07
90	25	2.184	0.0874
100	25	2.652	0.106
110	25	3.141	0.126
120	25	3.465	0.139

Figure 1 The linear response of the kilovoltage and the air kerma per milliampere-sec

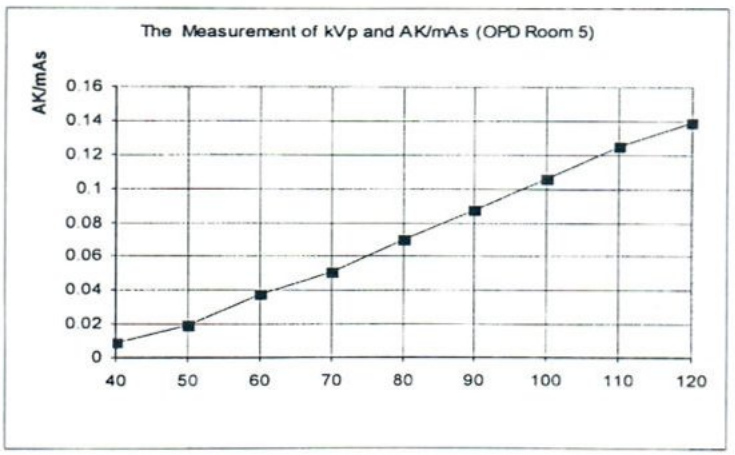

TABLE 4 Evaluation of ESAK for patient chest, lumbar spine, abdomen, skull and pelvis at OPD room 5.

Room No.	OPD Room 5		
Chest PA/ Patient ID	**kVp**	**mAs**	**ESAK, mGy**
1. 10279847	80	20	0.540
2. 3175549	77	16	0.407
3. 3916749	80	16	0.427
4. 11137047	80	16	0.421
5. 4533128	80	14	0.388
6. 4973649	80	16	0.438
7 .11049348	80	16	0.438
8. 3224049	80	20	0.550
9. 12348239	80	14	0.364
10.10969443	80	20	0.554
Lumbar spine AP/ Patient ID	**kVp**	**mAs**	**ESAK, mGy**
1. 1304437	80	64	5.919
2. 3175549	70	50	3.197
3. 2603449	80	64	6.349
4. 8195647	75	50	4.056
5. 11705444	75	64	5.315
6. 421845	75	64	5.574
7. 9434832	75	64	5.574
8. 3175549	80	50	4.96
9. 5236438	80	64	6.349
10.3928249	80	64	6.503
Lumbar spine lateral/ Patient ID	**kVp**	**mAs**	**ESAK, mGy**
1. 1304437	85	126	13.717
2. 3175549	80	64	6.663
3. 2603449	85	126	14.765
4. 8195647	80	100	10.937
5. 11705444	80	126	15.270
6. 421845	80	126	15.270
7. 9434832	80	100	11.216
8. 3175549	80	126	15.939
9. 5236438	85	126	17.0
10.3928249	80	126	14.132
Pelvis AP/ Patient ID	**kVp**	**mAs**	**ESAK, mGy**
1.121667	75	50	5.629
2.11938	75	52	5.262
3.122503	70	40	2.974

4.40853	70	42	3.452
5.23003	75	50	5.478
6.36432	75	50	4.444
7.58964	75	50	5.951
8.21193	75	50	5.06
9.11605	67	40	2.439
10.81977	70	40	2.5
Abdomen/ Patient ID	**kVp**	**mAs**	**ESAK, mGy**
1. 9969347	80	64	5.919
2. 6765843	75	50	3.622
3. 3631649	75	50	3.874
4. 13016233	80	64	6.349
5. 451947	80	64	6.662
6. 3926349	75	50	4.408
7. 11282048	75	64	5.507
8. 13100143	80	64	6.503
9. 9436429	75	64	6.15
10.7668243	75	64	6.0
SkullPA/ Patient ID	**kVp**	**mAs**	**ESAK,mGy**
1. 9182745	67	40	2.363
2. 94272	70	32	2.267
3.134998	70	32	2.267
4.126008	70	32	2.322
5.59645	75	40	3.75
6.125003	75	50	4.355
7.61786	70	32	2.379
8.128828	70	32	2.379
9.129416	70	40	2.903
Skull LAT/ Patient ID	**kVp**	**mAs**	**ESAK, mGy**
1.9182745	63	32	1.518

As the retake rates were higher than 5 percent for both OPD Room 5 and Emergency X-ray room as in Table 2, the major causes, patient positioning were discussed among radiologist, medical physicist and radiographers to overcome the problem. The ESAK determined from Hitachi X-ray at OPD room 5 at Chest PA was also high, the high kVp technique was recommended. The results are shown in Table 4.

TABLE 5 The result after education for the improvement of retake rate and the use of high kVp technique at OPD room 5.

Room No.	**OPD Room # 5**	
Time period of the analysis (mm.yy)	**From_19/06/06 to 30/06/06**	
At the level of RADIOGRAPHER		
Number of films used during 2 weeks	78	
Number of films rejected by radiographer	0	
Percentage of films rejected by radiographer	0	
At the level of RADIOLOGIST		
	Number	**Percentage**
A grade films	62	79.4
B grade films	16	20.6
C grade films	0	0
TOTAL	78	100%
Cause analysis (B and C graded films)		
Over- & under-exposure	0	0
Artifacts	0	0
Field size misplacement	0	0
Processing problems	0	0
Other -Positioning	16	100
TOTAL	**16**	**100%**

TABLE 6 ESAK determination from patient data of chest, lumbar spine and abdomen AP with the high kVp technique.

Room No.	OPD Room 5		
Chest PA/ Patient ID	**kVp**	**mAs**	**ESAK mGy**
1. 13776046	90	15	0.22
2. 5581849	90	12.5	0.19
3. 11753339	90	15	0.23
4. 6665433	90	15	0.22
5. 1933041	90	15	0.22
6. 5660349	90	17.5	0.25
7. 5588340	90	12.5	0.18
8. 10604568	90	12.5	0.18
9. 7543209	90	15	0.22
10. 4641549	90	15	0.22
Lumbar spine AP/ Patient ID	**kVp**	**mAs**	**ESAK mGy**
1. 845225	85	25.6	1.05
2. 8282944	85	51.2	2.19
3. 13270339	85	22.4	0.9
4. 5579249	85	25.6	1.07
5.11945441	85	22.4	0.96
6. 6390039	85	19.2	0.84
7. 5532749	85	12.8	0.52
8. 1943549	90	32	1.76
9. 5540346	90	64	3.79
10. 50719330	85	32	1.51
Lumbar spine lateral/ Patient ID	**kVp**	**mAs**	**ESAK mGy**
1. 845225	90	64	3.69
2. 8282944	90	102	7.18
3. 13270339	85	32	1.54
4. 5579249	90	32	1.85
5.11945441	90	32	1.48
6. 6390039	100	19.2	1.41
7. 5532749	100	12.8	0.94
8. 1943549	90	38.4	2.45
9. 5540346	90	102.4	5.11
10. 50719330	90	64	3.19
Pelvis AP/ Patient ID	**kVp**	**mAs**	**ESAKmGy**
1. 11536248	90	19.2	0.96
2. 50057130	90	25.6	1.28
3. 1943549	90	32	1.75
4. 12358448	85	25.6	1.18
5. 8533336	80	25.6	1.32

TABLE 7 After education on the causes of high retake rate, the record on lower retake rate at ER X-ray room.

Room No.	**Emergency(ER)**	
Time period of the analysis (mm.yy)	**From 05/06 to 05/06**	
Describe the corrective actions that were taken	**Arrange a meeting with radiologist, technologist to describe the cause of retake, patient positioning.**	
At the level of RADIOGRAPHER		
Number of films used during 2 weeks	**88**	
Number of films rejected by radiographer	**5**	
Percentage of films rejected by radiographer	**5.68**	
At the level of RADIOLOGIST (use Table 1)		
	Number	**Percentage**
A graded films	42	47.73
B graded films	41	46.59
C graded films	5	5.68
TOTAL	**88**	**100%**
Cause analysis (B and C graded films)		
Over- & under-exposure	1	2.17
Artefacts	4	8.7
Field size misplacement	0	0
Processing problems	0	0
Other -positioning	41	89.13
TOTAL	**46**	**100%**

TABLE 8 Evaluation of entrance surface air kerma (ESAK) at ER x-ray room

kVp	mAs	AK in 1 m (mGy)	AK/mAs (mGy/mAs)
50	25	0.993	0.040
60	25	1.546	0.062
70	25	2.116	0.085
80	25	2.692	0.108
90	25	3.374	0.135
100	25	4.107	0.164
110	25	4.9	0.196
120	25	5.722	0.229
130	25	6.609	0.264
140	25	7.610	0.304
150	25	8.401	0.336

FIGURE 2 The linear response of kVp and ESAK per mAs from Toshiba at ER room.

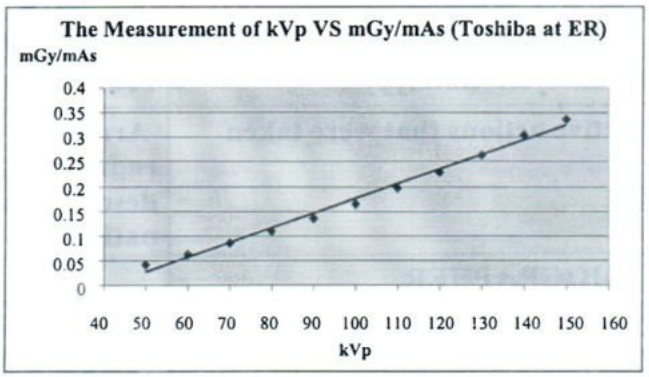

TABLE 9 The entrance skin air kerma determination from patient studies of chest, lumbar spine, abdomen and skull.

Room No.	**Emergency**		
Chest PA/ Patient ID	**kVp**	**mAs**	**ESAK mGy**
1. 9263529	90	3.2	0.067
2. 4981837	90	3.6	0.073
3. 3572949	90	4.8	0.105
4. 915333	90	2.4	0.05
5. 7797444	90	3.2	0.073
6. 6445346	90	2.8	0.057
7. 4223849	90	4	0.084
8. 4869849	90	2.4	0.049
9. 12764145	90	2	0.041
Lumbar spine AP/ Patient ID	**kVp**	**mAs**	**ESAK mGy**
1. 9343848	75	51	2.948
Lumbar spine lateral/ Patient ID	**kVp**	**mAs**	**ESAK mGy**
1.9343848	85	39.7	3.41
Abdomen/ Patient ID	**kVp**	**mAs**	**ESAK mGy**
1.1067447	81	11.5	0.794
2.5429644	81	5.1	0.31
3.4696932	81	13.4	0.925
4.10842042	81	10.2	0.622
5.12476548	81	8.3	0.531
6.12154348	81	9.6	0.6
SkullPA/ Patient ID	**kVp**	**mAs**	**ESAKmGy**
1.4932349	70	25	1.161
2.9239348	70	25	1.190
Skull Lat/ Patient ID	**kVp**	**mAs**	**ESAKmGy**
1.4932349	66	22	0.913
2.9239348	66	22	0.913

DISCUSSION AND CONCLUSION

The surveys of the radiographic image quality from 2 X-ray equipment at King Chulalongkorn Memorial Hospital show the highest percentage of film rejected by radiographers of 7.57 and 7.2% at the OPD and the ER of KCMH. The major cause of film rejection is from patient positioning commented by a radiologist. The meeting was arranged to inform the radiographers and the 2 week survey was followed up showing the reject rate reduce to 3.37 and 5.67% respectively of the same cause.

The measurement of kVp and AK/mAs showed the good linearity of 2 x-ray equipment at KCMH. The ESAK of chest PA at OPD (Table 5) was most likely higher than the guidance level (GL) from BSS as shown in Table 10.

TABLE 10 IAEA Guidance Levels of dose for diagnostic radiography for typical adult patient.

Examination		Entrance surface dose per radiograph[a] (mGy)
Lumbar spine	AP	10
	LAT	30
LSJ		40
Abdomen, intravenous urography and cholecystography	AP	10
Pelvis	AP	10
Hip joint	AP	10
Chest	PA	0.4
	LAT	1.5
Thoracic spine	AP	7
	LAT	20
Skull	PA	5
	LAT	3

[a] In air with backscatter. These values are for conventional film screen combination in the relative speed of 200. For high speed film- screen combination (400-600) the values should be reduced by a factor of 2 to 3.

The meetings among radiologists, physicists and radiographers were arranged for the discussion on several factors involved in ESAK measurement. It was concluded that for chest PA projection the kVp should be increased from 80 to 90 and mAs reduced from 14-20 to 12.5-15 for the machine of nearly 20 years old, a single phase generator. As the high kVp technique is set for all studies, these results in the reduction of ESAK to 0.18-0.25 in the chest PA projection which is less that GL of chest PA (Table 6). The other projections show the ESAK are within the GL. The maximum patient skin doses from the studies are shown in Table 11.

TABLE 11 The comparison of the maximum Entrance Surface Dose from our study to proposed Guidance Level (GL).

Examination		Entrance surface dose, mGy	Proposed GL, mGy
Chest	PA	0.25	0.4
Lumbar spine	AP	3.79	10
	LAT	7.18	10
Pelvis	AP	2.5	10
Abdomen	AP	3.4	10
Skull	PA	2.4	5

From the table, the proposed lumbar spine lateral can be reduced from the original value of 30 mGy to 10 mGy. The exposure techniques play the important role in the patient dose reduction and the meeting for the review of image quality with the patient dose should be arranged regularly at the radiology department as the part of quality assurance program. It is recommended that the patient dose from all simple radiographic studies and the routine retake rate analysis should be determined at the department level, then at the national level later in order to recruit the national guidance level of diagnostic imaging.

REFERENCES

1. International Atomic Energy Agency. International Basic Safety Standards for Protection against Ionizing Radiation and for the Safety of Standards Sources. Safety Series No. 115. Vienna Austria 1996.

2. EUR 16260 European Guidelines on Quality Criteria for Diagnostic Radiographic Images. European Commission, Brussels 1996.